ISTANBUL TECHNICAL UNIVERSITY ★ GRADUATE SCHOOL

INVESTIGATION OF THE CUTTING PERFORMANCES OF THE DIAMOND TOOLS USED IN THE NATURAL STONE INDUSTRY

Ph.D. THESIS

Berrak BULUT

Department of Metallurgical and Materials Engineering

Metallurgical and Materials Engineering Programme

OCTOBER 2021

ISTANBUL TECHNICAL UNIVERSITY ★ GRADUATE SCHOOL

INVESTIGATION OF THE CUTTING PERFORMANCES OF THE DIAMOND TOOLS USED IN THE NATURAL STONE INDUSTRY

Ph.D. THESIS

Berrak BULUT
(506142413)

Department of Metallurgical and Materials Engineering

Metallurgical and Materials Engineering Programme

Thesis Advisor: Prof. Dr. Murat BAYDOĞAN

OCTOBER 2021

İSTANBUL TEKNİK ÜNİVERSİTESİ ★LİSANSÜSTÜ EĞİTİM ENSTİTÜSÜ

DOĞAL TAŞ SANAYİSİNDE KULLANILAN ELMASLI KESİCİLERİN KESİM PERFORMANSININ İNCELENMESİ

DOKTORA TEZİ

Berrak BULUT
(506142413)

Metalurji ve Malzeme Mühendisliği Anabilim Dalı

Metalurji ve Malzeme Mühendisliği Programı

Tez Danışmanı: Prof. Dr. Murat BAYDOĞAN

EKİM 2021

Berrak BULUT, a Ph.D. student of İTU Graduate School student ID 506142413, successfully defended the thesis entitled "INVESTIGATION OF THE CUTTING PERFORMANCES OF THE DIAMOND TOOLS USED IN THE NATURAL STONE INDUSTRY", which she prepared after fulfilling the requirements specified in the associated legislations, before the jury whose signatures are below.

Thesis Advisor :	**Prof. Dr. Murat BAYDOĞAN** Istanbul Technical University	.....
Jury Members :	**Prof.Dr. Hüseyin ÇİMENOĞLU** Istanbul Technical University	.....
	Asst. Prof. Dr. Selim YILDIRIM Istanbul University Cerrahpasa	.....
	Prof.Dr. Hayrettin AHLATCI Karabuk University	.....
	Prof.Dr. Mustafa Lütfi ÖVEÇOĞLU Istanbul Technical University	.....

Date of Submission : 21 September 2021
Date of Defense : 28 October 2021

To my lovely mother Seyda Bulut,

FOREWORD

I would like to express my sincere gratitude and appreciation to many people who have made this thesis possible. Amongst them, I would like to a special thanks to my dear advisor Prof. Dr. Eyup Sabri KAYALI. From the day I started my graduate education, I felt all of his support and I have learned so much about research and life at every moment that I was with him.

I would like to express the most profound and sincere gratitude thanks to my advisor Prof. Dr. Murat BAYDOGAN for their enthusiasm, support, knowledge, motivation and guidance towards my development as a researcher and my academic life. I also wish to express special thanks to Asst. Prof.Dr. Selim YILDIRIM and Prof.Dr. Huseyin CIMENOGLU for their help, support and critical comments, which were very valuable for me and increase the quality of this thesis.

I would like to thank to Asst. Prof. Dr. Oguzhan Gunduz for accepting me as his student and providing all laboratory equipment and facilities for my thesis.

I would like to thank to dear members of the laboratuvary group and colleagues Res. Assist.Dogukan CETINERandDr. Faiz MUHAFFEL.

Iwould like to thank to Labrotary Director Alper BAYRAK, Microsture Laboratory Specialist Cetin BAGLAN and the all members of the microstructure and material analysis laboratory of the Materials Testing and Innovation Laboratories (MATIL).

I would like to thank to my dear best friend and colleague Dr. Fatma UNAL, who is always be with me with their ideas and support in my thesis.

I would like to a special thank to my mother Seyda BULUT. This doctorate would not have been possible without the unselfish support of her. She always encouraged me to pursue my dreams and made this process a success. I thank you all my familyfor helping me throughout my life and my academic career.

Finally,I would like to my deep special gratitude to my niece Nefes YILMAZ for being my sunshine in difficult times.

October 2021

Berrak BULUT
(M.Sc. Metallurgy and
Materials Enginner)

TABLE OF CONTENTS

Page

ABBREVIATIONS

FT4	:Freeman Rheometer
SEM	:Scanning Electron Microscopy
EDS	:Energy Dispersive Spectroscopy
BET	:Brunauer- Emmett- Teller
W-H	:Williamson-Hall Method
XRD	:X-ray Diffraction
S/T	:Streeping/Trimming Machine
SE	: Specific Energy
DCTs	:Diamond Cutting Tools
HIP	: Hot Isostatic Pressing
SPS	: Spark Plasma Sintering
ISRM	:International Scoiety of Rock Mechanics and Rock Enginnering
TSE	: Turkish StandardsInstitution

SYMBOLS

θ	:Diffraction angle
β	:Crytallite size boardening
λ	:X-ray wavelength
k	:Shape factor
D	:Cristallite size
Ɛ	:Lattice strain

LIST OF TABLES

Page

LIST OF FIGURES

Page

INVESTIGATION OF THE CUTTING PERFORMANCES OF THE DIAMOND TOOLS USED IN THE NATURAL STONE INDUSTRY

SUMMARY

Natural stone production has become an increasingly important sector with developments in the construction sector in recent years.In this process, new natural stone quarries were opened, and the open quarries were further deepened and enlarged.The development of the natural stone production sector has provided the research of natural stone production methods and technological gains in production machines. Natural stone production in open mining is carried out in the form of cutting the natural stone from the bedrock with different methods and reducing it to the desired dimensions. The diamond cutting wire and saws are the newest and most advantageous method, which has the most application area among the block natural stone production methods.In these methods, after the diamond toolsare contacted with the stone surface to be cut, it is moved at a certain speed with an electric or diesel drive unit, and the cutting process is carried out by breaking off a piece of natural stone with the abrasive wear.

Diamond segments are composite materials created by mixing diamond grains and metal powders. Generally, powder metallurgy method is used as production technology. There are many geological and physico-mechanical factors affecting the field performance of the diamond cutting tools; machine power, hardness and abrasiveness of the stone to be cut, operator experience, diamond segment design and production technology. In addition to these parameters, the most important factor affecting the cutting performance is the selection of the metal matrix composition of the diamond tools and the determination of the properties of the diamond such as concentration, grain size and coating type.

Diamond is used in cutting, drilling and polishing of hard materials due to its high hardness and high wear resistance.The size of the diamond grains used in the segment is in the range of 18-60 mesh. 20/30 mesh diamond size is for cutting very low hardness and coarse grained stones such as limestone and sandstone, 30/40 mesh diamond size is for cutting medium hard marble stone, 40/50 mesh diamond size is for cutting hard and fine grained stones such as granite and basalt, and 50/ 60 mesh diamond grain size is preferred for cutting flint and very hard granite type stone. As the diamond grain size gets thinner, the impact strength increases. Although high cutting speeds can be achieved with coarse-grained diamonds, fine-grained diamond is preferred as the hardness of the cut stone increases.In addition to diamond grain size, another characteristic that affects cutting performance is its concentration. Concentration refers to the volume of diamond in the insert mix and is calculated by the weight of the diamond in the metal matrix layer. The high diamond concentration provides high wear resistance for the diamond tools, even at high loads. However, a large contact surface requires lowering the grinding intensity. In this case, a lower diamond concentration should be used.

Diamonds segments wear during the production of natural stone. This wear can occur both on the diamond grain and between the diamond-matrix interface. The main task of the metal matrix in diamond tools is to hold the diamonds in its structure and to wear it in compatible with the diamond. The matrix should keep the diamonds that have not completed their cutting task in the structure, but should be worn so that the diamonds that have completed the cutting process leave the structure and are replaced by new diamonds with sharp edges. The cobalt (Co) powders and alloys are matrix materials that are widely used in cutting processes of marble and granites. Copper (Cu), tin (Sn) or bronze are used as a metal matrix materials for decrasing the porosity. Tungsten (W) can be used to for increasing the mechanical properties of the metal matrix material.

In this study, the metal matrix compositions were developed to improve the cutting performances of the diamond tools. Three different publications are presented in this thesis. The first publication is on the examination of the morphology, microstructure and mechanical properties of Co powders that can be used in the metal matrix composition, and the selection of the appropriate Co powder that can increase the field performance of the diamond tools. The second publication is on the determination of the matrix compositon to increase the cutting speed of the diamond toolsdue to the properties of the stone. In this study, iron (Fe)-based and Co-based metal matrices were formed. In the third publication, aluminum (Al) and silver (Ag)addition were used to increase the performances of thediamond tools in the production of Ankara andesite stone.

The first part of the thesis examines the effects of powder grain shape on the final product. The Co powders with spherical(Co-S) and rod-like(Co-R) grain shapes are preferred by the manufacturers in many countries. The effects of these grain shapes on the production of the segment and thus on the final product were examined comparatively. Freeman (FT4) rheometer analysis was performed to predict the behavior of the powders in the cold pressing process. The grain shapes, grain sizes and surface areas of the powders were determined by Scanning Electron Microscopy (SEM), grain size distribution measurement and Brunauer, Emmett and Teller (BET) analysis. The crystal size of the powders was determined by the Williamson–Hall (W–H) method. Microstructure analyzes were determined by SEM and X-ray diffraction method (XRD), and the density was determined by the Archimedes. The mechanical properties were determined by microhardness measurement, compression test and abrasion test. According to the results obtained by the powder characterization studies, the grain size of Co-S powder is lower than Co-R powder. According to the FT4 analysis results, it was determined that the cold press fluidity of Co-S powder is high, it can fill the cold press mold without creating deep cavities, and the powders are stable against air flow. The results obtained in Co-R powderrevealed that the powders are not stable with air flow, their fluidity is low and they created cavities in the cold press mold during powder filling. It was determined that Co-R samples contain 25% more porosity than Co-S samples. The highest mechanical properties were obtained in Co-S samples. According to the results of this study, the grain shape of the powders significantly affects the powder properties. The Co-S powders are more appropriate in the production of the diamond tools is and it was preferred in the metal matrix compositions in the next studies of the thesis.

In the second part of the thesis, the metal matrix compositions to be used in cutting marble and granite stones were examined. Fe-based and Co-based metal matrix

groups were formed. In order to determine the microstructure and mechanical properties, SEM, XRD, density measurement, hardness measurement, compression test and relative wear tests were performed. In order to determine the field performances, diamond cutting wires were produced. The hardness, compression strength and the relative wear resistance of Co-based samples are higher than Fe-based samples. The high cutting speeds were obtained with Fe-based matrices in marble stone production. The Fe-based metal matrix is worn during cutting and new diamonds with sharp corners come to the surface and increasing the cutting speed. In Co-based matrices, on the other hand, the cutting speed in marble stone production remained low, because the broken and damaged diamonds remained on the surface and could not perform well during the cutting process. In granite stone cutting, the higher cutting speeds were obtained in Co-based matrices. The high mechanical properties given by Co are maintained at high temperatures to provide high cutting speeds and high service life to the segments. In this study, it has been determined that the first step in the production of the diamond tools is to understand the characteristics of the stone to be cut.

In the last part of the thesis, similar to the second part of the thesis, the metal matrix compositions according to stone properties were examined to increase the cutting performance of the diamondsegments. Ankara andesite stone has high hardness and abrasiveness. Since it is in the volcanic stone group, it contains high porosity and glassy phases. Due to its structural features, the service life of the cutting tools is low. For this reason, Al and Ag were used as a matrix material to increase the service lifethe Co-based matrix composition. The microstructure and mechanical properties of metal matrices were determined comparatively. Diamond circular saws were used for field trials. According to the results of the analysis, Ag spread between the grain boundaries and filled the existing porosities. The mechanical properties of the samples increased with the formation of the $Al_{13}Co_4$ intermetallic phase and a decrease in the porosity. The high cutting speeds and long lifetimes were determined for Al and Ag added samples. 57.14%vol. more stone cutting was achieved. The cutting tools obtained from the matrix composition developed in this study are produced in series and the produced saws continue to be used in andesite and basalt stone cutting in Ankara and Kayseri, Turkey.

The matrix compositions developed in the thesis have been used in different stone types in different countries and mass production continues.

DOĞAL TAŞ SANAYİSİNDE KULLANILAN ELMASLI KESİCİLERİN KESİM PERFORMANSININ İNCELENMESİ

ÖZET

Doğal taş üretimi, son yıllarda doğal yapı malzemelerine olan talebin artması ve inşaat sektöründe yaşanan gelişmeler ile önemi gittikçe artan bir sektör haline gelmiştir. Bu süreçte yeni doğal taş ocakları açılmış, açık olan ocaklar ise daha fazla derinleştirilmiş ve büyütülmüştür. Doğal taş üretim sektörünün gelişmesi doğal taş üretim yöntemlerinin araştırılmasını ve üretim makinelerinde teknolojik kazanımları sağlamıştır. Doğal taş yatağının üzerindeki örtü tabakasının ekonomik sınırları zorlamadığı durumlarda açık ocak blok doğal taş işleme yöntemleri uygulanmaktadır. Açık işletmelerde doğal taş üretimi, doğal taşın değişik yöntemlerle ana kayadan koparılarak talep edilen boyutlara indirilmesi şeklinde gerçekleşmektedir. Açık doğal taş ocaklarında uygulanan blok üretim yöntemlerine örnekler; patlayıcı madde kullanımı, kamalama, helezon tel testere ile kesim, kollu kesiciler, elmaslı kesici teller ve testereler, elmaslı kayışlı kollu kesiciler, alevle kesme ve basınçlı su ile kesme olarak sıralanmaktadır. Blok doğal taş üretim yöntemleri içerisinde en fazla uygulama alanı bulunan ve teknolojik açıdan en yeni ve avantajlı olan yöntem elmaslı kesici tel ve testerelerdir. Bu yöntemlerde elmaslı kesici, kesilecek taş yüzeyine temas ettirildikten sonra, elektrikli ya da dizel bir tahrik ünitesi ile belirli bir devirde hareket ettirilerek, abrasif aşınma yöntemi ile doğal taştan parça koparark kesme işlemini gerçekleştirmektedir. Elmaslı kesici yöntemlerin avantajları; yer altı ve yer üstü kesim çalışmalarında kullanılabilmesi, doğal taş madenciliğinde 200 m^2'den büyük boyutlu kesimlerin yapılabilmesine olanak tanıması, ilk yatırım maliyetlerinin düşük olması, makine ve ekipmanların yıpranma payı sürelerinin kısa olması, dahaaz talaş oluşturması, düzgün şekilli blok çıkarımı, iş gücünün daha verimli kullanılmasına olanak tanıması ve yüksek kesim hızları ile üretim kapasitesinin artmasıdır.

Elmaslı kesici uçlar elmas ve metal tozları ile elde edilen kompozit malzemelerdir. Genellikle üretim teknolojisi olarak toz metalurji yöntemi kullanılmaktadır. Elmaslı kesicilerin saha performansını etkileyen jeolojik ve fiziko-mekanik birçok faktör bulunmaktadır; kullanılan makine gücü, kesilecek taşın sertliği ve aşındırıcılığı, operatör tecrübesi, kesici uç tasarımı ve üretim teknolojisidir. Bu parametrelerin yanı sıra kesim performansını etkileyen en önemli faktör elmaslı kesicilerin metal matris bileşiminin seçimi ve elmas konsantrasyonu, elmas tane boyutu ve elmas kaplama türü gibi elmasın özelliklerinin belirlenmesidir.

Elmas, kimyasal olarak saf karbondan oluşmaktadır ve elmas kübik yapısına sahiptir. Elmas, yüksek sertlik, mükemmel tokluk, yüksek termal iletkenlik, düşük sürtünme ve yüksek aşınma direnci gibi birçok üstün özelliğe sahiptir ve bu nedenle de sert malzemelerin kesim, delim ve parlatma gibi işlemlerinde yaygın olarak kullanılmaktadır. Kesici uçlarda kullanılan elmas tanelerinin boyutu 18-60 mesh aralığındadır. 20/30 mesh elmas boyutu çok düşük sertlikteki ve iri taneli kireçtaşı, kumtaşı gibi taşların kesiminde, 30/40 mesh elmas boyutu orta sertlikteki mermer

taşının kesiminde, 40/50 mesh elmas boyutu sert ve ince taneli granit ve bazalt gibi taşların kesiminde ve 50/60 mesh elmas tane boyutu çakmaktaşı ve çok sert granit türü taş kesiminde tercih edilmektedir. Elmas tane boyutu inceldikçe darbe dayanımı artmaktadır. İri taneli elmaslarla yüksek kesim hızları elde edilse de, kesilen taşın sertliği arttıkça elmas tane boyutunda ince ölçü tercih edilmektedir.

Elmasın tane boyutunun yanı sıra kesim performansını etkileyen bir diğer özellik ise konsantrasyondur. Konsantrasyon, kesici uç karışımındaki elmasın hacmini belirtir ve metal matris katmanındaki elmasın ağarlığı ile hesaplanır. Elmas tanesinin ağırlık birimi karattır ve bir karat elmas 0,2 grama eşittir. Örneğin; C100 olarak belirtilen konsantrasyon 4,4 karat/cm^3demektir ve bu da metal matris hacminin %25'ini elmasın oluşturduğunu belirtmektedir. Elmas konsantrasyonun belirlenmesi; kesme yüzeyine, elmas tane boyutuna, matrisin aşınma direncine ve çalışma koşullarına bağlıdır. Konsantrasyonun seçimi için genel bir kural olarak; kesme işlemi sırasında dairesel testere ve katrakkesici uç ile doğal taş arasında küçük bir temas yüzeyi varsa elmas konsantrasyonu yüksek olmalıdır. Yüksek elmas konsantrasyonu, elmaslı kesici için yüksek yüklerde bile yüksek aşınma direnci sağlar. Tersine, geniş bir temas yüzeyi, öğütme yoğunluğunun düşürülmesini gerektirir. Bu durumda daha düşük elmas konsantrasyonu kullanılmalıdır. Elmas ile metal tozları arasındaki bağın güçlendirilmesi için karbür kaplamalı elmaslar kullanılabilir.Bu yöntemle sinterleme prosesi sırasında elmasın oksidasyonunu (700 K) ve grafite dönüşmesini engellenir ve elmasın mekanik özellikleri korunabilir.

Kesici uçlardaki elmaslar, doğal taş üretimi sırasında maruz kaldıkları kuvvet nedeniyle aşınabilirler. Bu aşınma hem elmas tanesi üzerinde hem de elmas-matris bağ arasında gerçekleşebilir. Elmas tanelerinin aşınma davranışı dört başlıkta sınıflandırılabilir; yeni taneler, kırık taneler, aşınmış taneler ve dökülmüş taneler. Yeni elmas taneleri keskin köşeli yapısını korumaktadır ve elmas yüzeyinde hasar meydana gelmediği için kesim işleme devam etmektedir. Kırık taneler, termal stres ve ardından gelen hızlı soğutma, mekanik yük ile birleştiğinde elmas tanesinin uçlarında kırılmalar meydana gelmektedir ve yeni keskin köşeler de oluşmaktadır. Böylece elmas taneler kesim işlemine devam edebilmektedir. Aşınmış elmaslarda, sürtünme sonucu elmaslar keskin köşelerine kaybeder ve kesme işlemine katkısı olmayan, yuvarlatılmış, düzleştirilmiş kesme kenarları oluşur. Bu elmas taneleri körelmiş veya camlaşmış elmas olarak bilinmektedir. Son olarak elmas ile matris arasındaki bağın tutucu kuvvetinin yeterli olmadığı durumlarda elmas tanelerinin dökülmesi meydana gelir. Kesim işlemine devam eden ya da görevini tamamlayan elmas metal matrisin aşınması ile yapıyı terk eder.

Elmaslı kesici uçlarda metal matrisin temel görevi elmas tanelerini yataklama, elması yapıda tutma ve elmas ile uyumlu olacak şekilde aşınma özelliği göstermektir. Matris kesim görevini tamamlamamış elmasları yapıda tutmalı ancak kesim işlemini tamamlamış elmasların yapıyı terk edip yerine keskin köşeli yeni elmasların yüzeye gelmesi için aşınmalıdır. Matris bileşimikesilecek taşın sertliğine ve aşındırıcılığına göre kobalt (Co), bakır (Cu), kalay (Sn), demir (Fe), krom (Cr), nikel (Ni), gümüş (Ag), titanyum (Ti), tungsten (W) gibi elementlerden oluşur. Co tozları ve alaşımları, yüksek mekanik özelliklerinden dolayı mermer ve granitlerin kesim işlemlerinde yaygın olarak kullanılan matris malzemeleridir. Sıvı faz sinterleme yoluyla gözenekleri doldurmak amacıyla bileşime Cu, Sn ya da bronz eklenir. W ve diğer karbür oluşturucu elementler, tane büyümesini önlemek ve dolayısıyla matris malzemesinin mekanik özelliklerini arttırmak için küçük miktarlarda eklenebilir.

Elmas tanecikleri ile matris arasında elmasın hizmet ömrünü artırabilecek güçlü bir karbür bağı oluşturmak için Ti, Cr, Silisyum (Si), Vanadyum (V) gibi karbür yapıcılareklenebilir.

Elmaslı kesicilerin toz metalurjisi yöntemi ile üretimi metal matris karışımının hazırlanması ve içerisine elmas ilavesi yapılması ile başlamaktadır. Karışım 360 º dönebilen otomatik karıştırıcılarkullanılarak gerçekleştirilir. Elde edilen karışıma, elmas tanelerinin metal tozlar ile bağının arttırılması için granül işlemi uygulanır. Hazırlığı tamamlanan toz-elmas karışımı elmaslı kesici ucun belirlenen ölçülerine göre soğuk preslenir ve ardından sinterlenerek nihai ürün elde edilir. Dairesel testere ve katrak testeresi üretiminde kullanılacak soketler sert lehimleme işlemi ile testerelere kaynatılır. Elmaslı kesici tel üretiminde ise içi boş silindir olarak üretilen uçlar çelik halat üzerine dizilir. Uçlar arasındaki mesafe yay, plastik veya kauçuk malzeme ile sağlanır.

Bu çalışmada, elmaslı kesicilerin saha performansını arttırmak için metal matris bileşimleri geliştirilmiştir. Bu tezde üç farklı yayın sunulmuştur. Bu yayınlar sırasıyla, metal matris bileşiminde kullanılabilecek farklı tane şekillerine sahip Co tozlarının (küresel ve çubuksu tane şekli) morfoloji, mikroyapı ve mekanik özelliklerinin incelenmesi ve inceleme sonucuna göre elmaslı kesicilerin saha performansını arttırabilecek uygun Co tozunun seçimidir. Bir diğer çalışma, kesilen taşın sertliğine ve aşındırıcılığına uygun matris bileşiminin belirleyerek elmas kesicilerin kesim hızını arttırmaktır. Bu amaçla Co ve Fe esaslı olmak üzere iki ayrı grup metal matris bileşimleri oluşturulmuş ve numunelerin mikro yapıları, mekanik özellikleri ve aşınma özellikleri karşılaştırmalı olarak incelenmiştir. Son yayın olarak da yüksek sertlik ve yüksek aşındırıcılık özelliğinin yanı sıra yapısında porozite ve camsı fazlar barındıran Ankara andezit taşının üretiminde verimliliği ve kesici ucun kullanım ömrünü arttırmak adına Co esaslı metal matris yapısına alüminyum (Al) ve Ag ilavesi gerçekleştirilmiştir. Gerçekleştirilen çalışmada elmaslı dairesel testereler üretilmiş ve kesim denemeleri Ankara bölgesinde endüstriyel alanda tamamlanmıştır.

Tezin ilk bölümü toz tane şeklinin nihai ürün üzerine etkilerini irdelemektedir. Öncelikle sektörde kesici uçların üretiminde yaygın olarak kullanılan Co tozları belirlenmiştir. Yuvarlak tane (Co-S) ve çubuksu tane (Co-R) şekline sahip olan Co tozları birçok ülkede üretici firmalar tarafından tercih edilmektedir. Bu tane şekillerinin kesici uç üretim aşamalarına ve dolayısıyla nihai ürün üzerine etkileri karşılaştırmalı olarak incelenmiştir. Tozların soğuk presleme işlemindeki davranışlarını, akıcılıklarını ve soğuk pres kalıbını doldurabilme özellikleri öngörebilmek adına Freeman (FT4) reometre analizi gerçekleştirilmiştir. Tozların tane şekilleri, tane boyutları ve yüzey alanları Taramalı Elektron Mikroskobu (SEM), tane boyut dağılım ölçümü ve Brunauer,Emmett and Teller (BET) analizleri ile belirlenmiştir. Tozların kristal boyutu Williamson–Hall (W–H) yöntemi ile hesaplanmıştır. Mikroyapı ve mekanik özelliklerin belirlenebilmesi adına silindir şeklinde (7,5 mm çap x14 mm yükseklik) numuneler Spark Plazma Sinterleme (SPS) yöntemi ile 750 ve 800 °C sıcaklıkta ve 115 bar basınç altında sinterlenmiştir. Mikroyapı analizleri SEM ve X- ışını kırınım yöntemi (XRD) ile belirlenirken, yoğunluk Arşimet yöntemiyle belirlenmiştir. Mekanik özellikler mikro sertlik ölçümü, basma testi ve aşınma testi ile belirlenmiştir. Toz karakterizasyon çalışmaları ile elde edilen sonuçlara göre, Co-S toz taneleri Co-R tanelerinden daha küçük boyutludur. FT4 analiz sonuçlarına göre Co-S tozunun soğuk pres akışkanlığının yüksek olduğu, soğuk pres kalıbını derin boşluklar yaratmadan

doldurabildiği ve hava akışına karşı tozların stabil olduğu belirlenmiştir. Co-R tozunda elde edilen sonuçlar ise tozların hava akışı ile stabil olamadığı, akışkanlığının düşük olduğu ve toz dolum sırasında soğuk pres kalıbında boşluklar yaratacağı gözlemlenmiştir. Farklı sıcaklıklarda sinterlenen numunelerin XRD analizlerine göre faz farklılıkları bulunmamaktadır. Her iki toz türünde de kübik yüzey merkezli Co fazı tespit edilmiştir. SEM analizleri incelendiğinde Co-S numunelerinde düşük oranlarda porozite gözlemlenmiştir ve artan sinterleme sıcaklığı ile porozite oranında azalma gözlemlenmiştir. Co-R numunelerinde ise yüksek oranda porozite gözlemlenmiştir ve artan sinterleme sıcaklığının yüksek porozite oranına bir etkisi olmadığı gözlemlenmiştir. Co-R numunelerinin Co-S numunelerine göre %25 daha fazla porozite içerdiği tespit edilmiştir. Co-R numunelerinde sinterleme sonrasında tane aralarında derin boşluklar bulunduğu belirlenmiştir. En yüksek mekanik özellikler 800 °C sıcaklıkta sinterlenen Co-S numunelerinde elde edilmiştir. Co-S numunelerinin sertlik değerleri ve relatif aşınma direnci, Co-R numunelerinden sırasıyla %11 ve %44 daha yüksek olduğu tespit edilmiştir. Bu çalışmanın sonuçları, taneşeklinin, sinterleme kabiliyeti, akış kabiliyeti ve mekanik davranışlar dahil olmak üzere toz özelliklerini önemli ölçüde etkilediğini göstermiştir. Doğal taş kesme işleminde kesicilerin mekanik özelliklerinin özellikle sertlik ve aşınma dirençlerinin yüksek olması gerekmektedir.Bu nedenle, elmaslı kesici üretiminde Co-S tozlarının kullanımının daha uygun olduğu belirlenmiştir ve tezin sonraki çalışmalarında metal matris bileşimlerinde bu toz tercih edilmiştir.

Tezin ikinci bölümünde, mermer ve granit taşların kesiminde kullanılmak üzere metal matris bileşimleri incelenmiştir. Fe esaslı ve Co esaslı olmak üzere iki ayrı grup metal matris bileşimleri oluşturulmuştur. Mikroyapı ve mekanik özellikleri belirlemek adına SEM, XRD, yoğunluk ölçümü, sertlik ölçümü, basma testi ve aşınma testleri gerçekleştirilmiştir. Saha performanslarını belirlemek adına elmaslı kesici teller üretilmiştir. Saha testlerinde tek telli makineler (sayalama) kullanılmıştır. Kesim sonrası kesici uçların elmas görüntüleri incelenmiş ve hangi taş grubuna hangi metal matrisin yüksek kesim hızı sağlayabileceği belirlenmiştir. Fe esaslı ve Co esaslı numunelerin XRD sonuçlarına göre, Fe ve Co içeriklerinin artmasıyla Fe esaslı ve Co esaslı piklerin yoğunluğu artmış ve bu sonuçlara paralel olarak Cu esaslı piklerin yoğunluğu, matris bileşimlerinde Cu içeriğinin azalmasıyla azalmıştır. SEM analizinde gözlemlendiği gibi, sıvı faz sinterleme sonucunda oluşan Cu adacıkları, matris bileşimlerinin Cu içeriği azaldıkça azalmıştır.Toz bileşime eklenen bronz miktarındaki azalmaya paralel olarak, numunelerin Fe ve Co içerikleri arttıkça Fe esaslı ve Co esaslı numunelerin her iki türünde de sertlik ve basma dayanımı değerleri artmıştır. Co esaslı numunelerin mekanik özellikleri Fe esaslı numunelerden daha yüksektir. Saha kesim performansları karşılaştırıldığında, mermer taş üretiminde Fe esaslı matrisler ile yüksek kesim hızları elde edilmiştir. Fe esaslı matrislerin mekanik özelliklerinin Co esaslı matrise göre daha düşük olmasından dolayı, kesim sırasında metal matris aşınmış ve yüzeye keskin köşeli yeni elmaslar gelerek kesim hızı artmıştır. Co esaslı matrislerde ise aşınma meydana gelmediği için kırılan ve hasar gören, kesim işlemini gerçekleştiremeyecek elmaslar yüzeyde kaldığı ve matrisi terk etmediği için mermer taş üretiminde kesim hızı düşük kalmıştır. Granit taş kesiminde ise taşın sertliğinden dolayı Fe esaslı matrisler yüksek oranda aşınmış ve yoğun elmas dökülmesi meydana gelmiştir. Bu nedenle Co esaslı matrislerde daha yüksek kesim hızları elde edilmiştir. Co metalinin yapıya verdiği yüksek mekanik özellikler ve bu özellikleri yüksek sıcaklıklarda da kaybetmemesi kesici uca yüksek kesim hızları ve yüksek kullanım ömrü sağlamıştır. Bu çalışma ile

doğal taş üretiminde kesilecek taşın sertliğinin ve aşındırıcılığının metal matris bileşimi belirlenirken ki önemi vurgulanmıştır. Elmaslı kesici üretiminde ilk adımın kesilecek taş özelliklerinin iyi anlaşılması olduğu belirlenmiştir.

Tezin son bölümünde ise, tezin ikinci bölümüne benzer olarak elmaslı kesici uçların saha performansını arttırmak amacıyla taş özelliklerine göre metal matris bileşimleri irdelenmiştir. Kesilen taş Ankara andezit taşıdır. Ankara andezit taşı yüksek sertlik ve aşındırıcılık özelliğine sahiptir. Volkanik taş grubunda olduğundan aynı zamanda yüksek oranda porozite ve camsı fazlar içermektedir. Yapısal özelliklerinden dolayı kesim işleminde kesici ucun kullanım ömrü düşük olmaktadır. Bu nedenle verim artışı sağlamak amacıyla Co esaslı matris bileşimine Al ve Ag ilavesi gerçekleştirilmiştir. Metal matrislerin mikroyapı ve mekanik özellikleri karşılaştırmalı olarak belirlenmiştir. Saha çalışmaları için elmaslı dairesel testereler kullanılmıştır. Konik-dikdörtgen şeklinde üretilen soketler sert lehimleme yöntemi ile dairesel saca kaynatılmıştır. Analiz sonuçlarına göre metal matrise ilave edilen Ag tane sınırları arasında yayılarak var olan poroziteleri doldurmuştur. Al ve Ag ilavesi ile porozite oranında düşüş ve $Al_{13}Co_4$ intermetalik fazın oluşumu ile numunelerin mekanik özelliklerinde artış tespit edilmiştir. Saha performansları karşılaştırıldığında Al ve Ag ilaveli numunelerde yüksek kesim hızları ve yüksek kullanım ömürleri belirlenmiştir. %57 daha fazla taş kesimi gerçekleştirilmiştir. Bu çalışmada geliştirilen matris bileşiminden elde edilen kesici uçlar seri olarak üretilmektedir ve üretilen testereler andezit ve bazalt taş kesiminde Ankara ve Kayseri bölgelerinde kullanılmaya devam etmektedir.

Tez içerisinde geliştirilen matris bileşimleri farklı taş tiplerinde farklı ülkelerde kullanılmıştır ve seri üretimi devam etmektedir.

1. INTRODUCTION

1.1 Significance of Thesis

The natural stones on the earth crust are classified of three main groups according to their genesis forms; sedimentary, igneous, and metamorphic. The sedimentary stones are formed on Earth's surface (in seas, lakes and pits) by the accumulation of minerals or organic materials. The organic materials are formed from the plants and animals decayin the ground. Coal is a sedimentary rock formed from compressed plants. The mineralsare formed from broken rocks via erosion and weathering geological phenomenons andthe best-known type is sandstone [1-5].The stalagmites and stalactites of the cave and the limestone are also sedimentary stones. They are formed by calcium carbonate, the source of which is the shells of marine animals and chemically rich waters[6-8].The precipitation geological phenomenons create the stalagmites and stalactites of the cave and the lithification geological phenomenons create limestone [9-13].

The color of the sedimentary rock varies depending on the chemical content as grey, green, red and brown [14,15].Figure 1.1 presents examples of sediment stones named according to their region and color. All types of stones are known by these names in the commercial market and its qualities are known from producers.

The presence of organic material can give black and grey color to the stone. According to the mineralogically investigation of the sedimentary stones, their composition was generally composed of quartzite and calcite [15,16].Sedimentary stones have hardness of 3 Mohs and their abrasive property is low.

Figure 1.1 : Sediment stones examples with named their region and color.

Igneous stones are formed from the magma in the cracks of the earth's crust up to the earth's surface. The magma on the earth's crust melt and it quickly cools and crystallizes on the Earth's surface[17,18]. Igneous stones are divided into two classes according to their formation styles; intrusiveand extrusive igneous rocks. The intrusive rocks are coarse crystalline and the best known examples are rhyolite (containing quartz, mica, feldspar), syenite, diorite. The extrusive igneous stones, which cool down in a short time, become small crystals or glassy texture and the best-known examples are basalt, andesite, obsidian and volcanic tuff [19-21]. Igneous stones have hardness of 7 Mohs and their abrasive property is very high. Figure 1.2 presents examples of sediment stones named according to their region and color.

Figure 1.2 : Igneous stones examples with named their region and color.

Basalt has black, dark green or brown colors.Basalt is mainly composed of olivine, pyroxene, plagioclase, and possibly with minor glassy texture. Basalt stones have pumiceous structure and the steam cavities fill with secondary minerals as calcite, chlorite, and zeolites [21,22].

Andesite has a different color grey, pink brown from light to dark. Andesite stone has a similar mineral composition as rhyolite and basalt. Due to this similarity, darker andesite can be difficult to distinguish from basalt. Andesite stones contain large and small minerals were formed by the cooling phase of magma[23,25]. Andesite stones have a porous structure and they contain glassy phases. Andesite stones are highly abrasive and the production of these stones complicated. Andesite stones have a bright appearance and due to this property they are used in the exterior decoration of architectural structures.

Granite is the most abundant and best-known igneous stone at Earth's surface. Granite stones have a color groups as pink-red, white- grey and dark brown-black [26-29].Granite stones are formed by physical weathering or chemical weathering. In physical weathering, when the accumulation in the earth's crust is removed by erosion, the pressure decreases, the granite stone expands and breaks. In the formation of granite by chemical weathering, feldspar change occurs in the hydrolysis process [29-31].

Metamorphic stones arise from the transformation of sedimentary and igneous stones to new types of stone with heat and pressure on the Earth’s crust, in a process called metamorphism [32,33]. The metamorphism process of the sedimentary or igneous stones start at a temperature of more than 200 °C and a pressure of more than 100 MPa. These environmental circumstances cause physical and chemical changes of the stones. After this process, the stones have a new texture and mineral composition, for example the conversion of granite to gneiss and limestone to marble [34-39].

Marble is sediment origin stone and it is formed by the metamorphism of limestone. It consists predominantly of calcite and/or dolomite. The composition of marble is containedhigh amount of calcium carbonate [40,41]. Marble stones can be found in a wide variety of colors; white, bluish, grey, pink, yellow, or black. The color of the marble stone changes depending on the chemical composition of the limestone stone is formed by metamorphism.The white color of the marble stone is due to the pure

chemical composition of the limestone stone. When the impurities in the chemical composition of the limestone increase, the color of the marble stone becomes beige and yellow colors. [42-45]. Figure 1.3 presents the samples of the marble stones.

Figure 1.3 : The samples of the marbles stone types.

Marble is resistant to harsh weather conditions, has high bearing strength, is abundant in nature and has been the noblest building material in architecture for centuries. The most important feature that makes marble superior to other materials is that it allows building solid structures without the need for any connection.Regardless of the type and composition of the marble stone, large blocks can be obtained, cut and polished. For this reason, it is a type of stone with a very high use in the industrial field.The main consumption areas of marble are the construction industry, the field of fine arts and decoration. The largest usage area is the construction sector since ancient times. Interior and exterior coatings of buildings, decoration works, monuments, sculptures, ornaments and souvenirs are important consumption areas.

Natural stone quarries have various morphological structures, different depths and geological features. Depending on these features, natural stone quarries are divided into two as outdoor and underground.The difference between underground and outdoor quarries is that underground are preferred when the cover layer does not allow open mining, has high mechanical properties and has limited natural cracks. Outdoor stone quarries are the most common type of quarry [41,46].Figure 1.4 presents the outdoor deposits.

Figure 1.4 : The outdoor mining quarry.

Natural stone production in open and underground stone enterprises is carried out in the form of slicing the natural stone in desired sizes by detaching it from the bedrock with various methods. For the production of slabs from stone blocks coming from the quarry, sizing and polishing processes are applied according to the purpose of use in the processing facilities. After these processes, smooth-surfaced stones are obtained.For this purpose, different tools and methods have been used since ancient times. Outdoor stones production methods are generally divided into two groups as primitive methods and mechanical methods. Primitive methods are gutter-grooving, drilling (triple wedge), modern triple wedge and explosives methods and are few and only local applications [47-50].The mechanical methods are cutting with diamond disc, cutting with diamond wire, cutting with a lever cutter, cutting with flame and pressurized water.

Diamond tools perform the cutting process as a result of moving them at a certain speed on the surface to be cut and rubbing the stone with the applied tension. Diamond tools are available in the form of wire, circular and linear saw for cutting, grinding and polishing of the natural stones. The diamond cutting wires consist of a steel rope anddiamond beads.There are varieties of diamond cutting wires as spring wires, plastic coated wires and rubber coated wires. The type of wire is decided according to the stone to be cut and the quarry and its location.Figure 1.5 and Figure 1.6 shows the components of the diamond cutting wires and a schematic view of the diamond cutting wire, respectively.

(a) (b)

(c)

Figure 1.5 : The components of the diamond cutting wires a) steel rope b) diamond beads.

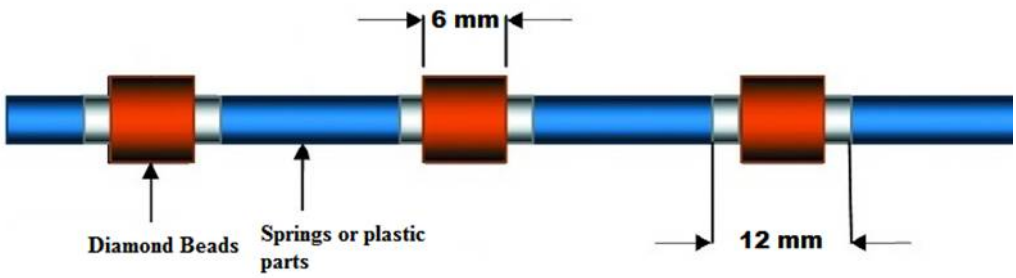

Figure 1.6 : The schematic view of the diamond cutting tools.

Diamond beads are arranged on the steel rope that there are 25-40 diamond beads per meter depending on the type, structure, hardness and abrasiveness of the stone to be cut.The diamond wire is passed through the pulleys of the cutting machine. The pulleys are moved by the motor and the wire rotation movement is provided. With the tension force applied to the wire during the cutting process, the wire rubs against the stone and performs the cutting process with abrasive wear. The wire cutting machine can be mono and multi wire as seen in Figure 1.7.

(a)

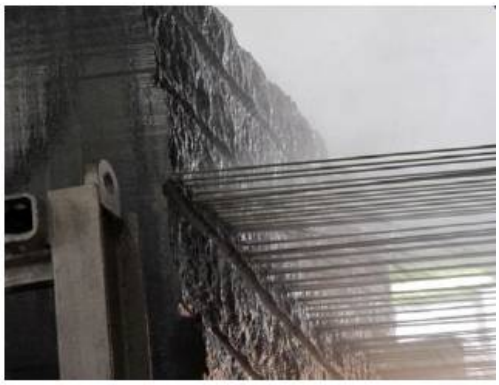

(b)

(c)

Figure 1.7 : The diamond wire machines a) diamond wire b) multiwire c) monowire.

The circular and linear saw blades are welded with diamond rectangular segment. The linear saw blades are named as gang saw. The segments are composed of binder, diamond grain and metal matrix and the segments are prepared with powder metallurgy process as diamond beads. Figure 1.8 present the segments, diamond circular saws and gang saws. Streeping (S)/ Trimming (T) block cutting machines are used for slicing large masses of natural stones in certain sizes and separating them from the block, and diamond cutting discs are used in cutting processes.Two different circular saw blade, horizontal and vertical, are placed on S/T machines. The vertically working saw performs the cutting operation and the horizontally working saw performs the task of separating the cut slice stone from the main block. The diameter of the vertical saw making the cutting operation should be larger than the diameter of the horizontal saw performing the cutting operation.As with diamond cutting wires, circular saw machines and gang saw machines can be mono or

multi.The saw blade welded with segments is driven by the crankshaft to realize the horizontal reciprocating motion and driven by the stone block lifting mechanism to achieve smooth upward feeding motion [50-52]. The combination of these forward and upward movements realizes the effective processing of the stone material. The sawing force of the gang saw machines and the position of the blades change during the cutting process. The process steps are the blades sawing the stone and then separating from the stone and after a period of time, the blades sawing the stone again and separating from the stone. The sawing force is zero, when the blade separate from the stone surface. Figure 1.9 shows the samples of the S/T and gang saw machine.

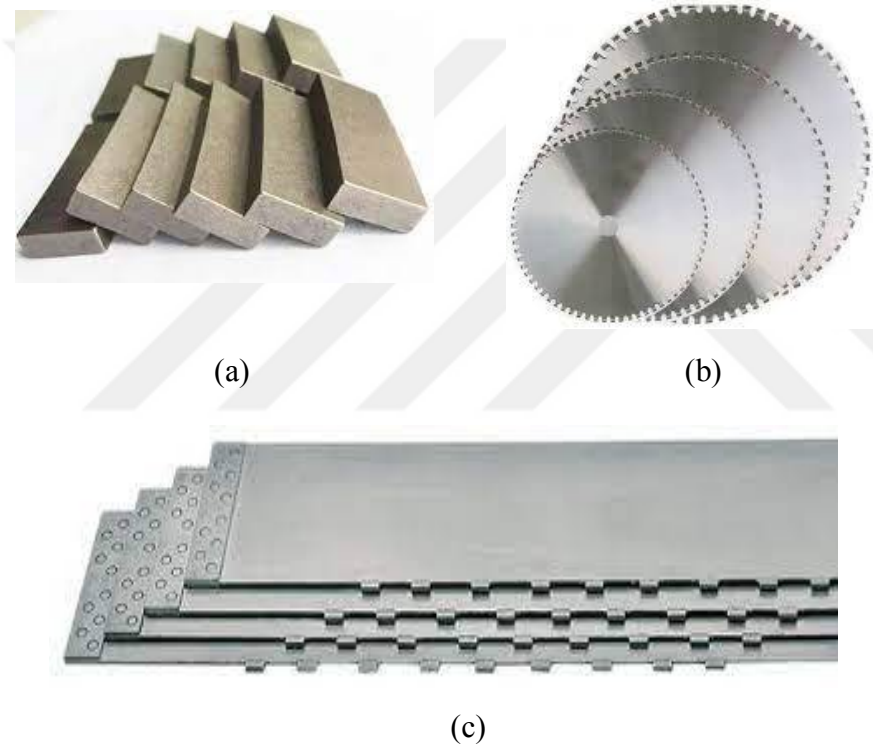

(a) (b)

(c)

Figure 1.8 : The samples of the diamond saws a) diamond cutting segments b) circular saw blades c) gang saws.

(a) (b)

Figure 1.9 : The circular and linear saw machine a) S/T cutting machine b) Gang saw machine [43].

Numbers of factors have effect on the field performances of the diamond tools; the rock types, the cutting depth, load, force, cutting speed, peripheral speed, saw design, diamond and matrix properties. There are several studies about investigation of the relationship between these parameters and field performances of the diamond tools. Ersoy et al.[53] have studied on the cutting function, wear characteristics and properties of the natural stone in order to determine the suitable diamond cutting tools for use in the production of natural stones.According to the results obtained in this study, the optimization of cutting tool's design and operating parameters according to natural stone properties increases the cutting efficiency, increases the tool's lifetime and reduces the cost of marble production.

Kaplan et al. [54] have investigated the effect of Co metal powder to the matrix composition of diamond cutting tools.The effects of diamond grain size on cutting performance were also investigated. As a result of the examinations, it was emphasized that the use of fine-grained diamonds in high hardness stones such as granite, and the use of coarse diamond grains in the production of soft marble class stones. It was stated that the hardness and strength of the cutting segments increased when cobalt powder was added to the matrix consisting of Fe, Cu and Sn elements.

Similarly, Rosa et al.[55] have investigated the effects of tungsten carbide (WC) additive on metal matrix composition of the diamond tools. They added 10 wt % and 20 wt % WC to the matrix structure consisting of Co and bronze elements. It was observed that the added WC increased the mechanical properties of the segments, and high wear rates were detected in the samples without WC.

Yu et al. [56]studied on the concentration of the diamond grains in composites. According to the results of this study, the surface roughness was decreased with increasing diamond concentration.

Das et al.[57]have examined onthe diamond concentrations. According the results of this study, the wear resistance of the samples was increased with increasing diamond consentrations. The sample with high diamond content was created relatively smoother surface.

Che et al. [58] have studied on the Titanium (Ti)-coated diamond particles in Al reinforced matrix. The Ti on the coating surface of the diamonds is observed to react with the Al from the matrix at the beginning of the infiltration process. It was determined that strong chemical bonds were formed between the coated diamonds and the matrix.

Aslantas et al. [59] have studied on circular diamond saw blade used in marble cutting process. During the cutting processes, the axial forces of the saw blade were measured by a dynamometer. According to the field test results, an increase of the traverse speed and depth of cut also increases the axial force on the saw blade.

Bayram and Kulaksiz [60] have examined the gang saw to evaluate of its cutting performances. The carbonate originated metamorphic stones from Turkey were chosen. According to the results of this study, an increase the advance rate were increased stress on the saw blades.

Sun et al. [61] have determined the effect of the rock properties on the wear of the gang saw during the cutting of granite stones. This study have indicated that the principal wear mechanism of the diamond toolsis abrasion and the matrix must wear to improve the self-sharpening ability of the diamonds.

1.2 Purpose of Thesis

The purpose and scope of the thesis can be explained with 3 parts. The first part includes the investigation about Co powders used for producing diamond cutting tools. The physical, mechanical, and microstructure of the spherical grain and rod-like grain shapes Co powders were studied. The grain shapes of the powders were changed due to the production methods. The spherical Co powder were produced using gas atomized process and the rod-like Co powder were produced using

chemical decomposition process. The grain shapes of the powders were conducted using SEM. The crystallite size values were determined using the W-H method. For determining the cold press parameters of the powders, FT4 rheometer analysis was used.So in this study the most appropriateCo powder was determined for production of diamond tools.

At the second part, Fe- based and Co- based matrices of the diamond wires were investigated. The compositions containing Fe in three different ratios were prepared. It was prepared in mixtures using Co metal instead of Fe in the same composition. The grit sizes of the diamonds were 35/40 and 40/50 mesh at the diamond concentrations of 15 and 5 for all samples. Marble and granite stones were used for cutting tests. In this study, the hardness and abrasiveness of the cut stone were taken into consideration while interpreting the metal matrix investigations. It was determined that the hardness and relative wear resistance of Co-based samples were higher than Fe-based samples.It has been observed from the cutting tests, the Fe-based matrix is convenient for cutting marble and the Co-based matrix is convenient for cutting granite.

The last part is about the cutting process of Ankara andesite stone with diamond circular saw blades.The cutting process of this stone is complicated due to the porosities and glassy phases on the structure of the stone.The circular diamond saw blades are used in this study. The main matrix was composed of Co, Ni, Sn, and W elements. Al and Ag were used as metal matrix materials for improving the cutting performances of the circular saw blades. Ag addition was used to improve the mechanical properties of the metal matrix of the diamond segments and Al addition was used high wear resistance under a load. The mechanical properties of the samples are enhanced with the addition of Al and Ag to the metal matrix of the diamond segments.The matrix composition developed in this thesis is used in the production of andesitic and basaltic stones in the in Turkey's Central Anatolian Regionwith ongoing mass production.

2. EFFECT OF PARTICLE MORPHOLOGY ON PHYSICAL, MECHANICAL AND WEAR PROPERTIES OF COBALT METAL POWDERS[1]

2.1 Introduction

Diamond cutting tools are important for machining materials in industrial manufacturing used to process hard and brittle non-metallic materials, rocks, concretes and glasses. A variety of diamond tools are needed including circular, frame and wire saws, and core drilling [53,62]. The diamond-impregnated metal matrix segments are produced with diamond grit embedded in a metal matrix. The diamonds are responsible for the cutting process using a combination of physical and chemical interactions [63]. Determining the metal matrix hardness according to the natural stone leads to self-sharpening diamonds, which results in good wear behaviour [64]. In the selection of the metal matrix, W is frequently used in tools to cut hard materials like concrete. Co and W-Co alloys are used for hard materials like granite. Co-Bronze, Fe-Co, and Fe-Bronze alloys are bonding matrices used to cut moderately hard materials like marble [55,65].

Cobalt has been used in the production of super alloys, magnetic materials, rechargeable alkaline batteries, cemented carbides and diamond cutting tools because of its high density, magnetic property, hardness level, wear resistance, durability at high temperatures and excellent impact resistance property [66,67]. Co plays an important role in diamond cutting tools as a binder because it combines adequate diamond retention and excellent wear resistance during the cutting operation. Co powders improve the mechanical properties of diamond cutting tools [54].

[1]This chapter is based on the paper "Bulut B., Unal F., Baydogan M., Kayali ES., Trans IndianInst Met 2021; 74: 2345-2355. https://doi.org/10.1007/s12666-021-02331-5".

The use of Co as an alloying element for matrices increases the strength, ductility, and impact strength of the alloy. The occurrence of Co provides solid solution strengthening of the binder matrix and strengthens the matrix interface.

The toughness of diamond cutting tools is determined by their Co content [68- 70]. The properties of Co powdersdepend on their size and morphology; therefore improving fabrication methods can enhance the properties of Co powders [71,72]. Currently, Co powders may be prepared using atomization, hydrothermal reduction, ultraviolet irradiation, chemical vapour condensation, electrochemical decomposition and thermal decomposition [73]. The particle size and morphology of the final product depend on the production methods. The shape of the powder affects its compactness, flow properties, and porosity. Therefore, the powder shape determines the strength and mechanical and microstructural properties of the final product. The powder grain shapes are formed based on the production methods presented in Figure 2.1 [74-76].

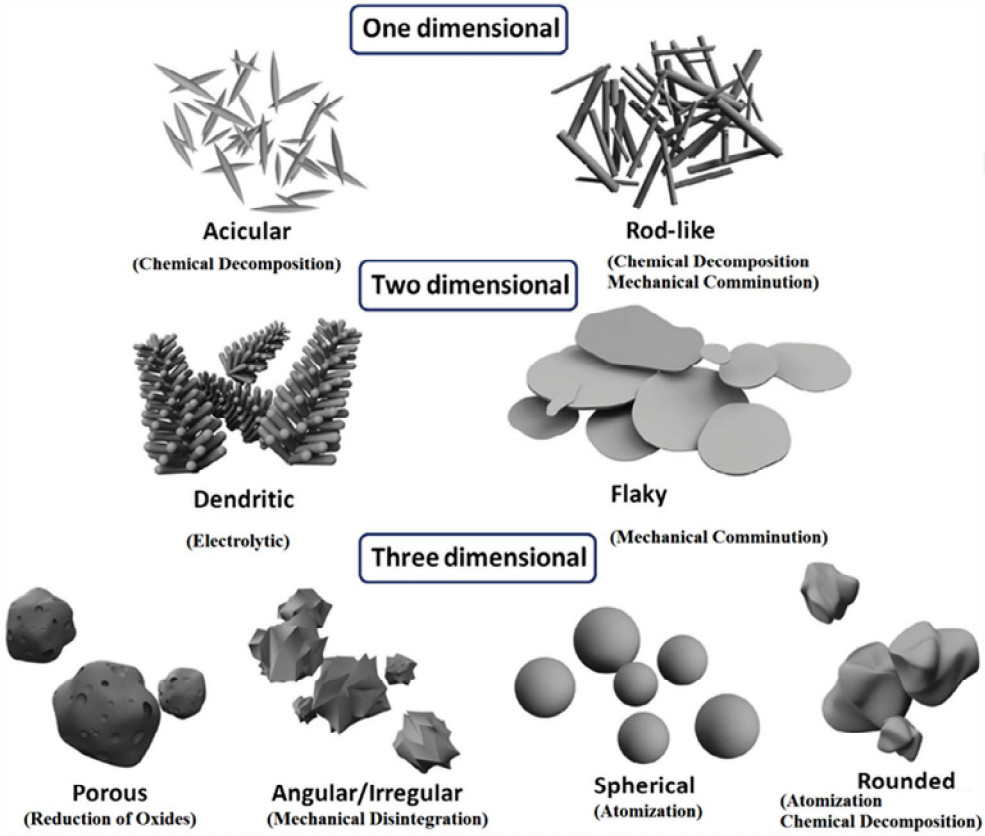

Figure 2.1 : Change of powder grain shapes depending on the production method [75].

The sintering of Co powders and its alloys using the conventional technique requires high dwell time. Different sintering techniques, such as microwave sintering and spark plasma sintering (SPS), have evolved to process the alloys at a faster heating rate [77-79]. The process can be conducted within a few minutes due to the rapid rate of heating, and better mechanical properties are achieved [80,81].

This study aimed to examine the structural and mechanical properties of the two different shapes of Co powders to determine the most suitable Co powder for diamond tools and improve their cutting performance.

2.2 Material and Experimental Methodology

Commercial Co powders with two different grain shapes, spherical and rod-like, were investigated. The powder- producing company (Freeport Cobalt; Finland) stated that the spherical shape (Co-S) (S series at Freeport Cobalt Company) and rod-like shape (Co-R) (R series at Freeport Cobalt Company) powders were produced using the gas atomized and chemical decomposition processes, respectively. The Co powders were treated using the freeze-drying method to obtain ultrafine particles. The ultrafine Co powders were used due to their high uniformity.

The particle size distributions were determined using Malvern Instruments Mastersizer 2000. The morphologies of the particles were investigated using a Zeiss Evo 18 Scanning Electron Microscope (SEM).The specific surface areas of samples were measured using the Brunauer, Emmett and Teller (BET) analysis. For the BET surface area analysis, the low-pressure volumetric gas adsorption measurements were performed at 77.40 °K and maintained using a liquid-nitrogen bath on a Quantachrome Quadrasorb automatic volumetric instrument.

The flow properties of the powders were characterized using a universal powder tester, the FT4 Powder Rheometer (Freeman Technology) to measure the flow energy, aerated flow energy, compressibility and permeability. This test indicates how easily a powder will move from a static condition to a dynamic form. The FT4 powder rheometer consists of a stainless steel blade with a diameter of 48 mm that rotates on a vertical axis as shown in Figure 2.2. The blade rotates and moves up and down through the powder bed, which is contained within a cylindrical vessel that has a diameter and height of 50 and 80 mm, respectively. The blade operates at a tip

speed of 100 mm/s with a -10° helix angle. The torque and axial force required to move the blade through the powder were recorded and used to calculate the total energy. The flow energy, which is calculated from the measured force and torque, represents the flow ability of the powders [82].

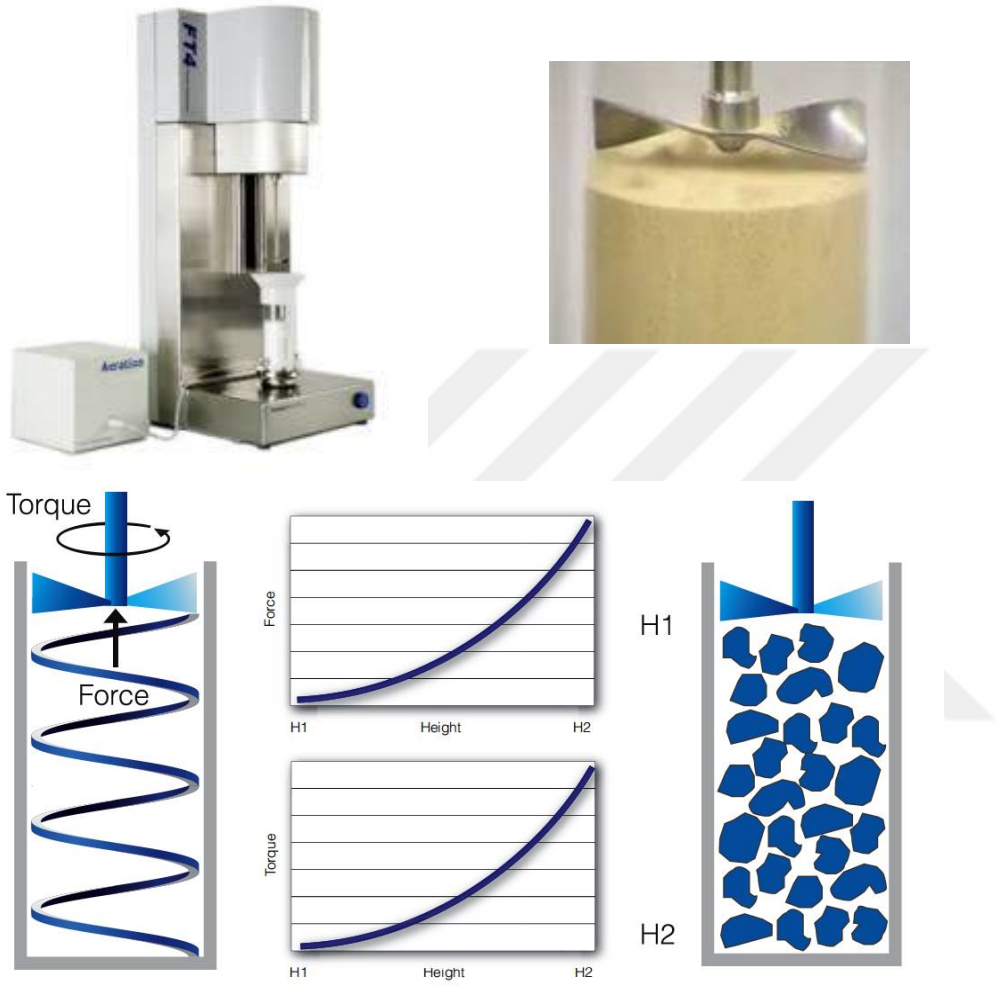

Figure 2.2 : Freeman FT4 Powder Rheometer instrument and operation [83].

After conducting the powder analysis, both powder groups were cold pressed as filled cylinders (7.5 x14 mm) and sintered using SPS at 750 and 800 °C under 115 bars. The microstructural, physical, and mechanical properties of the sintered samples were investigated using SEM-EDS examinations, XRD analysis, density measurements, hardness measurements, compression tests and abrasion wear tests. The X-ray diffraction analysis (XRD) was conducted using Cu Kα radiation to determine the crystalline phases using a Bruker D8-Advanced X-ray diffractometer. The measurements were performed with a 0.02° step size and scan rate of 1 step/min. The range of 2θ was set between 10° and 90°. Based on the XRD patterns, the

crystallite sizes of the powders were calculated using the Williamson–Hall (W-H) method. The instrumental broadening was measured using the standard silica sample XRD data. The line broadening of the diffraction peaks was calculated using Equation 1 [83].

$$\beta_{hkl} = [\beta_{hkl}^{2}{}_{measured} - \beta^{2}{}_{instrumental}]^{1/2} \quad (2.1)$$

The crystallite size values of the powders were calculated using the XRD patterns of the powders based on the W-H method using Equation 2 [83].

$$\beta_{hkl}\cos\theta = (\lambda k / D) + (4\varepsilon\sin\theta) \quad (2.2)$$

The densities of the samples were determined using the Archimedes method. The hardness measurements were conducted using the Shimadzu HMV-2 micro hardness tester using a Vickers indenter with a 300 g load. The compression tests were performed using a Dartec universal testing machine at a crosshead speed of 1 mm/min. Abrasion wear tests were conducted using a Rotary Drum Abrader DVT DA6 model abrasion tester. The samples were vertically installed in the rotary table of the tester which is covered with 80 grade sandpaper. The table was rotated with 40 rpm and 1 kg vertical load was applied on the processed samples. The samples were moved on the table for 20 m. The weights of the samples were measured before and after the wear tests by an electronic balance with an accuracy of 0.1 mg. The relative wear resistance of each sample was calculated as the ratio of the maximum weight loss of that sample to the weight loss of the reference sample. The sample with the highest rate of wear was taken as the reference sample and the relative wear resistance value of this sample was accepted as 1.The wear tests were repeated 5 times using fresh abrasive in each test.

2.3 Results and Discussion

The particle size distributions and the SEM micrographs of the powders are given in Table 2.1 and Figure 2.3, respectively. The Co-S powders had a finer grain size, although the grain size distributions of powders were similar. An examination of the SEM analyses of the powder samples showed that the shapes of the two powders were spherical and rod-like, respectively.

Table 2.1 : The particle size distribution of the Co powders.

Powder Sample	Particle Size Distribution (µm)			
	D10	D50	D90	D95
Co-S	1.0	1.7	3.1	3.5
Co-R	1.1	2.2	4.2	5.0

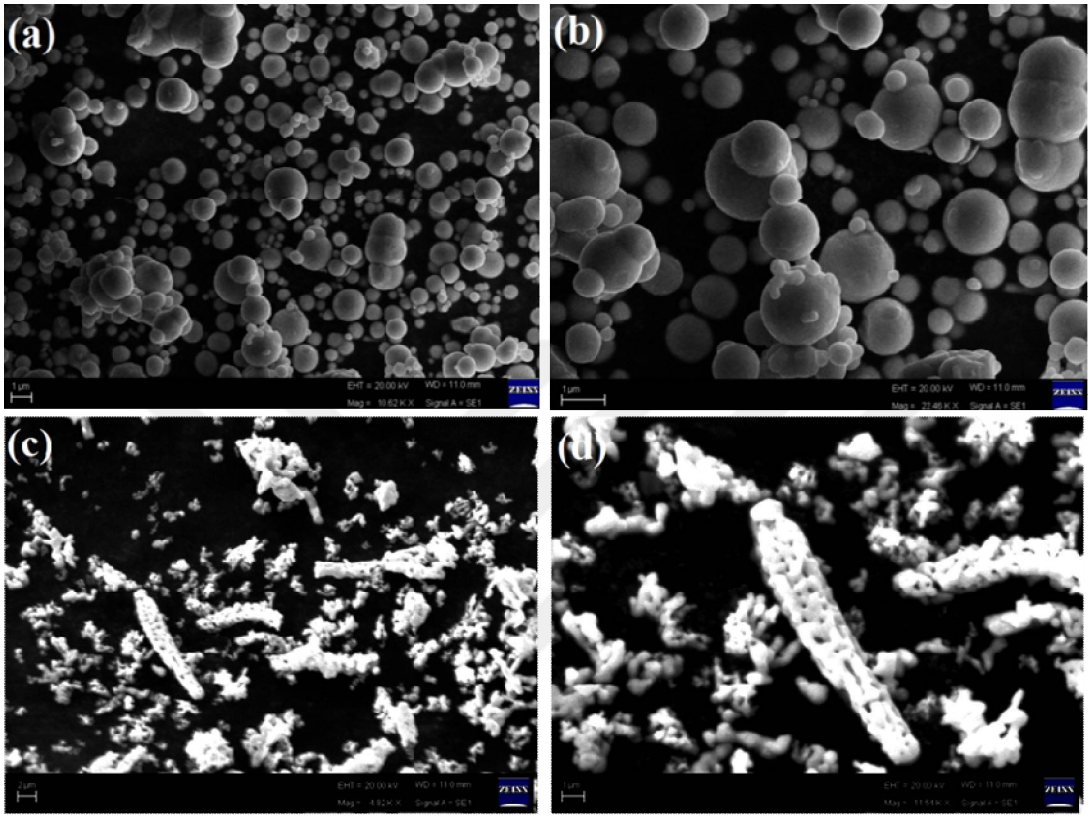

Figure 2.3 : SEM micrographs of powders a-b) Co-S powders c-d) Co-R powders.

Figure 2.4-a and Figure 2.4-b shows the 1.2473 m^2/g and 1.3367 m^2/g BET surface areas of the Co-R and Co-S powders, respectively. The BET surface area of the Co-S powder was larger than that of the Co-R powder.

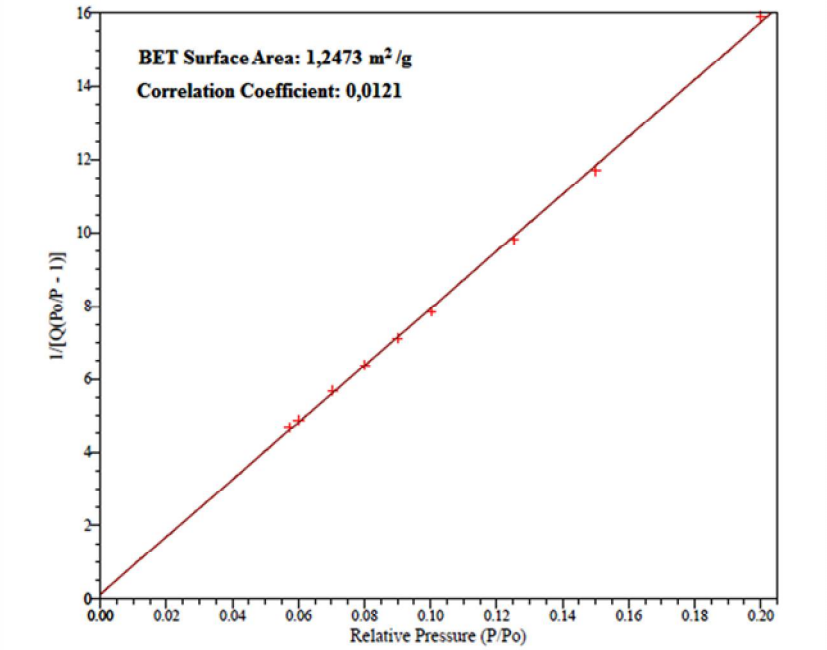

(a)

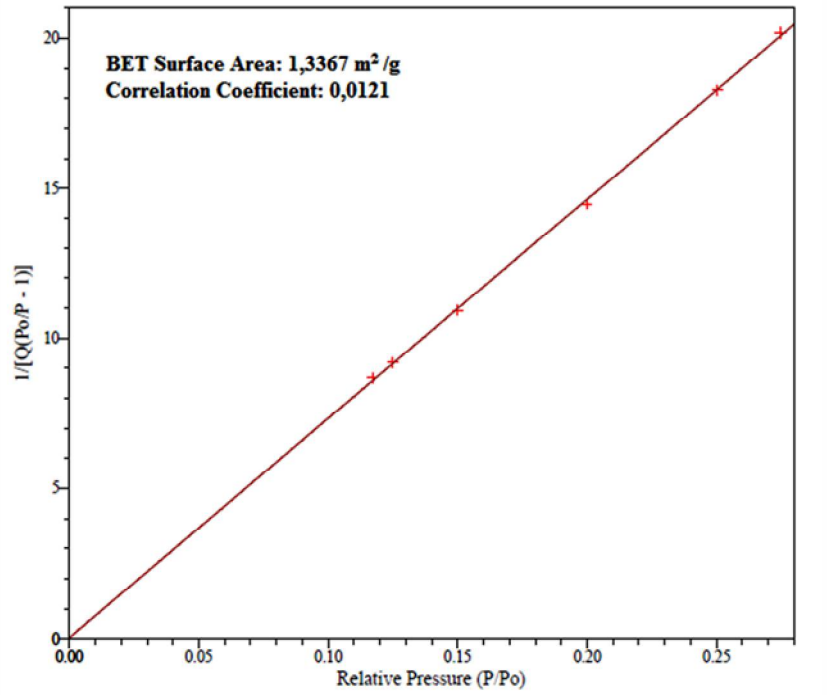

(b)

Figure 2.4 : BET surface area analysis of samples a) Co-R powders b) Co-S powders.

The specific energy, stability index and flow rate index of the Co powders were determined using the FT4 powder rheometer analysis. In addition to these examinations, the powders behaviour was investigated using aeration tests and their permeability and compressibility were determined. The Specific Energy (SE) is a measure of how easily a powder will flow in a gravity-induced flow or low-stress

environment [83]. The SE values of the powders are given in Figure 2.5. According to the results, the Co-R powders generated the highest SE value, indicating increased mechanical interlocking and frictional effects. The SE value of the Co-R powders was 28.8% higher than that of the Co-S powders.

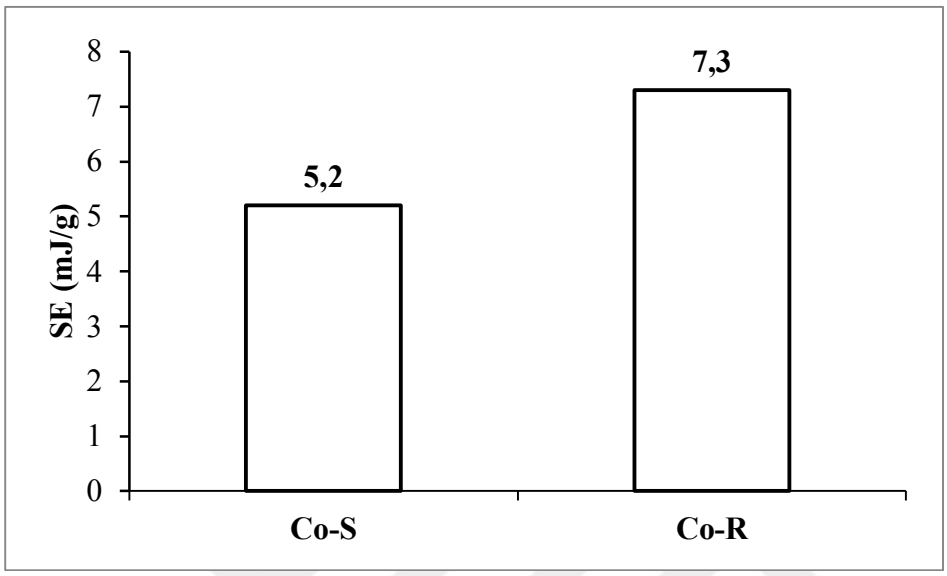

Figure 2.5 : Flow energies of the powders under different conditions.

The flow characteristics of the Co powder samples are summarized in Table 2.2. The Co-S powder was physically stable in the repeated tests with an approximately uniform stability index value. The Co-R powder was more unstable than the Co-S powder in terms of its physical effects. The flow rate index of the Co-R powder (1.0) was more favourable than that of the Co-S powder (2.9); this meant that the Co-R powder was more sensitive to changesin flow rate. The aeration test measurements changed in the flow properties due to the introduction of air into the sample. The aeration ratio of the powders identifies how a powder behaves during mixing, pneumatic conveying and fluidization, providing an indication of the absolute cohesive strength [83,84]. The Co-R powder was significantly more sensitive to the introduction of air and had a higher aeration ratio than the Co-S powder.

Table 2.2 : Primary flow characteristics of the powders determined by FT4 powder rheometer.

Flow characteristics	Co-S	Co-R
Stability index	0.98	1.20
Flow rate index	1.0	2.9
Conditioned bulk density (g/ml)	1.5	1.5
Aeration Ratio, AR10	1.1	2.0
Aerated Energy, AE10 (mJ)	521	87
Pressure Drop, PD15.2 (mBar)	2.2	82

The permeability measures how easily the powder bed will transmit or release air over a range of stress conditions; a higher pressure drop values indicate that the material is less permeable. Permeability is necessary for aerosolization, hopper flow, direct compression, pneumatic transfer and filling applications [85]. Figures 2.6 and 2.7 show the permeability and compressibility of the powders. The compressibility measures the ability of the powder to become compacted when subjected to normal stress. It indicates changes in volume and packing during storage and transport and in processes such as direct compression and roller compaction. The Co-S powder generates the lowest pressure drop and is the more permeable and compressible of the two powders. Based on these results, the Co-S powder will show better performance in the filling operations.

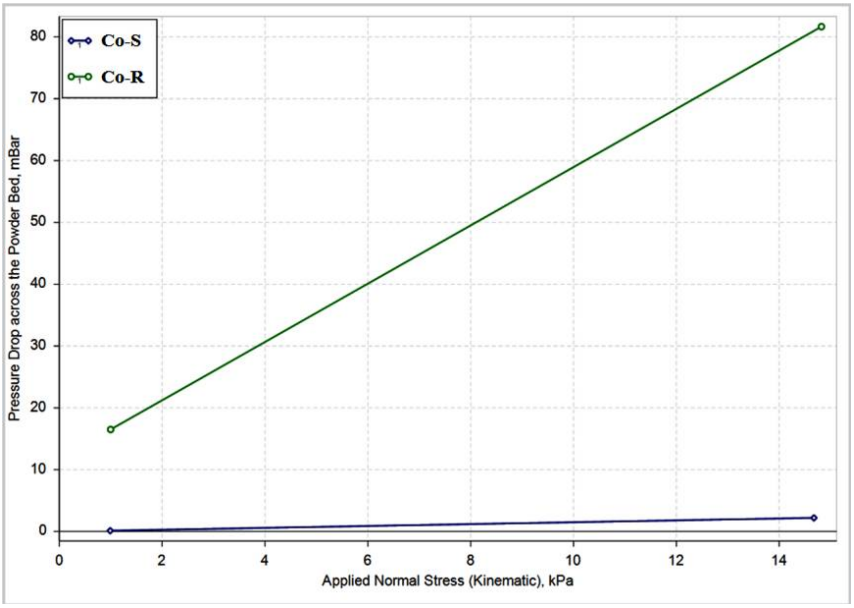

Figure 2.6 : Permeability of the powders as a function of normal stress at constant air velocity.

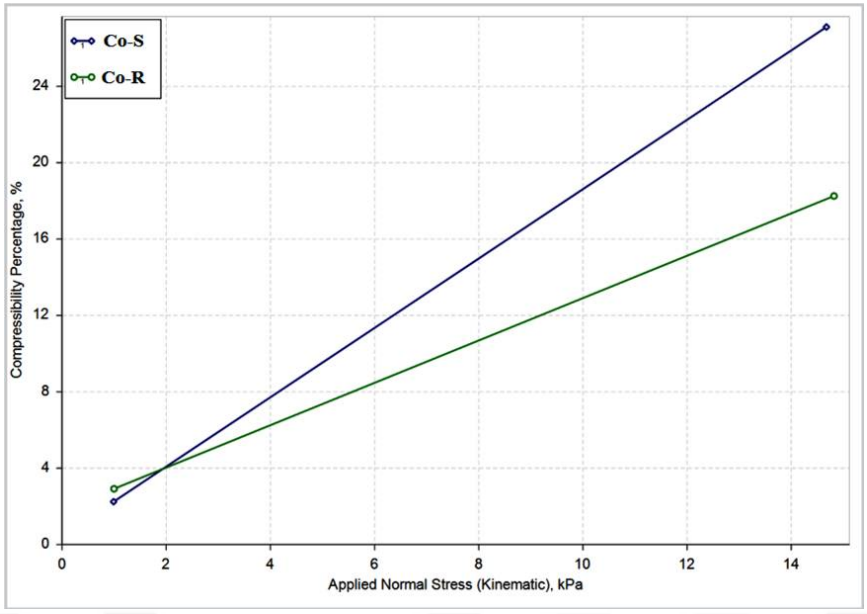

Figure 2.7 : Compressibility of the powders versus normal stress**.**

According to the result of the FT4 powder rheometer analysis, the Co-R powder generated a high Specific Energy (SE) and low permeability. These results indicated that the Co-R had a high degree of mechanical friction and interlocking, and it had a high resistance to air passing through the powder bed. Nan et al. [86] analyzed the effect of the particle shape on the bulk powder flow. They used the FT4 powder rheometer from Freeman Technology to experimentally characterize the particle flow as a function of the shear strain rate, and to predict its dynamics for rod-shaped particles. The polyethylene and glass beads samples were investigated with two kinds of particle shapes: spheres and rods. They found that the particle shape has a strong influence on the bulk powder flow dynamics. Based on the results, the flow energy required for agitating the bed of rod-like particles was much larger than the flow energy required by the spheres, and the flow energy of the rod-like particles was also affected by the microscopic structure of the initial bed. It was suggested that the addition of spherical beads could improve the flowability of the rod-like particles.

Bharadwaj et al. [87] investigated the flow properties of spherical and non-spherical glass beads using FT4 powder rheometer analysis. That study simulated blade resistance to powder flow in FT4 rheometer and showed that the flow energy was sensitive to the particle shape and friction coefficient. Bharadwaj et al. [87] specified that the particle shape could affect the flow ability of the materials. The bulk powder flow of the non-spherical particles was more difficult due to the interlocking of the particles and particle orientation. The perfect spherical glass beads led to a low shear

strength compared to that of the non-spherical beads. Moreover, the non-spherical particles showed decreased flow ability compared to the spherical particles.

Jakub et al. [88] studied the effect of particle shape and size on the compressibility and bulk properties of powders via the FT4 powder rheometer. They investigated Fe, Cu and Al metal powders using two grain shapes: round and irregular. The study indicated that the metal powders with a round grain shape exhibited better flow properties than the irregular particles in mixtures. They also determined that the flow properties of irregular particles increased with the addition of round particles. Fu et al. [89] presented data that quantified the effect of the particle shape and size of three different lactose powders on their respective flow and bulk characteristics. They specified that the particle size and shape have a significant impact on powder compressibility and permeability. The SE value of the spherical powders was 12% lower than that of the irregular powders. The spherical powders generated the lowest pressure drop and were the most permeable ones. The compressibility of the spherical powders was 51% higher than that of the irregular powders. This study stated that an understanding of the correlation between the particle shape and size distribution, and the associated powder flow properties would help improve the design and processes of particles to enhance their performance.

The XRD patterns of the samples sintered at 750 and 800 °C are given in Figure 2.8. The peak obtained corresponded to the Co. The peaks obtained after sintering the Co-S and Co-R had approximately the same intensity. No effect of the powder grain shapes was observed on the phases formed in the structure.

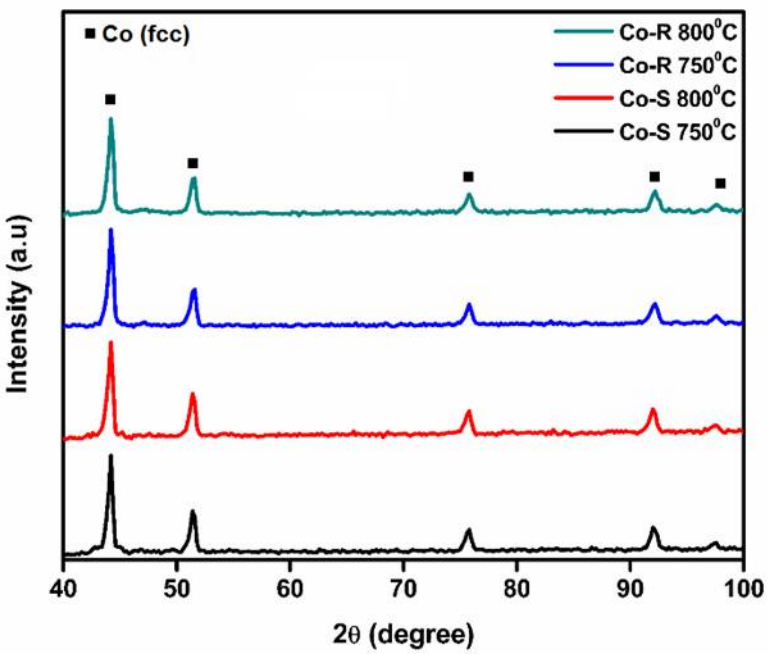

Figure 2.8 : XRD analysis of sintered samples at 750 and 800 °C.

The calculated crystallite size values are given in Table 2.3. The crystallite sizes of the Co-S and Co-R samples sintered at 800° C were 10.31 and 11.43 nm, respectively.

Table 2.3 : The crystallite size values of samples sintered at two different temperatures.

Samples	Sintering Temperature (°C)	Crystallite Size (nm)
Co-S	800	10.31
Co-R	800	11.43

Figure 2.9 (a-d) shows examples of the SEM performed on the sintered samples. When the SEM images of Co-S samples were examined, low rates of porosities were observed in the structure, and the occurrence of porosity decreased with increasing temperature. The Co-R samples showed multiple porosities in the structure. No difference was observed in porosity levels of each sample as the temperature was increased.

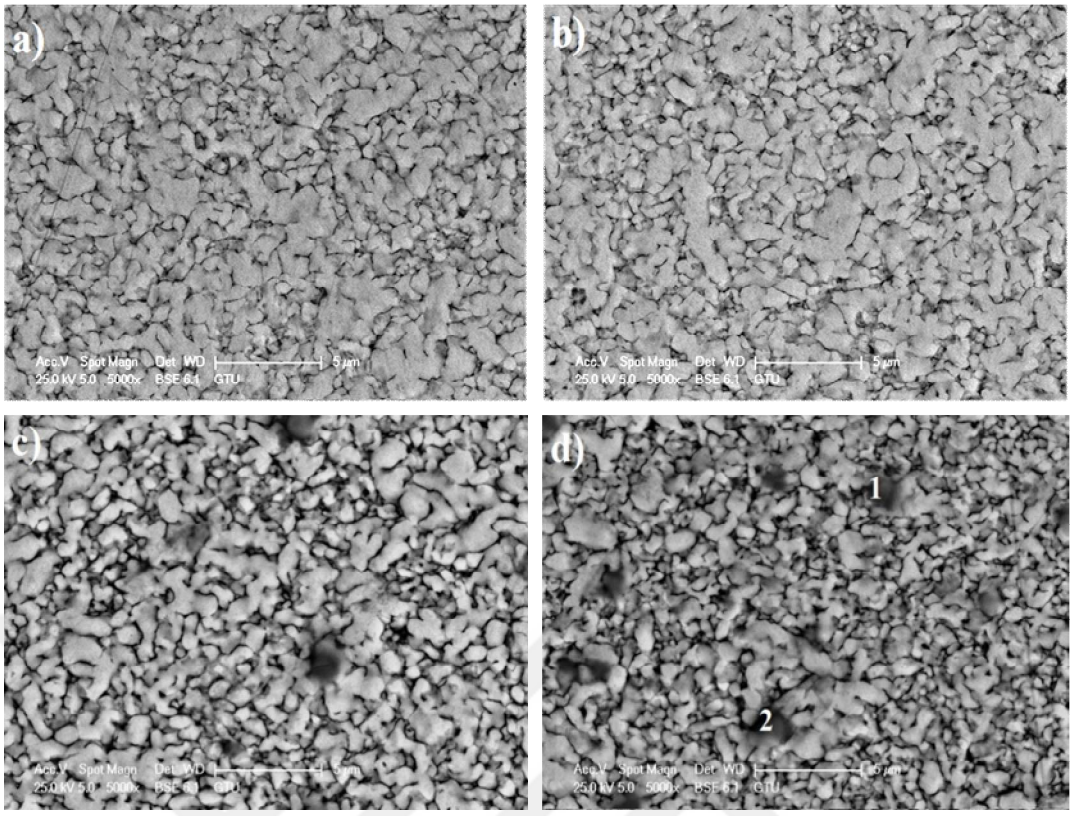

Figure 2.9 : SEM micrographs of a) Co-S at 750 °C b) Co-S at 800 °C c) Co-R at 750 °C d) Co-R at 800 °C.

Table 2.4 and Figure 2.10 summarize the relative density, hardness, compressive strength and relative wear resistance of the sintered samples, respectively. The highest mechanical properties (density, hardness, compressive strength and wear resistance) were obtained in the Co-S samples sintered at 800 °C. The mechanical properties of the Co-S samples were better than those of the Co-R samples at all temperatures.

Table 2.4 : The mechanical properties of the sintered samples.

Sample	Sintering Temperature (°C)	Relative Density (%)	Hardness ($HV_{0.3}$)	Compressive Strength (MPa)
Co-S	750	98.5	340±2.2	324±1.1
Co-S	800	99.1	344±2.9	335±1.4
Co-R	750	97.2	265±2.4	299 ±2.1
Co-R	800	98.0	305±1.5	312±2.7

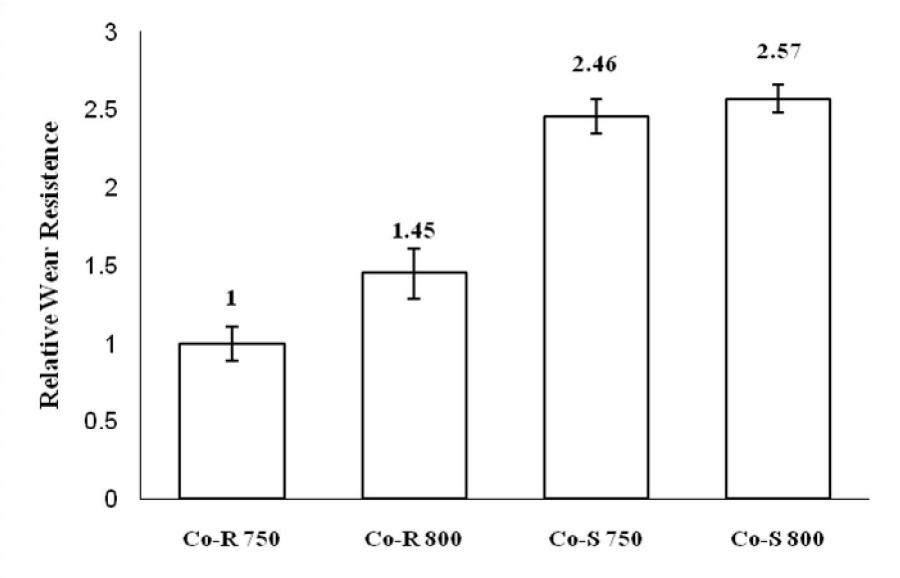

Figure 2.10 : The relative wear resistance values of the sintered samples.

As shown in Figure 2.11a and b, the mechanical properties of the samples increased with increasing sintering temperature. Moreover, the mechanical properties of the samples increased with increasing density and decreasing porosity. The effect of powder grain shapes on the properties of the sintered samples was also observed. The Co-R sintered samples' porosities were 25% higher than those of the Co-S sintered samples. The hardness values and relative wear resistance of the Co-S sintered samples were 11.3% and 43.5% higher than those of the Co-R samples, respectively. The spherical shape of the powder caused an increase in the hardness value of the sintered samples; however, it was mainly the relative wear resistance of the samples that was affected by the grain shape.

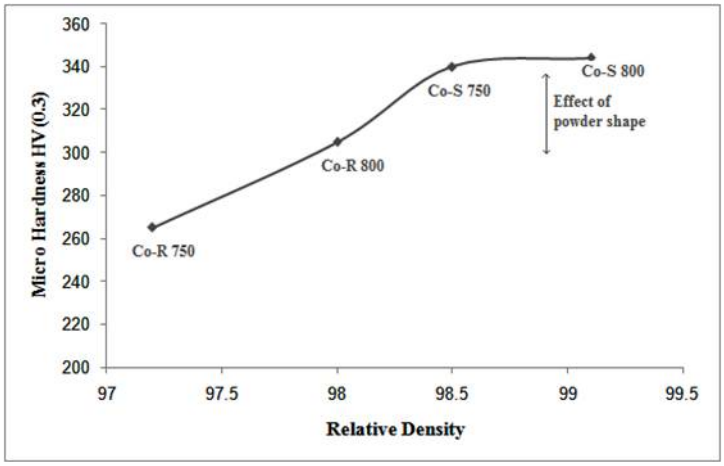

(a)

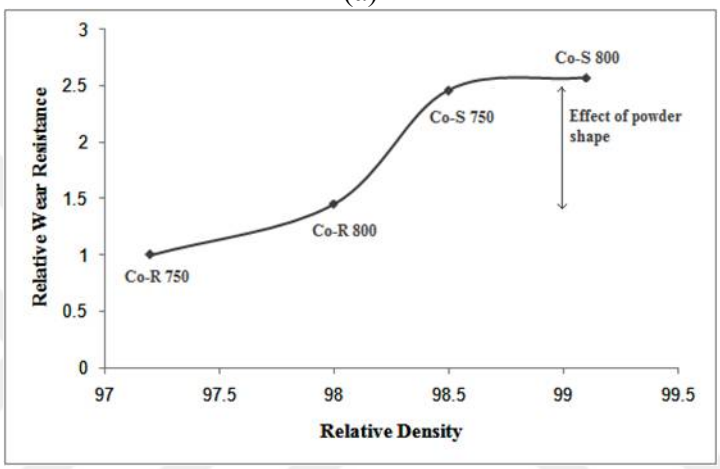

(b)

Figure 2.11 : Effects of density values on hardness and wear resistance values of sintered samples.

The Co-S powders were more permeable and compressible than the Co-R powders, and the Co-R powders were more sensitive to the introduction of air with a higher ratio due to their grain shapes. The Co-R powders had a high degree of mechanical friction and interlocking. Because of these properties, the powders did not completely fill the mould during the cold pressing process. The gaps caused internal porosity and low mechanical properties after sintering.

In a similar study, Danjo et al. [90] examined the influence of the particle shape on the packing density for organic and inorganic powders such as calcium carbonate, crystalline cellulose, and sodium glutamate. They determined an increase in density with increasing sphericity of the particles, and the more spherical particles had less shear strength in their powder bed. Jakub et al. [88] also studied the effect of the particle shape and size on compressibility, in their article about rheometer properties. According to Jakub et al. [88], spherical powders had low porosity, and the irregular

particles of copper and iron had a porosity that was 60% more than that of the equivalent spherical powders. Moreover, the round Al particles showed 46% lower porosity than irregular Al particles. As summarized in this study, the porosity level of the samples decreased with increasing sphericity of the grains. Zhou et al. [91] investigated the effects of grain size and shape on the mechanical properties of nanocrystalline copper using molecular dynamics simulations. In the simulation study, they determined that the spherical and cylindrical grain shape of Cu had an evident effect on the Young's modulus of the samples that depends on the difference of the volume fractions of the grain boundaries. Uddin et al. [92] characterized carbon nanotubes reinforced with Cu and Cu alloy composites to improve the hardness and electrical properties using different sizes and shapes of Cu powders. They used spherical and dendritic Cu powders produced via gas atomization process and the electrolytic decomposition method, respectively. The samples reinforced with spherical Cu powders had higher densities and hardness values than the dendritic-Cu powders. Wu et al. [93] analyzed the how effect of the shape of hydroxyapatite regulated porosity and mechanical properties. They prepared mixtures with rod-shaped (r-HA) and spherical- shaped (s-HA) hydroxyapatite with polyacrylamide. It was found that adding s-HA into r-HA mixture decreased the porosity of the sintered HA and enhanced the compressive strength of the sample. The increase was proportional to the increase of s-HA content. These findings suggested that adding s-HA into r-HA mixtures might provide a new and facile way to improve the compressive strength of porous HA.

The results of this study showed that particle shape significantly affected powder characteristics, including sinter ability, packing density, flow ability and mechanical behaviours. Moreover, the shape of the powder affected the properties of powder metallurgy products. The flow ability of the Co-R and Co-S powders decreased as the particle shape diverged from sphericity. The Co-R powders tended to cause more friction and flow problems than the Co-S powders. The Co-R powders had a strong resistance to flow, despite having low surface friction. The Co-S powders rearranged more easily than the Co-R powders and had lesser mechanical interlocking; thus, they exhibited higher compressibility due to their resistances against the filling up of their internal pores. The mechanical properties of the Co-S powders were better than those of the Co-R powders due to their favourable flow ability, compressibility, and

sinter ability. After the sintering process, there were only small pores in the structure of the Co-S powders that resulted in good mechanical behaviours. In the natural stone cutting process, diamond tools need robust mechanical properties. The hardness and wear resistances of the diamond cutters should be high. Because their high packing densities and low porosities with low oxygen contents, the Co-S powders are preferred in producing diamond cutting tools via SPS.

2.4 Conclusion

The following results can be drawn from this study;

- Even though the grain size distributions of both powder samples were similar, the grain sizes of the Co-S powder were smaller than those of the Co-R powder. Moreover, the BET surface area of the Co-R powder was smaller than that of the Co-S powder. The Co-S powder was finer than the Co-R powder.
- The XRD analysis of the sintered samples showed that the powder grain shape did not effect on the phase structure.
- The Co-R powder generated the highest specific energy, which indicated mechanical interlocking and frictional effect. The Co-S powder was physically stable. The Co-R powder was significantly more sensitive to air with a higher aeration ratio. The Co-S powder generated the lowest pressure drop and was more permeable and compressible than the Co-R powder.
- When the crystallite sizes calculated from the XRD analysis of the sintered samples were compared, at the same temperature the crystallite size of the Co-S powder was smaller than that of the Co-R powder.
- The Co-R powder had porosity after the sintering process based on the SEM analysis of the sintered samples.
- The highest mechanical properties (relative density, compressive strength, hardness and wear resistance) were obtained in the sample Co-S sintered at 800 °C. The mechanical properties of the Co-S samples were better than those of the Co-R samples.
- These results support the use of Co-S powders for the production of diamond cutting tools. Metal matrix mixtures prepared with Co-S powder might have

increased mechanical properties and thus enhanced field performance for the diamond tools.

3. DETERMINATION OF MATRIX COMPOSITION FOR DIAMOND CUTTING TOOLS ACCORDING TO THE HARDNESS AND ABRASIVITY PROPERTIES OF ROCKS TO BE CUT[2]

3.1 Introduction

The Earth's crust is composed of three general types of rocks; oceanic, magmatic and metamorphic. Each rock has distinct characteristics, mineral and chemical compositions, colours, specific gravitics and behaviours [94,95]. The main examples of magmatic and metamorphic rocks are granite and marble, respectively [94]. Granite is a very hard (7-8 Mohs), tough, granular and crystalline igneous rock which mainly consists of quartz, mica and feldspar, while marble is a soft rock having a hardness of 3-4 Mohs [42,96]. The classification of rocks with respect to their hardness is given in Table 3.1.

Table 3.1 : Classification of natural stones according to their hardness [95,42,96].

Natural Stones		
Oceanic Stones	**Metamorphic Stones**	**Magmetic Stones**
Hardness: 3 Mohs 105-130 Vickers **Samples:** Travertine **Location:** Denizli, Bucak Konya (Turkey)	**Hardness:** 3-5 Mohs 105-250 Vickers **Samples:** Marble, Burdur Beige, Bursa Beige, Afyon Rose, Elmalı White **Location:** Burdur, Bursa, Afyon, Antalya (Turkey)	**Hardness:** 7 Mohs Hardness Scale 400-500 Vickers **Samples:** Granite **Location:** Giresun, Aksaray, Bergama (Turkey) Iran, Saudi Arabia, Brazil

[2]This chapter is based on the paper "Bulut B., Gunduz O., Baydogan M., Kayali ES., J. Refract. Met. Hard Mater. 2021; 95: 105466. https://doi.org/10.1016/j.ijrmhm.2020.105466".

Diamond is chemically pure carbon with a diamond cubic crystalline structure and it is the hardest substance known naturally occurring [97]. Diamond has many outstanding properties such as high hardness, great toughness, high thermal conductivity, low friction and high wear resistance [98]. Therefore it is exceptionally suitable for grinding and cutting very hard materials such as hard metals, glass, rocks and concrete [99,100]. Metal matrix reinforced composites produced with imbedded diamond grits in a metal matrix, are widely used in diamond tools fabrication for cutting, grinding, drilling, and polishing processes of rocks [101,102]. Processing of diamond in metal bonds often results in a reaction between the diamond surface and the surrounding metal matrix [55,103]. The extent of this reaction depends upon the specific composition of metal powders, their particle size, particle distribution and processing temperature and time [104].

Performance of diamond cutting tools (DCTs) mostly depends on their diamond-holding ability and wear resistance of the matrix [62,105]. Number of operating conditions including cutting depth, peripheralspeed, load, pressure, velocity, cutting mode, properties of rock, design and working conditions governs the wear rate of DCTs [106].DCTs partly covered and penetrated by strongly adhered rock materials after cutting process. This layer of the rock materials appear very firmly integrated into the surface of the cutting tools as three basic types; partical rock cover, intermixed layer and rock channels. The Cobalt in matrix composition was frequently intermixed with rock materials, forming a new layer with a radically modified binder. The surface filled rock materials act like a wedge and this situation cause a surface crack and lower wear resistance of the DCTs. The design of the DCTs should be developing to avoid rock materials penetration [107]. Beside the all parameters mentioned above, the most important parameter to choose right matrix material by taking into account the properties of rock in the manufacturing process of DCTs. Depending on hardness and abrasivity of the rock, the metal matrix contains the metals or alloys such as cobalt, iron, tin, bronze and tungsten carbide[104,62].

Cobalt (Co) powders and alloys due to their high mechanical properties are more commonly used matrix materials in the cutting process of marbles and granites [101]. Only a few countries produce cobalt powders and this leads to a fluctuation in the Co price. Due to their high cost and limited availability, DCTs manufacturers initiated several research works to find an alternative matrix material having similar service

performances of Co-based matrices. An example of such an alternative matrix material is Co-free, iron (Fe)-based powders. Besides Fe and Co, bronze is added to the composition to fill the pores via liquid phase sintering. Tungsten (W) and other carbide forming elements can also be added in small amounts to prevent grain growth and hence to increase mechanical properties of the matrix material [99]. Tungsten can also be added to form a strong carbide bonding between diamond grit and matrix, which may enhance diamonds service life [100]. Moreover, diamond particles are coated with Ti, Cr, Si, V and W to improve the cutting performance and degradation resistance [42,101].

Sintering method is another issue which determines the properties and performances of DCTs. DCTs can be produced by different production methods such as electroplating, powder metallurgy and brazing [105,106]. Hot Isostatic Pressing (HIP), Spark Plasma Sintering (SPS) and Conventional Sintering (Pressureless sintering) are the widely used techniques by the manufacturers in powder metallurgy based processes [63]. SPS has recently been revealed as an extremely efficient sintering technique for the production of high density and low porosity DCTs. In this technique, the powders are heated to the sintering temperature in a conductive graphite mold at very high heating rates by the action of electric pulses and hold at this temperature under a uniaxial pressure as seen in Figure 3.1. This provides sintering with significantly shorter times at lower temperatures than those used in the conventional methods. In addition, as a more efficient method, it allows a tight control of grain growth during sintering. In these regards, SPS is a short and effective way to produce diamond tools [63,108].

The aim of this study is determination of the suitable matrix composition according to the properties of rocks with the investigation of two different Fe based and Co based metal matrices.

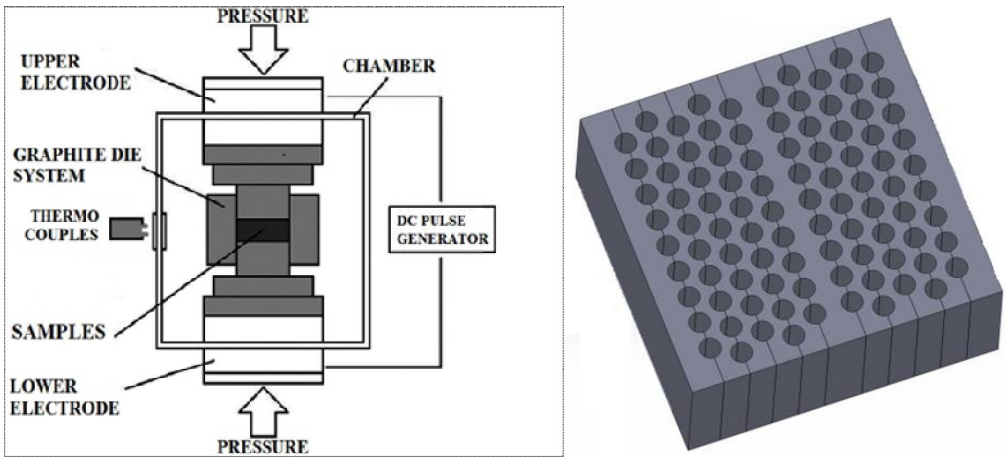

(a) (b)

Figure 3.1 : Process of SPS (a) Schematic view of SPS technique, and (b) Graphite mold.

3.2 Materials and Experimental Methods

3.2.1 Materials

Two different types of powders are comparatively investigated in this study; Fe powders and Co powders. Both powders are spherical in shape, and average particle size of Fe and Co powders are 2.50 μm and 1.5 μm, respectively. Beside Fe or Co, additional elements such as Ni, Cu and Sn were also added in the powder composition. Each powder mixture was designated according to the weight percent of the base metal. Powders were first mixed in a 360° rotating chamber, and then compacted in a cold press and finally the green samples were sintered via SPS method. Chemical compositions of matrixes and sintering parameters are given in Table 3.2.

Table 3.2 : Chemical compositions of the samples.

Reference Name	Chemical Composition (in wt%)					Sintering Temperature (°C)	Pressure (MPa)
	Co	Fe	Ni	Cu	Sn		
Fe30	-	30	10	54	6	900	15
Fe50	-	50	10	36	4	900	15
Fe80	-	80	10	5	5	930	23
Co30	30	-	10	54	6	900	15
Co50	50	-	10	36	4	900	15
Co80	80	-	10	5	5	930	23

3.2.2 Characterization and mechanical tests

Microstructure, physical and mechanical properties of sintered diamond cutting tools (DCTs) were investigated by SEM-EDS examinations, XRD analysis, density measurements, hardness measurements, compression tests and abrasion wear tests.

Microstructures of the samples were examined by a Zeiss Evo 18 Scanning Electron Microscope (SEM) equipped with an EDS (Energy Dispersive Spectroscopy) unit. X-ray diffraction (XRD) analysis was used for quantitative identification of the phases by a Bruker D8-Advanced X-ray diffractometer using Cu Kα radiation. Density of the samples was determined by the Archimedes method. Hardness measurements were carried out by using Shimadzu HMV-2 microhardness tester using Vickers indenter by the application of 300 g load for 15 sec. The compression tests were performed by using cylindrical sample with a diameter of 7.3 mm and a height of 12 mm on a Dartec universal testing machine operating at a crosshead speed of 1 mm/min. Abrasion wear tests were conducted in accordance with ASTM D 5963 standard on a Rotary Drum Abrader DVT DA6 model abrasion tester. The samples were vertically installed in the rotary table of the tester and pressed against 80 grade sandpaper by a normal load of 1 kg. The drum of the tester was rotated with 40 rpm and the samples were moved on the drum for 20 m. The wear path of the sample on the sandpaper was spiral in shape and thus the samples were abraded by a fresh abrasive along the wear path during the test. Weight of the samples were measured before and after the wear tests by an electronic balance with an accuracy of 0.1 mg. Fe-30 sample is taken as the reference. Relative wear resistance of each sample was calculated as the ratio of maximum weight loss of that sample to the reference's weight loss. According to this definition, the relative wear resistance of Fe-30 sample was 1. Wear tests were repeated three times by using fresh abrasive in each test, and the results were averaged and reported with standard deviations. On-site field test were performed by an attempt to cut marble and granite rocks. The cutting wires used in the on-site field tests were 30 meters long and the wires have consisted of 30 cutting segments per meter. The cutting tests were performed by using a block-cutting machine with 15 kW power and operating at 1500 rpm. The cutting fluid was fresh water. The Burdur Beige rock (having a hardness of 3-4 Mohs) was used for marble cutting and the Bergama Kozak rock (having a hardness of 7 Mohs) was used for granite cutting process. The Burdur Beige and Bergama

Kozak rocks have more homogeneous structures and low glassy phase ratio. During the cutting process, more than three cuts were performed on the same rock block and both groups of wires, Fe-based and Co-based, were tested at the same rock regions.

3.3 Results and Discussion

XRD patterns of the investigated samples are given in Figure 2 and 3 for Fe-based and Co-based samples, respectively. The acquired peaks for Fe-based samples are FeNi, $Ni_{17}Sn_3$ and $FeCu_4$. The acquired peaks for Co-based samples are Co, NiCu and $Ni_{17}Sn_3$. When the XRD analysis results of all samples were examined, the multiple peaks were determined at same 2θ due to the lattice parameters of the obtained phases are close to each other and they have the same face centred cubic micro structure. The deconvolution methods were used to separate the various peaks from the total XRD spectrum. The deconvolution of the XRD patterns was performed with Origin Pro software considering the Gaussian function as the shape of the resolved peaks. Also the resolved peaks of the sample are shown in Figure 3.2 and 3.3.

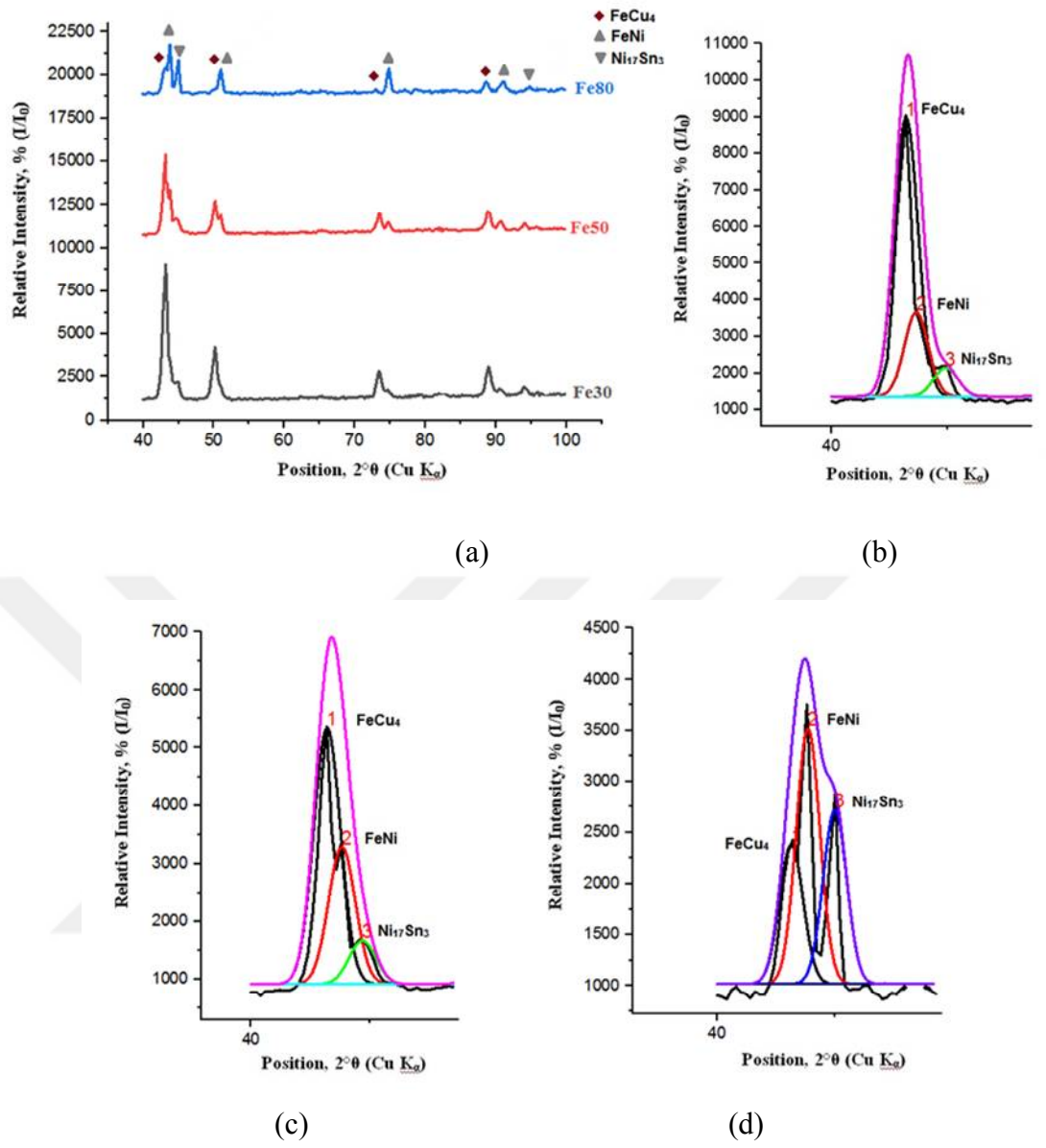

Figure 3.2 : XRD patterns and deconvolutionof XRD pattern of Fe-based samples a) XRD patterns b) Deconvolution of Fe-30 c)Deconvolution of Fe-50 d)Deconvolution of Fe-80.

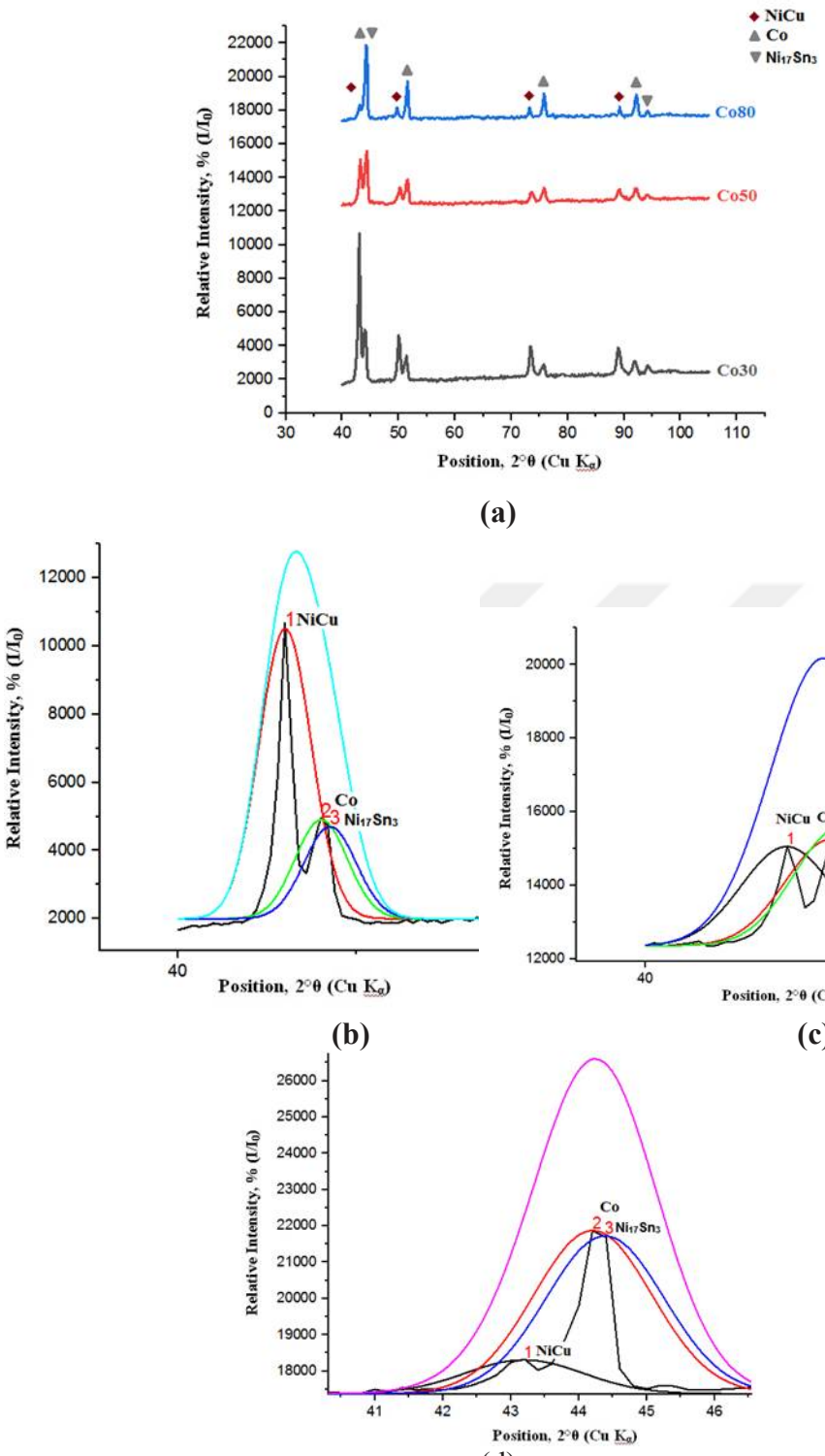

Figure 3.3 : XRD patterns and deconvolutionof XRD pattern of Co-based samples a) XRD patterns b) Deconvolution of Co-30 c)Deconvolution of Co-50 d)Deconvolution of Co-80.

According to the XRD analysis result of Fe-based samples, the relative intensity of the $FeCu_4$ peak is the most remarkable in Fe-30 sample (with the lowest Fe content), and the relative intensity gradually decreased with increasing Fe content. Decreasing

intensity of $FeCu_4$ with increasing Fe content can be clearly attributed to the fact that Fe-80 sample has the lowest Cu content as shown in Table 2. A similar situation applies in the FeNi phase. The intensity of the phase increases with increasing Fe content. The FeNi peak is the most significant in Fe-80 sample. The relative intensities of $Ni_{17}Sn_3$ are similar in Fe-30 and Fe-50 samples; however in Fe-80 samples the relative intensity of this phase is increased. The increasing of the intensity of $Ni_{17}Sn_3$ is not expected because all Fe-based samples contain almost equal amount of Ni and Sn. This suggests that formation of $FeCu_4$ suppress the formation of $Ni_{17}Sn_3$.

According to the results of XRD analysis of Co-based samples, the relative intensities of the NiCu samples decreased with decreasing Cu content. The intensities of the Co peak are the most significant in Co-80 sample. The relative intensities of the $Ni_{17}Sn_3$ are approximately the same values in Co-30 and Co-50 samples and the intensity of the peak increased in Co-80 sample. This situation is due to the suppression of the Cu-containing phase as in Fe-based samples.

Figure 3.4 (a-f) shows SEM micrographs of the samples, Figure 3.5 shows the corresponding EDS patterns of the samples. According to the results of SEM-EDS analysis, the existing islets in the Fe and Co based structures are Cu accumulation as a result of liquid phase sintering. Reductions of Cu accumulation were observed with decrease Cu content.

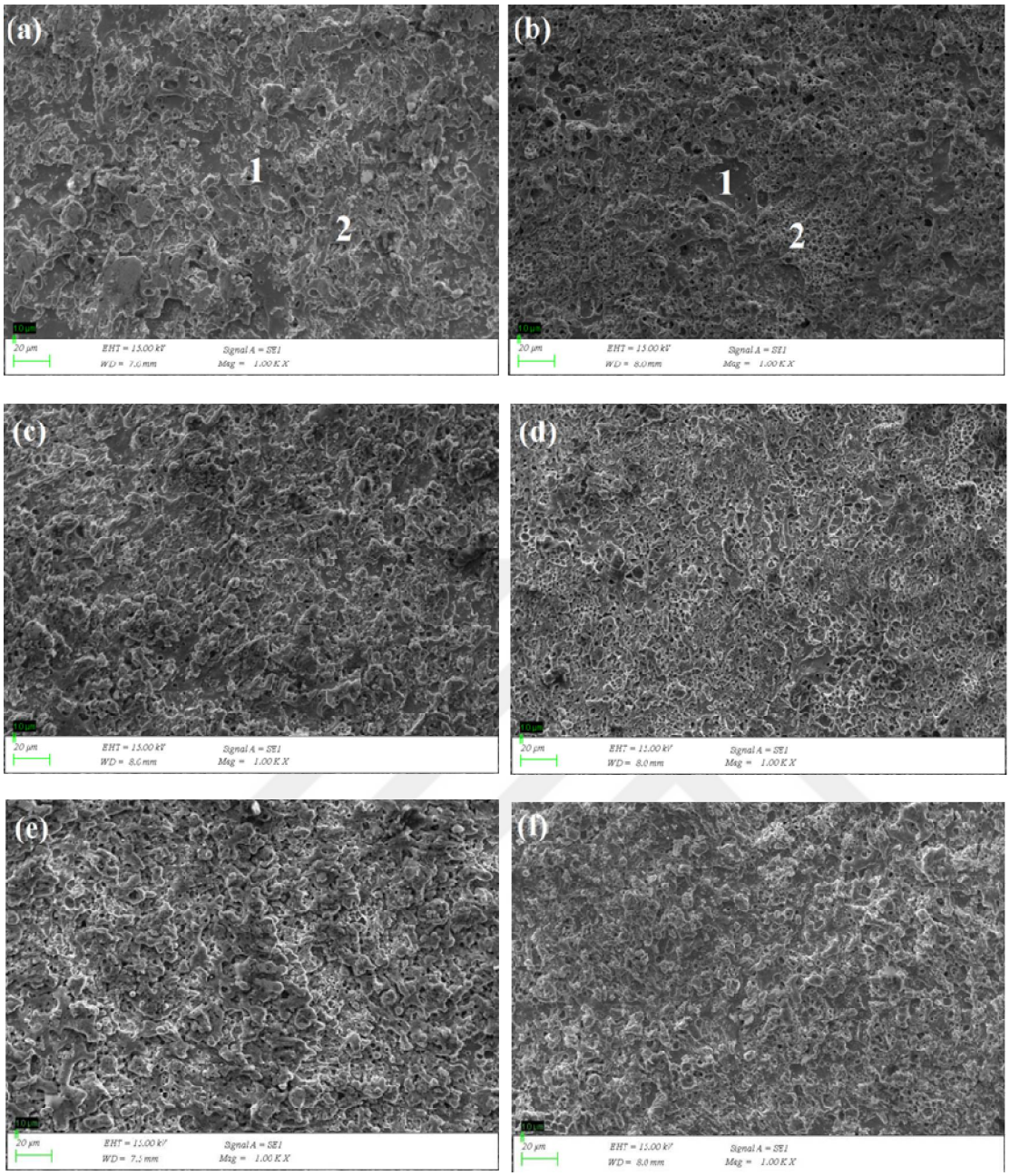

Figure 3.4 : SEM micrographs of (a) Fe30, (b) Co30, (c) Fe50, (d) Co50, (e) Fe80, (f) Co80 samples.

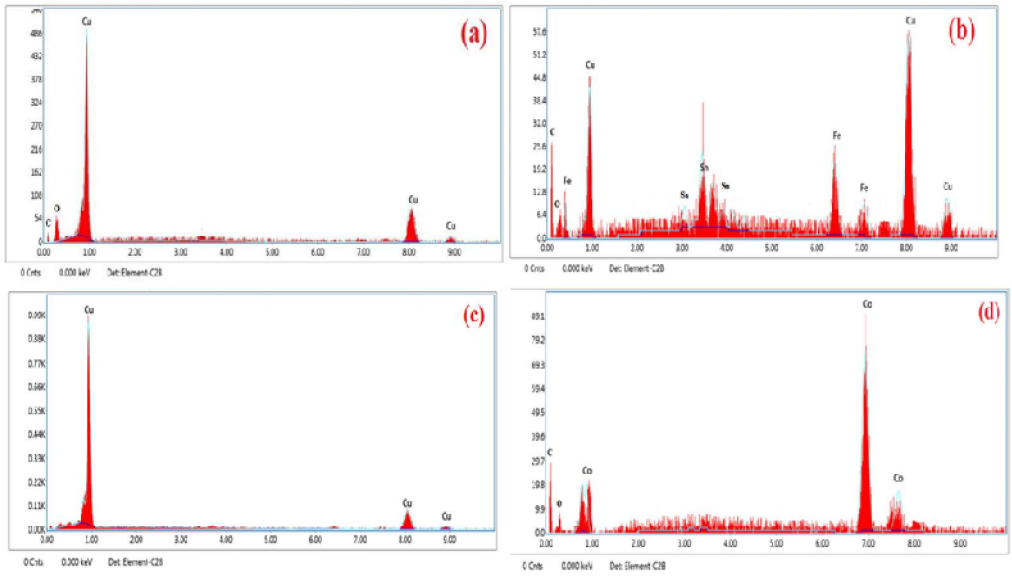

Figure 3.5 : EDS analysis of (a) Fe30-zone 1, (b) Fe30- zone 2, (c) Co 30- zone 1, (d) Co30- zone.

Table 3.3 lists relative density, hardness, yield strength and compressive strength and Figure 3.6 present relative wear resistance of the samples investigated. Figure 3.7 present the effect of copper amounts on hardness and wear resistance properties of the samples. The density values of the samples were close to each other. There was less than 1% difference between the highest value and the lowest value. Although the chemical composition especially Cu element percentage changes, the approximate density values in all samples were related to the sintering method used. The hardness and compression strength were increased with the increasing Fe and Co contents of the samples, parallel to decreasing amount of bronze addition into the powder composition. Increasing amount of bronze addition led to more significant decrement in hardness and compression strength than that observed in the relative wear resistance.

Table 3.3 : The mechanical properties of the samples.

Sample	Relative Density (%)	Hardness ($HV_{0.3}$)	Yield Strength (MPa)	Compressive Strength (MPa)
Fe30	98.9	211±2.2	131±2.3	258±1.1
Fe50	99.1	305±3.1	147 ±2.2	343±1.4
Fe80	98.7	381±2.4	162 ±1.1	365 ±2.1
Co30	99.0	230±1.5	145±1.6	286±2.7
Co50	99.4	318±2.1	156±2.7	359 ±3.2
Co80	99.1	414±1.9	173±1.2	369 ±2.5

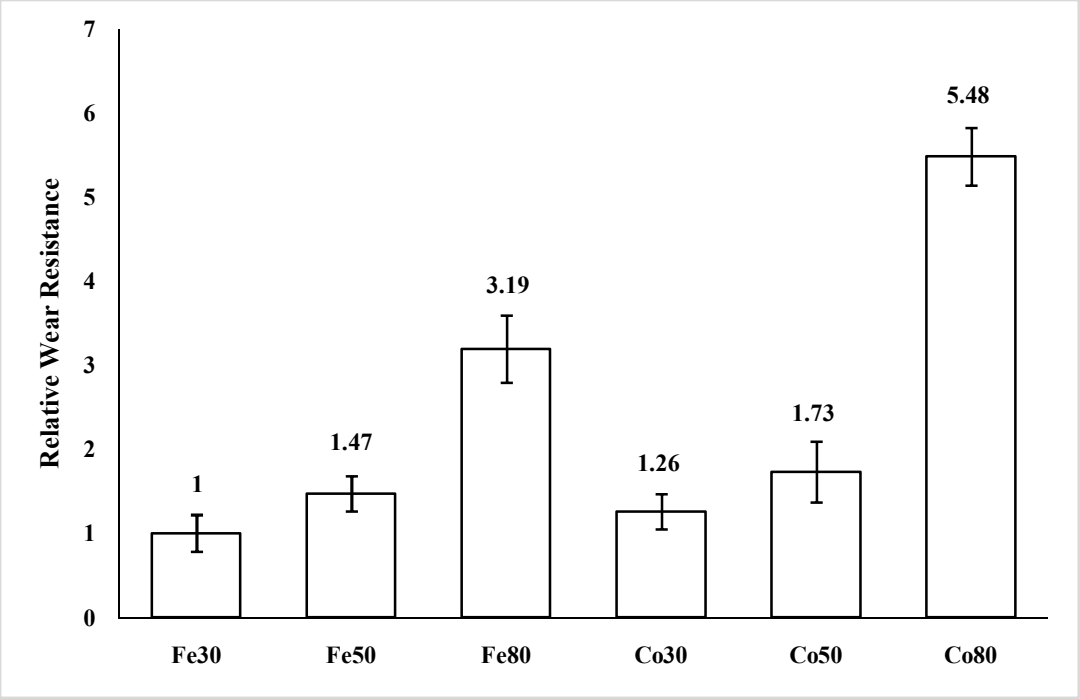

Figure 3.6 : Relative wear resistance of the samples.

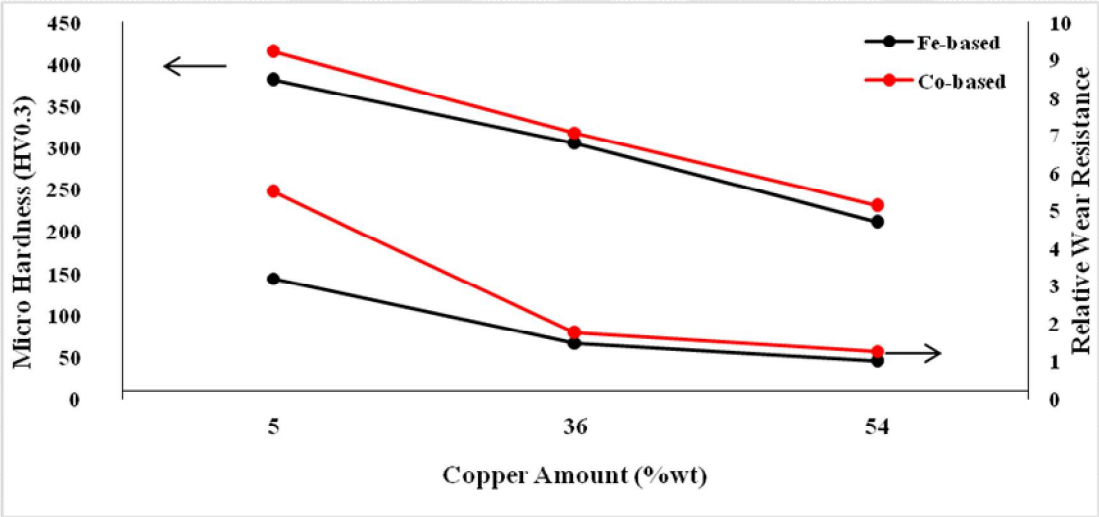

Figure 3.7: The effect of copper amounts on mechanical properties.

Figure 3.8 examine of hardness and wear resistance of the samples according to the percentage of the Fe and Co. It has been observed that the mechanical properties of Co-containing samples are higher than Fe-containing samples. The highest mechanical properties (density, hardness, compressive strength, yield strength and wear resistance) were obtained at Co80 samples. Similarly, Villar et al. [109] have analyzed the Cu-Co-Fe based pre alloyed metal powders for producing diamond cutting tools. They investigated two different Cu based pre-alloyed powders. It was

found that the densities of the samples were increased with increasing Cu content, while the hardness values of the samples were decreased. According to the Oliveira and Filgueira [110], at the Fe-Cu alloys using as a matrix for diamond cutting tools, there was the presence of a liquid phase formed by copper in the first minutes of sintering. Following, liquid copper penetrates in a progressive manner into the boundaries of iron particle were formed a film, promoting a straight contact. Due to the facilitating copper diffusion, the densities of the samples were increased. However the mechanical properties of the samples were decreasing with increasing Cu content.

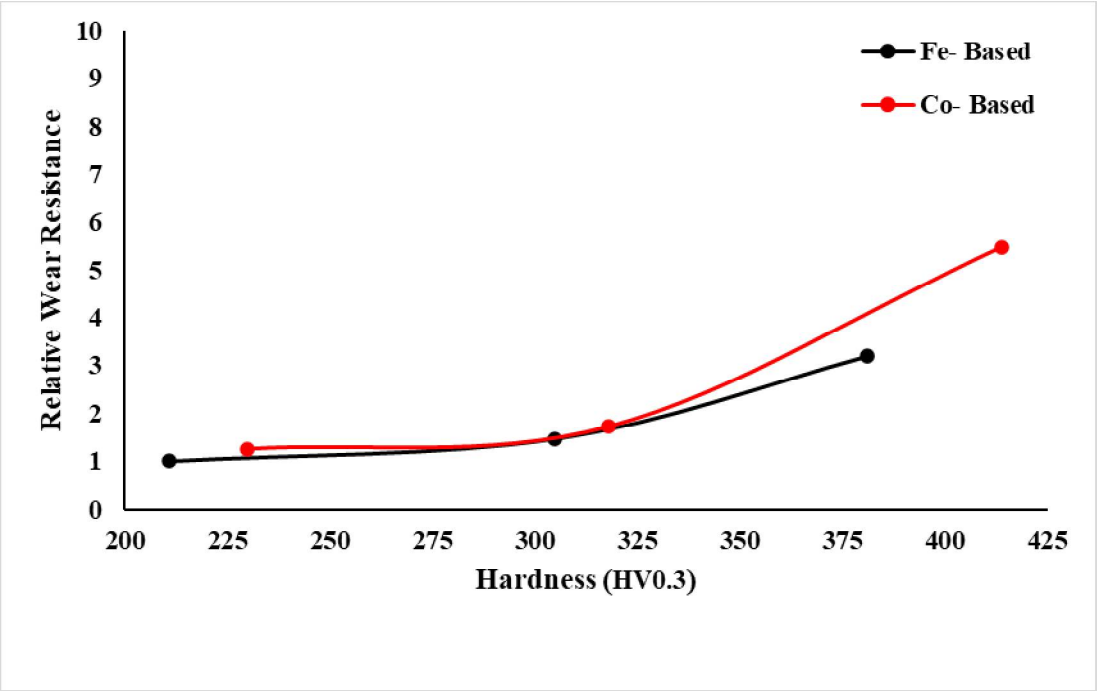

Figure 3.8 : The examination of hardness and relative wear resistance of samples.

In addition to the studies related to diamond cutting tools, there are studies in different fields that examine the effect of Co-Cu-Fe metals on mechanical properties. Xu et al. [111] had prepared and characterized the tungsten-copper alloys by microwave hot pressing sintering. A mixture of Cu and W powders was prepared with different copper content (8 and 20 %wt). This study were explained the increasing of copper content was beneficial for the flow of copper in the matrix and promotes the uniform distribution in the alloy, resulting in improved relative density. According to the ASM Handbook [112], the main effect of cobalt in high-speed tool steel was to increase the hot hardness and thus to increase the cutting efficiency when high tool temperatures were attained during the cutting operation. The

necessity of using deep cuts and fast speeds or of cutting hard and scaly materials justifies the used of cobalt high-speed tool steels. The addition of cobalt in various amounts allows higher hot hardness; the degree of hot hardness was proportional to the cobalt content. Cobalt steels gave better performance on hard, scaly materials that are machined with deep cuts at high speeds more than the non-cobalt types. Cobalt had the effects on other properties of high-speed steels; increased the hardness and the thermal conductivity. Gulyaev et al [113] had investigated the effect of Co addition on the properties of high speed tool steels. As a result of their study, they mentioned that cobalt increase the binding strength and reduces the grain boundary energy. Karaca et al [114] had compared Fe-Mn-Si and Co-Mn-Si superalloys by measuring Vickers hardness. In this study it was found that the hardness values of the samples containing Co were higher than the hardness values of Fe samples at the same Fe and Co contents. Chandrashekar and Prasad [115] had studied the effect of Co on wear behaviour of WC cutting tools for machining of Ti alloys. Three grades of samples were prepared by varying Co percentages (3, 5, 7 %wt). According to the experimental results, the sample's hardness values were decreased by increasing the percentage of Co content. High Co content showed low hardness values. The reason for low hardness values are, as the Co content was increased, the hard phase WC content in matrix was decreased. As the sample's hardness values were decreased, the wear rates were increased due to the high Co content in matrix. Gant et al [116] had studied the wear mechanism of the WC-Co-diamond composites with performing percussive drilling test. In this study, composites with three different cobalt percentages were prepared; 5, 10, 13% wt. As a result of the examinations, it was observed that the hardness and fracture toughness of the samples decreased with the increasing Co ratio in the WC-Co metal matrix. When the wear behaviour was examined, it was determined that the highest wear percentage was in the samples with 13% wt Co additive.

Figure 3.9 present the SEM images of the worn surface of all samples. The wear grooves characteristic of abrasive wear is typical of the worn surfaces of the all samples. The majority of the surfaces are smooth and a few small pits are clearly observed for all samples except Fe-80. The worn surface of the Fe-80 has been deteriorated after wear tests. This change in the wear surface of the Fe-80 sample is a sign that it may cause diamond loss during field testing. When the SEM images were

examined comparatively, it was found that the wear marks were narrow and shallow in the samples with high abrasion resistance, whereas those with low abrasion resistance were found to be large and deep. The results of the study are similar to the studies in the literature [117].

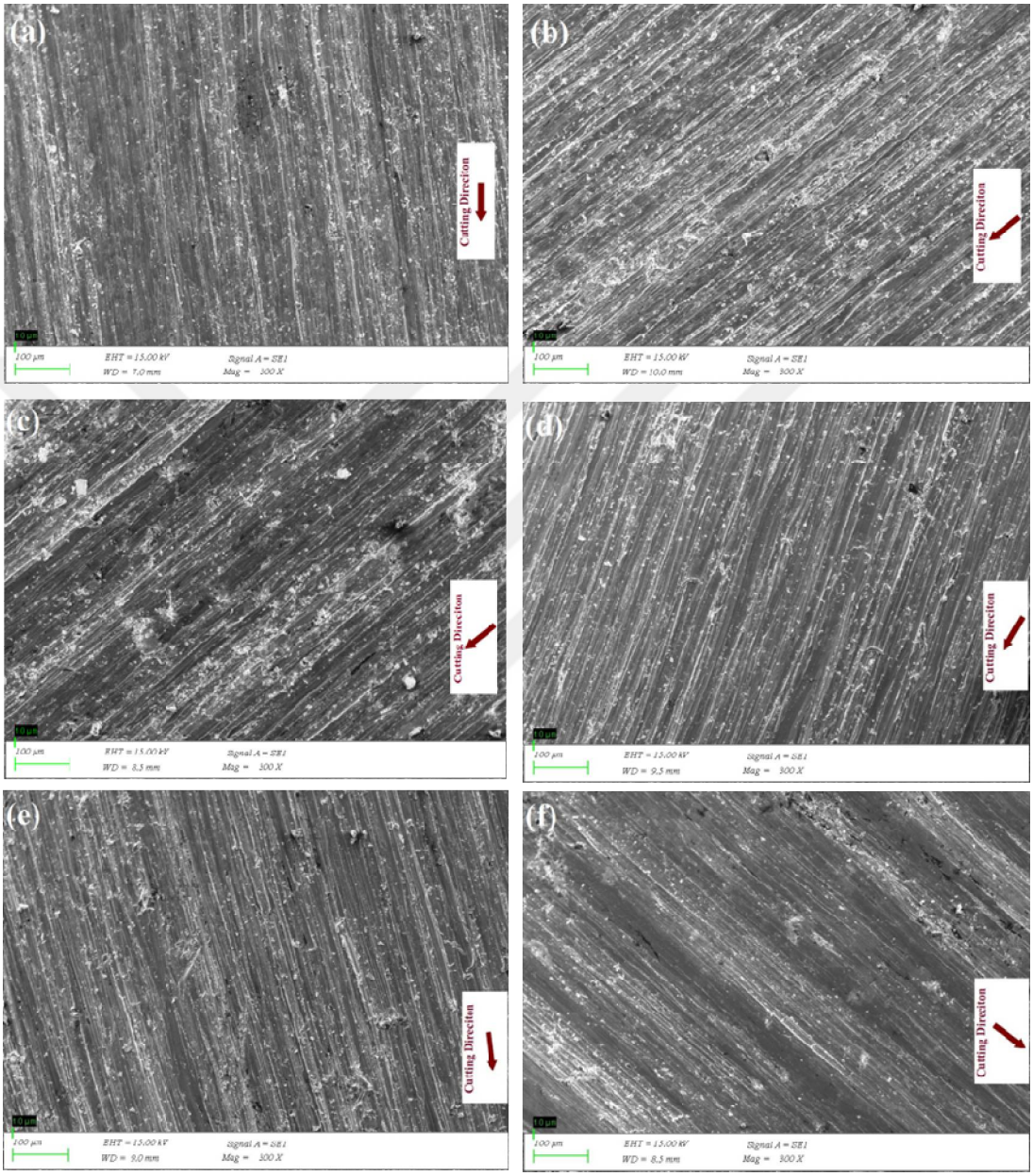

Figure 3.9 : Worn surface SEM micrographs of (a) Fe30, (b) Fe50, (c) Fe80, (d) Co30, (e) Co50, (f) Co80 samples.

Figure 3.10 shows an overview of the diamond bead and cutting wire processed in this work. The working principle of diamond wire; the diamond wire which is passed through two holes which are opened vertically and horizontally on the surfaces to be cut is passed through the flywheel (drum) of the machine and it is the joining of the

two ends and cutting the rock by the motor with the movement of the flywheel. The tensioning force that provides the cutting operation is ensured by the backward movement of the diamond wire cutter on a rail. The visuals from the fields of the diamond wire cutting method given in Figure 3.11. In order to evaluate the cutting performance of diamond beads produced by using the matrix materials studied in this work, matrix mechanical properties were investigated and appropriate stones were determined for field tests. As a result of the investigations, marble cutting with Fe-30, Fe-50, Co-30 and Co-50 content products were appropriate, and granite cutting with Fe-80 and Co-80 samples was appropriate due to their high hardness. The visuals of the stones are present in Figure 3.12. As a result of field tests, determined cutting speeds of the products are given in Figure 3.13 and after cutting processes the SEM images of diamonds of each composition are given in Figure 3.14 and 3.15.

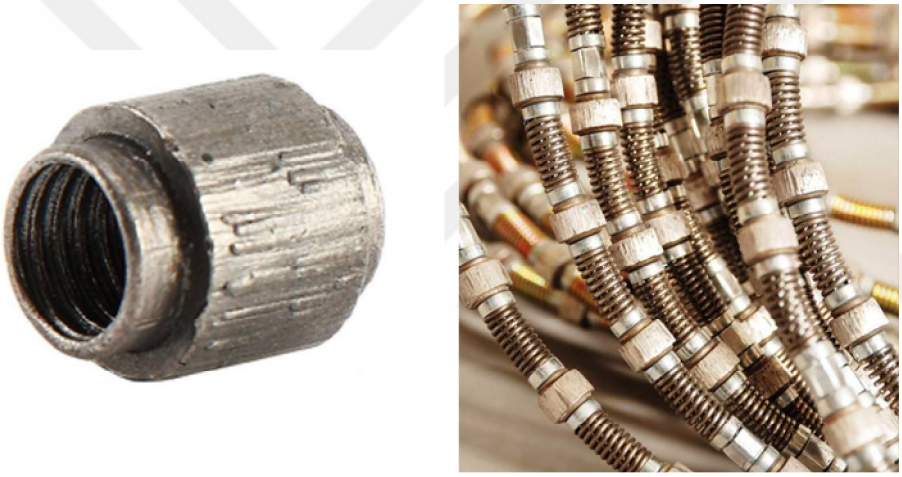

(a) (b)

Figure 3.10 : Overview of products used in on-site field tests; (a) Diamond bead, (b) Diamond cutting wire.

(a) (b)

Figure 3.11 : (a) The visuals from the fields and (b) Diamond wire cutting method.

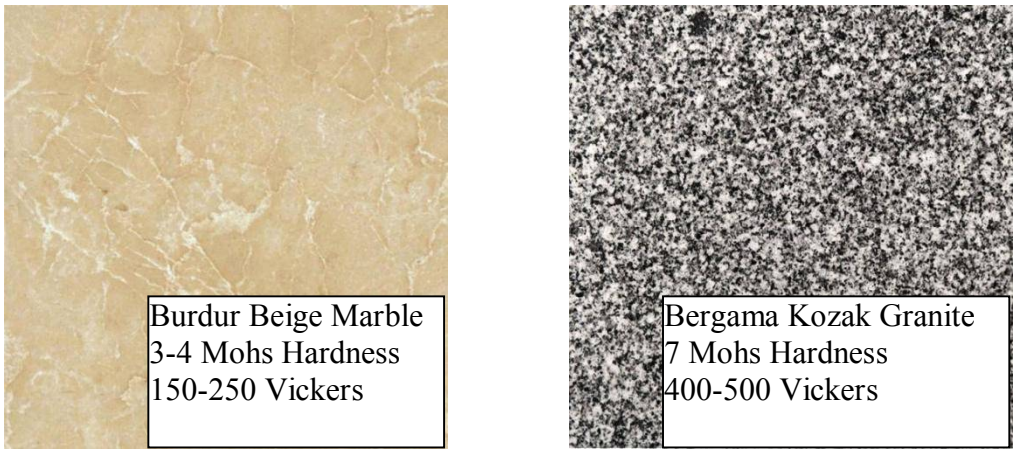

(a) (b)

Figure 3.12 : Surface appearance and hardness of (a) Burdur Beige Marble and (b) Bergama Kozak Granite.

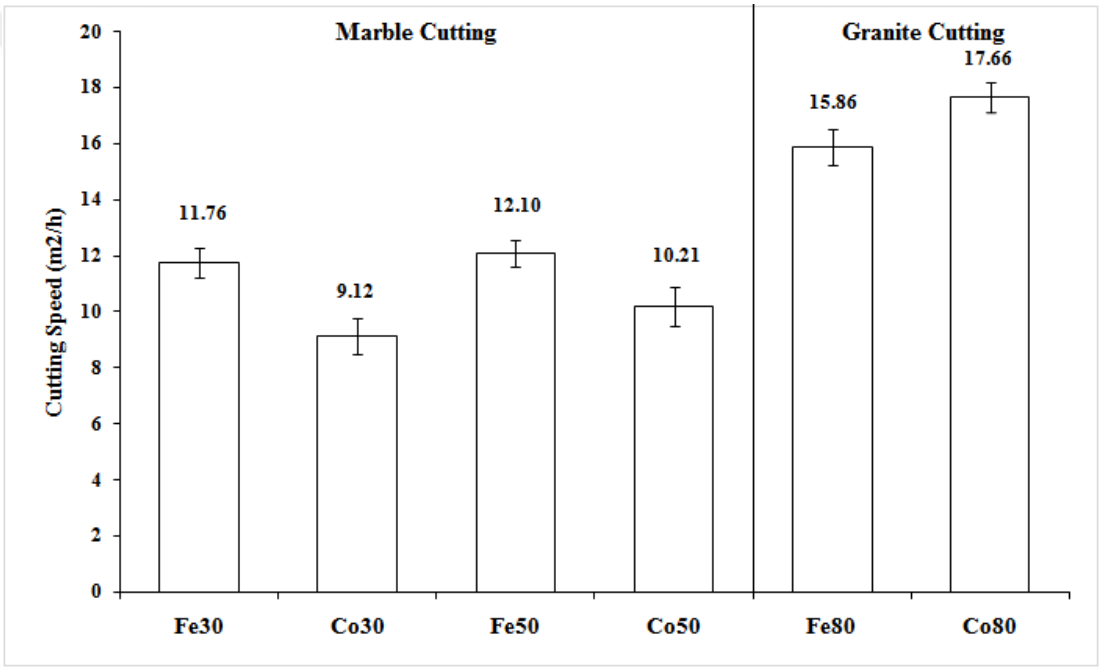

Figure 3.13 : The cutting speeds of the compositions.

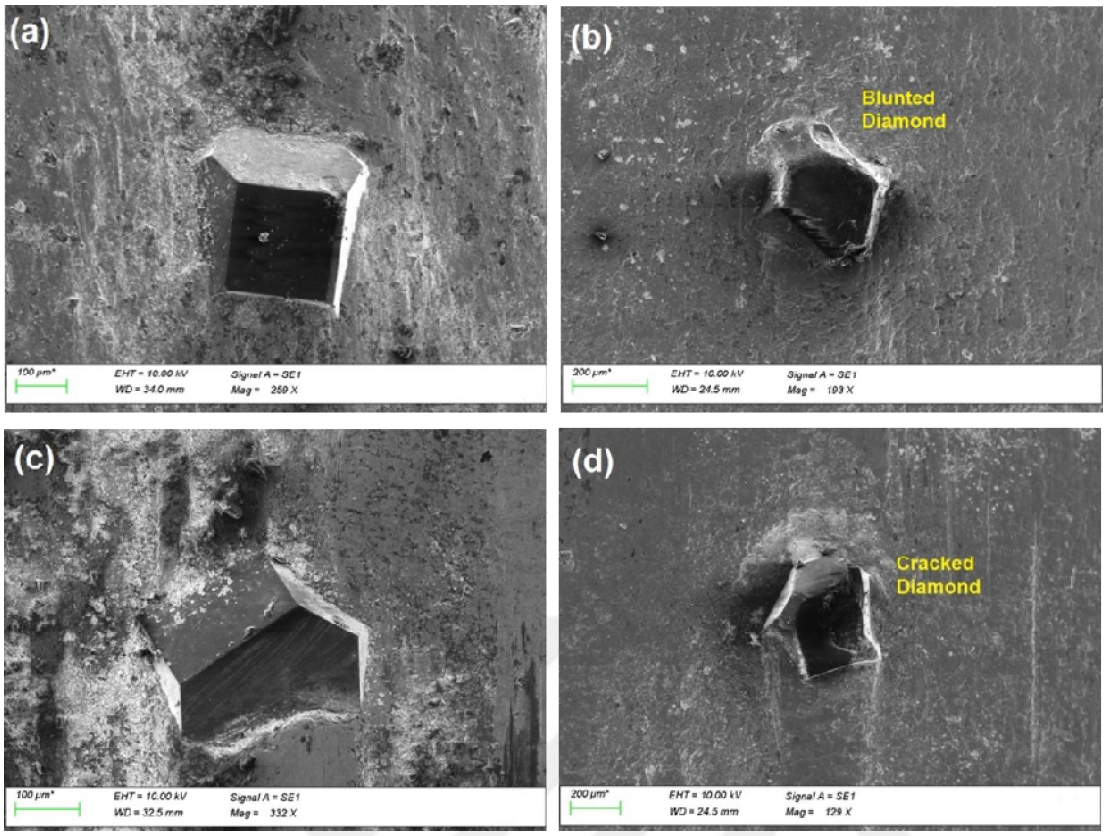

Figure 3.14 : The SEM images of the diamonds after marble cutting process (a) Fe30, (b) Co30, (c) Fe50 and (d) Co50 samples.

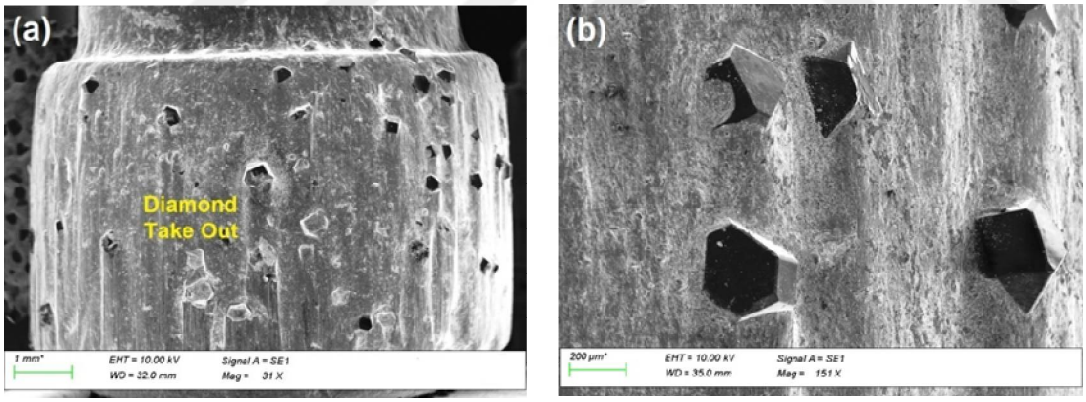

Figure 3.15 : The SEM images of the diamonds after granite cutting process (a) Fe80 and (b) Co80 samples.

When the marble cutting references are investigated; Diamonds of Fe-30 and Fe-50 references were not detected blunting and fracture. They have sharpened corners. According to the investigation of Co-30 and Co-50 references, it was observed that diamonds were blunted in Co30 samples and diamonds were broken in Co-50 samples. Since the mechanical properties of the Co-30 and Co-50 references were higher than the hardness of the marble, the diamonds completing the cutting task did not leave the matrix. Parallel to this, new diamonds were not able to start cutting. In

the field tests, the decrease in the cutting speeds of the Co-30 and Co-50 references in the marble group is due to the inadequacy of the wear of the matrixes. According to the investigation of Fe-80 and Co-80 references for granite cutting, intense spills of diamonds were determined at the Fe-80 reference. As other diamonds in the same structure were not blunted or breakage, it was found that diamonds abandoned the structure without completing cutting tasks. Because the mechanical properties of the Fe-80 references are low compared to the characteristics of the granite stone, the diamonds that can make the cuts had leaved from the matrix and the cutting speed has remained low. One of the reasons for obtaining good results with Co-80 samples in granite cutting is the increase in the mechanical properties of the structure with increasing hard phase amount. Another reason is that the high amount of Co metal in the structure gives thermal resistance to the matrix. In the production of granite stone, the matrix becomes warm during cutting and the matrices with low thermal resistance may lose their mechanical properties. In samples containing a high proportion of Co, Co metal increases thermal resistance while at the same time increasing the hardness and abrasion resistance of the high temperature matrix [23]. Therefore, Co-80 samples are determined to be the most suitable matrix mixture for granite stone cutting because they have high mechanical properties and they do not lose these properties at high temperature.

The optimization of wear rates of diamond and the matrix in a diamond containing cutting tool is necessary for a better cutting performances. Therefore the Fe-based matrix suitable for cutting marble and the Co-based matrix suitable for granite cutting operations according to the hardness level of stones.

3.4 Conclusion

Following results can be drawn from the present study;

1) The highest mechanical properties (relative density, compressive strength, hardness and wear resistance) are obtained in the sample Co-80.
2) The mechanical properties of Co-based samples are higher than Fe-based samples.

3) The intensities of Cu and Sn based phases are decreased with increasing Fe and Co percentage. And with decreasing Cu content, reduction of Cu accumulation were observed in SEM images.
4) According to the results of field tests, the cutting speed of Fe-30 and Fe-50 samples are higher than Co-30 and Co-50 samples for marble stone production. The cutting speed of Co-80 is higher than Fe-80 samples for granite production.
5) According to the hardness level of stones and wear resistance of matrixes, the Fe-based matrixes suitable for marble cutting and the Co- based matrix is suitable for granite cutting.

4. EFFECT OF ALUMINIUM AND SILVER ADDITION ON THE WEAR CHARACTERISTICS OF CIRCULAR DIAMOND SAW BLADES FOR CUTTING ANKARA ANDESITE ROCKS[3]

4.1 Introduction

Rocks are classified into various categories depending on their physical and mechanical properties and are broadly divided into three groups of igneous (volcanic), sedimentary, and metamorphic rocks [3,2]. Igneous rocks are formed from magma in the Earth's mantle. When the magma in the deep crust overflows through fractures or erupts onto the surface, it rapidly condenses in the air and crystallizes to form igneous rocks. Common igneous rock types include rhyolite, andesite and basalt [2,118,119]. Andesite has a compact structure and different colours such as bluish-grey, pink, reddish-brown, and blackish violet from light to dark. These differences are due to variations in the minerals amount, chemical composition, and locations [15]. Andesite has a porphyritic texture with plagioclase and quartz phenocrysts embedded within a microlite matrix. Due to the plagioclase crystals and ferric minerals, andesite has a bright appearance and is mostly used in the decoration of exterior surfaces and public areas as tourist sites, foundations, building walls, park and gardens, and in the restoration of historical buildings, mosques and minarets [15,120,121].

Ankara andesite is igneous rocks common in Central Anatolia in Turkey. The most common of these that form certain communities are the Early Neogene aged Kizilcahamam or Galatya volcanic [122,123]. In addition, there are erupted rocks in the form of pyroclastic and lava flows in the basaltic, andesitic and rhyolitic composition between Ankara-Haymana, around the Ballikuyumcu village between Ankara and Polatli (Golbasi, Bala, Elmadag) [124]. These rocks are rather representative of the volcanic outlets of the Early and Middle Miocene age that are

[3]This chapter is based on the paper "Bulut B., Baydogan M., Kayali ES., Wear 2021; 474-475: 203867. https://doi.org/10.1016/j.wear.2021.203867".

covered by sediments in the Late Miocene and Pliocene period, rather than being part of a particular volcanic system [125]. Ankara andesite rocks have a porous structure.They are generally composed of small crystals with some specimens containing a significant amount of glass and some specimens displaying vesicular and amygdaloidal texture. Ankara andesite is highly abrasive due to its chemical composition and structure. The cutting process of this andesite rock is complicated because while andesite is hard and abrasive it also has a high porosity [23,126].

Segmented circular diamond saw blades are the predominantly used tools in the sawing process of hard rock such as andesite [62]. Circular saw blades consist of two major components, namely the diamond segment and the steel core. The diamond segment is a composite material composed of diamond particles dispersed in a metal matrix [62,55]. The size of the diamond particles range from 120 Mesh (125 μm) to 18 Mesh (1000 μm). The metal matrix materials initially consist of ultra fine powder particles (with size up to 4 μm). Typical materials include Co, Fe, W, Ni, Cu, Sn, and bronze [97]. It is very important to know the properties of rocks and their distribution in the quarry prior to determining the composition of the matrix of the circular diamond saw blade. The matrices of the segments have two basic functions of holding the diamond and eroding at a rate compatible with the diamond loss [102]. To produce the segments, first, diamond grits and metal powders are mixed. The prepared mixtures are pressed and sintered using different methods such as pressureless sintering, spark plasma sintering (SPS) , and microwave sintering [63,110]. After production is completed, the segments are mounted on the steel body by a brazing process. The saw blade rotates around the blade centre at a certain angular speed and cuts the rocks at a constant traverse rate. The diamond particles on the segment cut by scratching and cracking the stone surface [27,127]. The saws are successfully used in rock cutting because they cut rapidly, are flexible, and are easy to operate with a good accuracy on the cutting surface [28]. The sawing performance and life of a circular saw blade is affected by many factors with the diamond and matrix properties (diamond type, diamond concentration, grit size, hardness of the metal bond), sawing conditions (peripheral speed, cutting depth), and physic-mechanical and mineralogical properties of the stone to be cut as some of the most important factors [28,53]. Ucun et al. [128] investigated the effect of matrix materials on the cutting performance of circular saws and analyzed the cutting forces and the

specific cutting energy. It was found that Co is a binder with a good wet ability and W provides fastening of diamond particles within the matrix. They showed that W and Co determine the hardness of the segment and Cu-Sn composition is preferred for filling the pores during the sintering process. It was concluded that the use of a high W-Co ratio increases the hardness of the segments and performances of the cutting disc and also considerably decreases the power consumption, cutting forces, specific energy values and segment wear amounts. Oliveira et al. [129] examined the possibility of adding Nb to the Fe-Cu system instead of Co without losing the wear properties needed for the diamond tools. In their study, cutting tests under real conditions were carried out for Porrinog granite. It was found that the mechanical properties the matrices with Nb were improved relative to those of the matrices with Co and both matrices were found to show similar cutting behaviour, indicating that the replacement of Co by elements such as Nb is a promising method for use in the near future. Luo [29] investigated the worn surface of diamond segments in circular saws for sawing hard and relatively soft granites. In this study, sawing tests were performed using a bridge sawing machine with a motor power of 15 kW. He found that for the sawing of hard granite, the worn particles were mainly of the macro-fractured crystal and/or pull-out whole type. When cutting the relatively soft granite, the worn particles produced a greater portion of whole crystal and micro-fractured grit on the worn surface and the amount of crystal pull-out was also high. Therefore, it was suggested that the diamond breakdown and the pull-out of the saw blade should operate in the correct wear mode in order to provide optimal blade performance. Tönshoff and Warnecke [130] stated that in the application of circular saw blades, a medium grit size and a high concentration at high cutting rates, and a smaller grit size and a low concentration at low cutting rates, provided favourable cutting conditions for tool stability and economic operation. Büttner [131] found that if the diamond is too friable it wears faster than the bond material and this causes the blade to act hard, which may cause glazing. Conversely, if the bond material is too soft, the diamond is lost prior to completing its effective service life, leading to excessive tool costs. Thus, the bonding material must wear at the same rate as the diamond particles in order to facilitate constant efficient cutting. Eyuboglu et al. [24] investigated the saw ability for andesitic rocks. In this study, the blade wears investigations were performed for Ankara andesite with block -cutting machines with a 24-disc type blade. They used 50/60 Mesh synthetic diamond particle size with the

diamond concentration of 20 (0.88 carats/ cm^3). After cutting operation, it was determined that a higher proportion of fractured crystals were observed than of the whole crystals and pull out crystals on the top surface of the worn segments. In this study, the possible causes of this problem were listed as a high cutting speed, inadequate particle size of diamonds, inappropriate matrix composition for andesite rocks, and random diamond distribution in the matrix. Atıcı and Ersoy [132] examined the correlations between brittleness of the rocks and cutting specific energy (SE) when producing Andesite rock blocks using circular diamond saw blades. In this study, the grit size of the diamond was 40/50 Mesh and the diamond concentration was 35. The composition of the matrix was Co-bronze. They defined the SE as the amount of energy required to cut the rocks. Based on the results of the tests, they concluded that low SE values indicate that the saw and the bit were cutting and drilling more efficiently, and SE values of 970 and 1138 J/m^3 were obtained for Afyon Basaltic Andesite and Kayseri Basaltic Andesite, respectively.

The aim of the present study is to enhance the cutting performances of diamond tools with the addition of Ag and Al for the cutting of Ankara andesite rocks. Ag was chosen as the matrix material from among the other metals in order to obtain superior wear resistance. Ag addition is often used to enhance the hardness, wear resistance, and strength of the metal matrix [133,134]. According to previous investigations, Ag does not perturb the crystallographic structure or forms impurity phases, and distributes only at the grain boundary regions. The use of Ag is also attractive because of its large diffusion coefficient that allows the metal to rapidly provide lubrication [135]. Al was chosen as the matrix material for its high strength and reasonable ductility and because it is known from the literature that Al materials show superior wear resistance under a large load [136]. Since a large load is applied to the diamond tools for the cutting process of abrasive rocks such as andesite, it is predicted that the cutting performance of diamond tools can be increased with Ag and Al additions.

4.2 Material and Experimental Methodology

Diamond cutting tool segments were manufactured by mixing different ratios of metal powders and diamond crystals and using the powder metallurgy method. Co, Ni, Sn, and W ultrafine metal powders were used as the matrix materials for the C

samples and 4 wt% Al with a particle size of 6.5 µm and 5 wt% Ag with a particle size of 8 µm were added to the metal matrix of the CAA samples. The grit size of the diamonds was 40/50 and 50/60 Mesh at diamond concentrations of 25 and 28 (1.07 and 1.23 carats/cm^3), respectively. The diamonds were carbon coated. The carbon-coated diamonds are cube-octahedral with minimal inclusions, high strength, and high impact toughness. The diamonds have a uniform shape as shown in Figure 4.1. Powders and diamonds were mixed in a 360° rotating chamber, compacted in a cold press, and the green samples were sintered via SPS at 920 °C and 40 MPa pressure. The chemical compositions of the matrices are given in Table 4.1 and the dimensions of the produced segment are shown in Figure 4.2. Since the produced segment will be used in natural stone cutting in the field, the dimensions of the segments produced are conical in order to prevent the dust of the stone from blocking the cutting path and to facilitate sludge removal from the cut surface while wet cutting. To determine the mechanical properties, filled cylindrical samples with a diameter and height of 7.5 and 14 mm, respectively, without diamonds were produced with the same method.

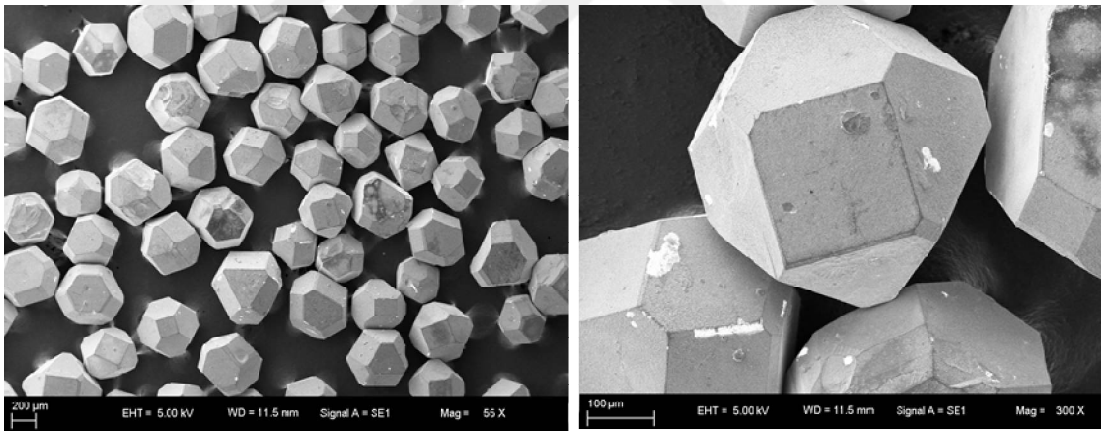

(a) (b)

Figure 4.1 : The SEM images of the 40/50 mesh carbon coated diamonds a) 55x b) 300x.

Table 4.1 : The chemical composition of the matrices.

Reference Name	Chemical Composition (wt%)					
	Co	Ni	Sn	W	Ag	Al
C	88	5	4	3	-	-
CAA	78	5	4	3	5	5

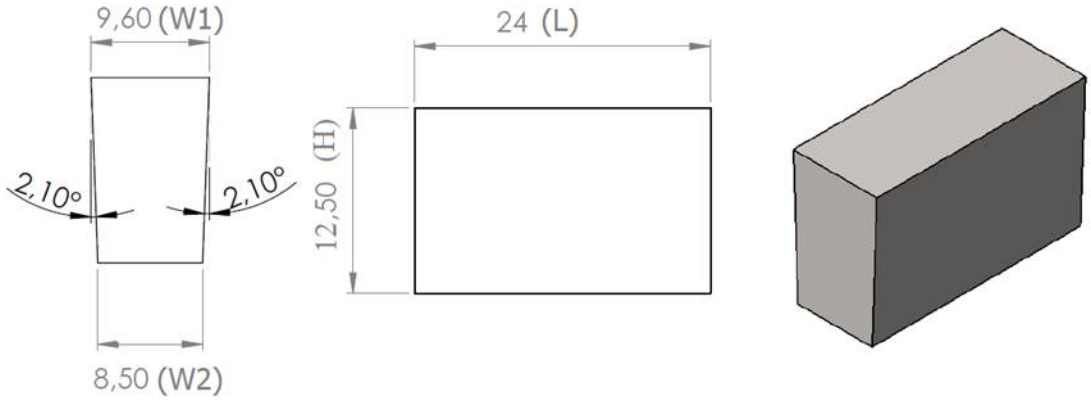

Figure 4.2 : The dimensions of the segments.

The microstructures of the samples were examined by a Zeiss Evo 18 scanning electron microscope (SEM) equipped with an energy dispersive spectroscopy (EDS) unit. X-ray diffraction (XRD) analysis was used for the quantitative identification of the phases and was carried out with a Bruker D8-Advanced X-ray diffractometer using Cu Kα radiation. The measurements were performed with a step size 0.02° and a scan rate of 1 step/min. The 2θ range was set to 30- 110°. The density of the samples was determined by the Archimedes method. Hardness measurements were carried out with a Shimadzu HMV-2 micro hardness tester using a Vickers indenter by the application of a 300 g load for 15 sec. The compression tests were performed using a Dartec universal testing machine operating at a crosshead speed of 1 mm/min. Abrasion wear tests were conducted using a Rotary Drum Abrader DVT DA6 model abrasion tester. The samples were vertically installed in the rotary table of the tester which is covered with 80 grade sandpaper. The table was rotated with 40 rpm and 1 kg vertical load was applied on the processed samples. The samples were moved on the table for 20 m. The weights of the samples were measured before and after the wear tests by an electronic balance with an accuracy of 0.1 mg. The relative wear resistance of each sample was calculated as the ratio of the maximum weight loss of that sample to the weight loss of the reference sample. The all mechanical characterization (density and hardness measurement, compression test and wear test) were performed repeated with 5 samples at the same properties.

The circular diamond saw blades used in the on-site field tests had a diameter of 1400 mm and the steel cores had a thickness of 4 mm. Ninety- two diamond segments (the dimensions are shown in Figure4.2) were brazed to the periphery of circular steel core. The blades wear investigations in andesite rock cutting were

performed in Ankara, Turkey on an industrial scale. The mineralogical structure, composition, and physical and mechanical properties of these andesite rocks were determined in the laboratory according to the International Society of Rock Mechanics and Rock Engineering (ISRM) standard [137] and the Institute of Turkish Standards (TSE) [138]. The measured strength and deformation properties were determined with uniaxial compressive strength and bending strength measurements. The index tests were performed for Mohs hardness; Schmidt rebound hardness, and Bohme surface abrasion strength. The porosity, density, and water absorption by weight and volume were calculated. The sawing tests were performed using block-cutting machines and the saw movements were forward-backward in the horizontal plane and up-down in the vertical plane. The sawing tests were carried out under a traverse rate of 20 m/s. The depth of the cut was 6 mm and the peripheral blade speed was kept constant at 12.5 m/min throughout the tests. The cutting fluid was fresh water. After cutting, the diamonds on the surface of the segments were examined by SEM.

4.3 Results and Discussion

The XRD patterns of the investigated samples are given in Figures 4.3 and 4.4 for the C and CAA samples, respectively. The acquired peaks for the C sample correspond to Co and NiSn. The acquired peaks for the CAA sample with the addition of Ag and Al are assigned to Co, NiSn, Ag, and $Al_{13}Co_4$. Since the C and CAA samples have the high Co content, the Co peak has the highest intensity and Co is the most significant phase according to results of the XRD analysis. In the XRD analysis of the CAA sample, due to the addition of Al and Ag, the Ag phase and the $Al_{13}Co_4$ intermetallic phase were observed. Due to the presence of these new phases, a decrease in the intensity of the NiSn peak was detected.

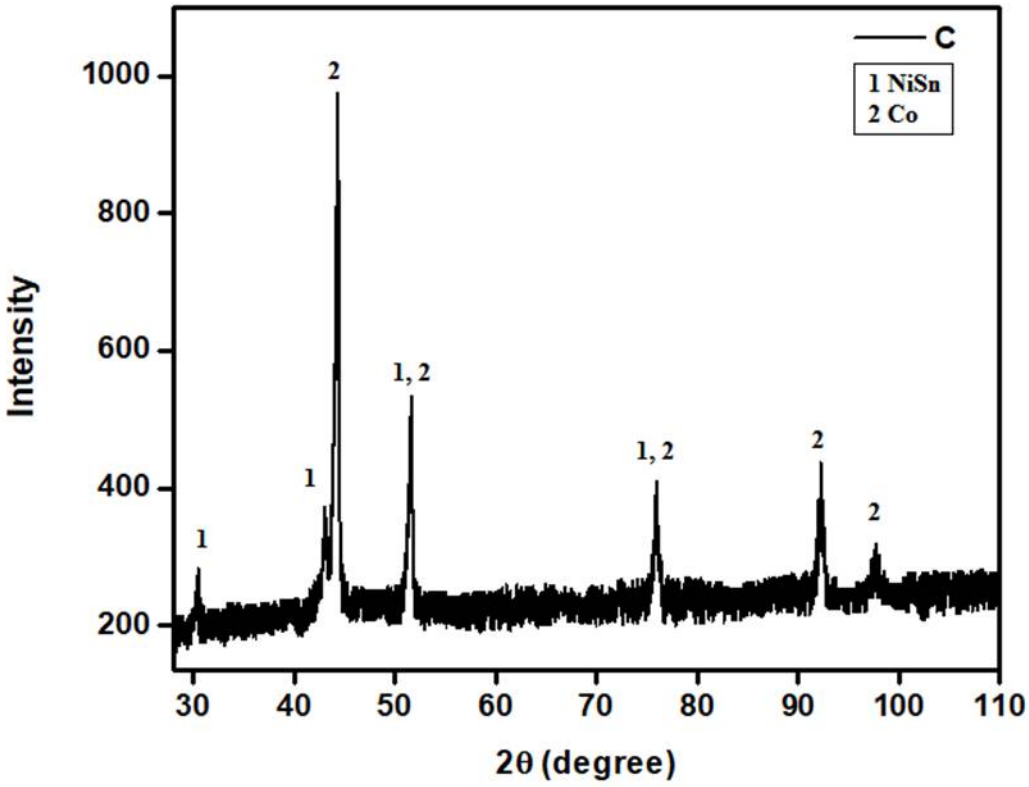

Figure 4.3 : The XRD pattern of the C samples.

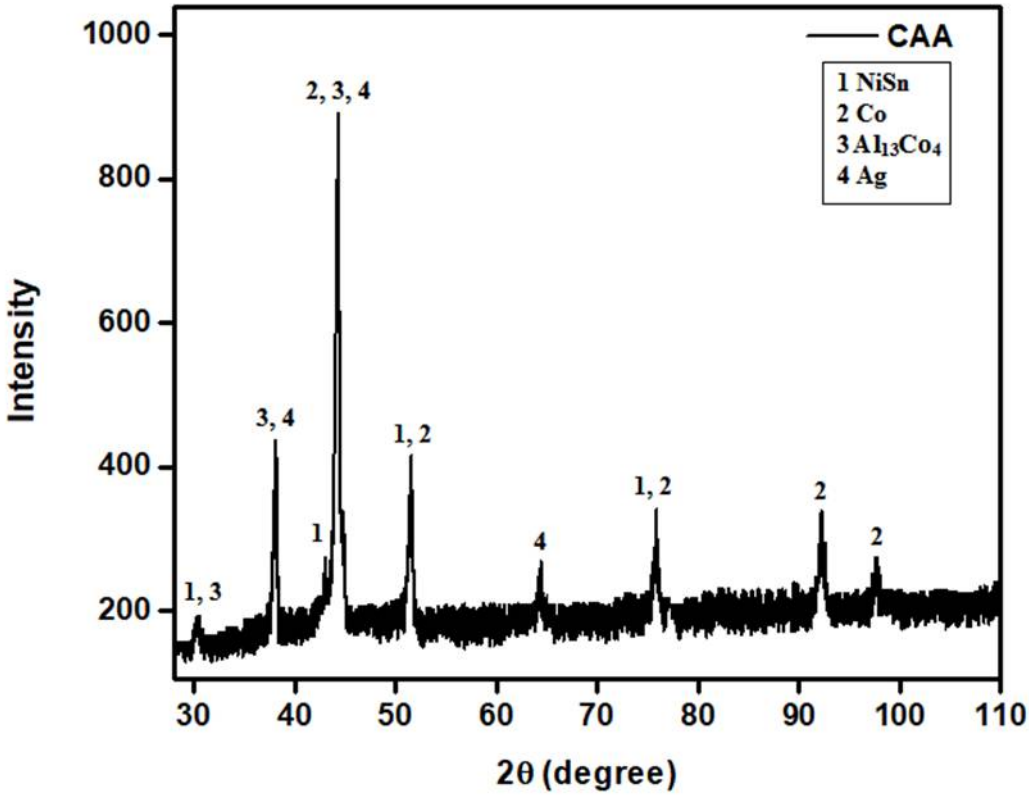

Figure 4.4 : The XRD pattern of the CAA sample.

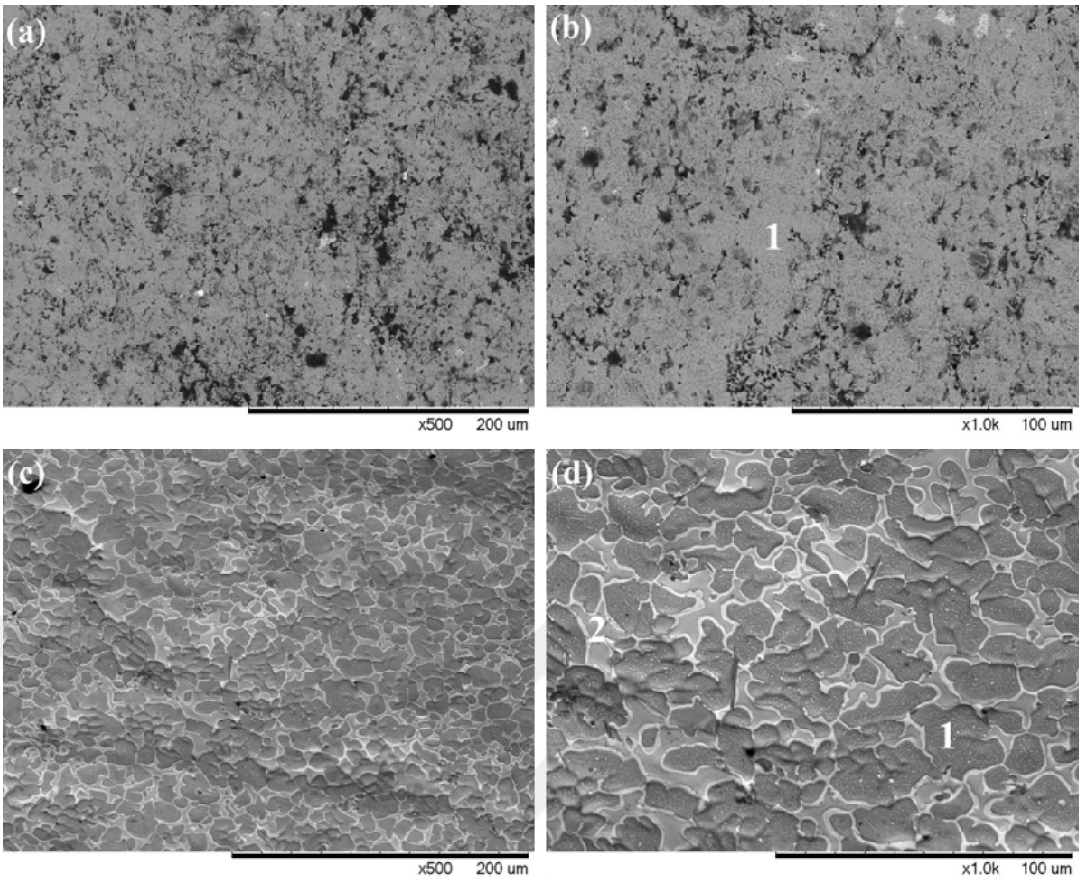

Figure 4.5 : SEM micrographs of (a) C samples x500, (b) C samples x1000, (c) CAA samples x500, (d) CAA samples x1000.

Figure 4.5 (a-d) shows the SEM micrographs of the samples and Figure 4.6 shows the corresponding EDS patterns. An examination of the SEM images of the C and CAA samples shows that the C sample structure has multiple porosities while low porosity is found for the CAA samples. According to the results of the SEM-EDS analysis, the existing bright islets in the grain boundaries of the CAA samples are Ag accumulation.

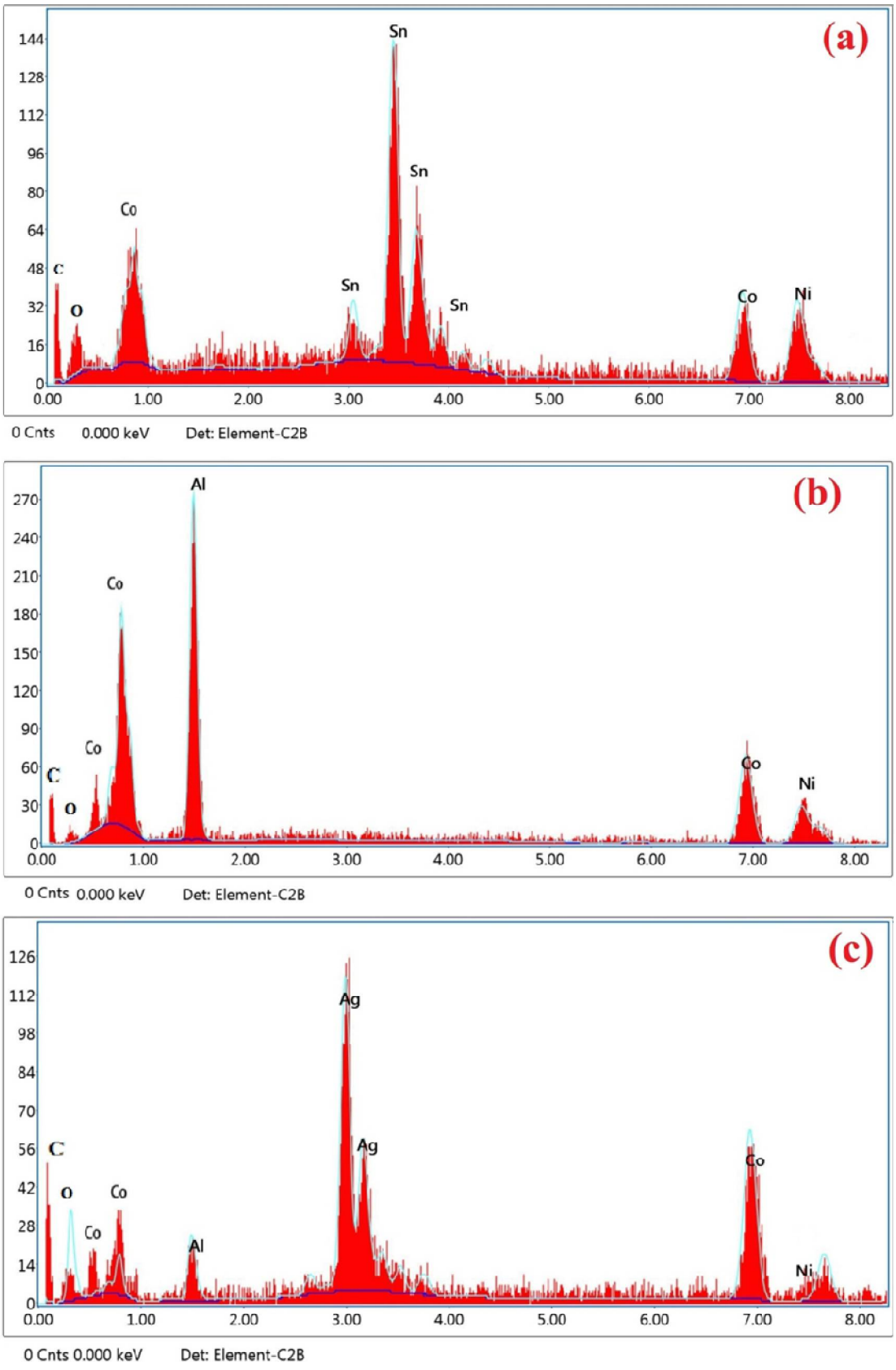

Figure 4.6 : EDS analysis of (a) C-zone 1, (b) CAA- zone 1, (c) CAA- zone 2.

Table 4.2 summarizes the relative density, hardness, compressive strength, and relative wear resistance of all samples. The highest mechanical properties (density, hardness, compressive strength, and wear resistance) were obtained in the CAA sample. The mechanical properties of the sample improved with the addition of Al and Ag that is accompanied by the decreasing porosity. The $Al_{13}Co_4$ intermetallic phase formed in the structure with the addition of Al and the solid lubricating layer formed with Ag on the surface of the material provided an enhancement of the mechanical properties. It was observed that the mechanical properties of the CAA samples were better than those of the C samples. Similarly, Ruiz et al. [139] investigated the wear resistance of the Al 7075 and Al-Ag composites and found that Ag prevents the wear of the material by acting as an obstacle to dislocation movements during the plastic deformation of the contact surface, and also acts as a solid lubricant when separated from the metal-matrix. In a different study [140], the same research group investigated the mechanical properties of the Al 7075- Ag nanoparticles powder composite. They found that Ag is beneficial for refining the powder particle size and for refining the crystallite size of the composite. The mechanical properties were enhanced with increasing Ag content. Azar et al. [141] studied the synthesis of W-Cu with addition of Ag via the chemical precipitation method. Their results showed that an increase in the amount of Ag powders led to improved sinterability and that the relative density and hardness of the samples increased with increasing Ag amount. Zhang et al. [142] studied the influence of Ag addition on the microstructure and corrosion behavior of Mg-Nd-Zn-Zr alloys. They found that the microstructure was refined with increasing Ag addition and the increased second phase distributed more continuously. The corrosion resistance of the alloy with 0.2 wt% Ag is approximately that of the alloy without Ag. Wu et al. [143] examined the effect of Ag addition on properties of Al-Zn-Cu- Mg-Zr alloys and found that the tensile strength of the base alloy increasd with Ag addition. Mandal and Robi [144] investigated the properties of Al-Cu-Zn-Fe-Ti-Mg alloys with Ag addition. They found that yield strength, ultimate tensile strength, and hardness increased with increasing Ag content in combination with reasonable ductility. Chou et al. [145] studied a polyether type polyurethane (PU) containing Ag and observed a significant enhancement in mechanical properties with increasing Ag content.

Table 4.2 : The mechanical properties of the samples.

Sample	Relative Density	Hardness (HV0.3)	Compressive Strength (MPa)	Relative Wear Resistance
C	98.6±0.052	414±1.5	369±2.3	1±0.61
CAA	99.7±0.048	437±1.1	415±2.2	3.70±0.55

Figure 4.7 presents the SEM images of the worn surfaces for the two types of samples. The wear grooves characteristics of abrasive wear are typical of the worn surfaces of the samples. The majority of the surfaces are smooth and a few small pits are observed for all samples. Comparison of the SEM images found that the wear marks of the C samples with low abrasion resistances were large and deep, whereas those of the CAA samples with high abrasion resistances were narrow and shallow.

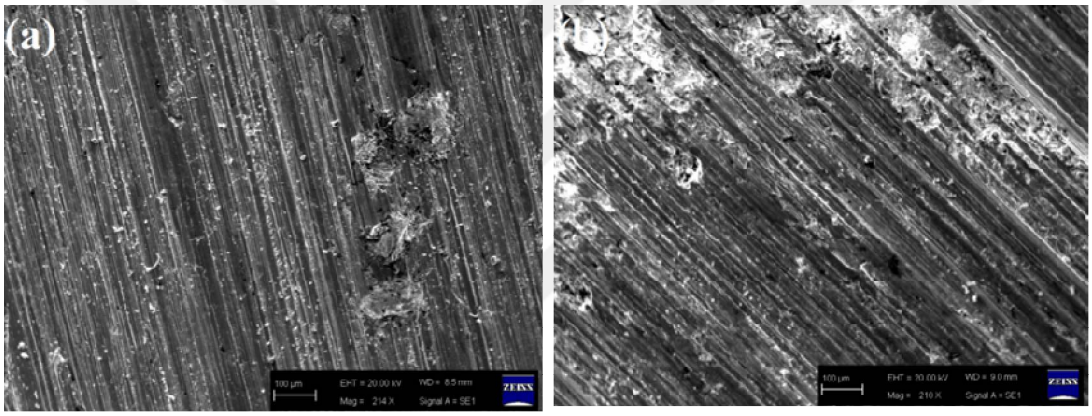

Figure 4.7 : The SEM micrographs of the worn surface of a) C sample b) CAA sample.

To evaluate the performance of circular diamond saw blades in cutting the Ankara andesite rock, on-site field tests were carried out on industrial scale with the C samples that are currently used commercially and the CAA samples prepared in this study to improve the cutting performance. Sawing tests were performed using a single- block cutting machine. The vesicular structure of the stone is present in Figure 4.8 and the mineralogical analysis is given in Table 4.3. The andesite rock had microlithic hyaline as the matrix and showed a vesicular texture. In the thin section of the rock, plagioclase, pyroxene, biotite, quartz, and opaque minerals were detected. The physical and mechanical properties of the andesite block are given in Table 4.4.

Figure 4.8 : The image of the vesicular structure of the Ankara andesite rock.

Table 4.3 : The mineralogical analysis of the Ankara andesite rock to be cut.

Mineral	%
Paste (matrix)+ vacancy	85
Plagioclase	7
Quartz	3
Pyroxene	2
Biotite	2
Opaque (magnetite)	1

Table 4.4 : The physical and mechanical properties of the andesite rock.

Basic Index Properties	
Density	2.00 g/cm^3± 0.20
Porosity	14.01 %± 0.34
Water Absorption by Weight	7.21 %± 0.90
Water Absorption by Volume	14.40 %± 0.33
Mohs Hardness	6.5± 1.00
Schmidt Rebound Hardness	52± 1.37
Strength and Wear Properties	
Uniaxial Compressive Strength	45.235 MPa± 0.60
Bending Strength	100.003 kgf/cm^2± 0.25
Bohme Surface Abrasion Strength	11.475 cm^3/50cm^2± 0.76

The cutting speeds of the products obtained in the field tests are given in Figure 4.9. It is observed that the cutting speed of the CAA sample is higher than the cutting speed of the C sample. During the cutting process, the relative wear of the saw blade

was measured on the 10 segment using a micrometer. The thickness (W1 -9.60 mm) and the height (H1- 12.50 mm) of the segments as a function of the amount of the stone cut are shown in Table 4.5 and Figure 4.10, and the wear loss of the segments for the W1 and H1 dimensions are shown in Figure 4.11. The lowest values of wear are found in the CAA sample rather than the C sample. As observed from Figure 4.10, the W1 dimension of the C sample is 9.55 mm and the H1 dimension of the C sample is 12.35 mm after cutting 70 m^2 rock, and after cutting 820 m^2 rock, the W1 and H1 values of the C sample are 8.00 mm 2.50 mm, respectively. The cutting process was finished because W1 of the segment is less than W2 (8.50 mm) of the segment and the H1 value is 2.5 mm at this stage. The C segments totally cut 820 m^2 andesite rocks. The W1 dimension and the H1 values of the CAA sample are 9.60 mm and 12.50 mm respectively, after cutting 70 m^2 rocks. At 820 m^2 rock, the W1 value of the CAA sample is 9.25 mm and the H1 value of the C sample is 8.50. At the end of cutting of 1400 m^2 rock, the W1 and H1 of the CAA samples are 8.00 mm and 2.70 mm, respectively. The cutting process was finished at the cutting of 1400 m^2 rock for the same reason as for the C samples. The CAA segments totally cut 1400 m^2 andesite rock and cut 57.14% more rocks than the C samples. Figure 4.12 presents the images of the segments cut in the on-site field tests. The SEM images of diamonds of each composition after the cutting process are given in Figure 4.13 and intense spills of diamonds are observed at the C segments. The diamonds abandoned the structure without completing the cutting tasks. Because the mechanical properties of the C samples are low compared to the characteristics of the andesite rock, the diamonds that can make the cuts detached from the matrix. The diamonds present on the segment surface were also broken. Therefore, the cutting speed remained low. By contrast, no spill was detected for the diamonds of the CAA sample. These diamonds have sharpened corners, and due to the abrasiveness of the cut rock, small breaks were observed at the corners of the diamond in the CAA samples. However, this does not affect the cutting speed and cutting life because the broken diamond corners are sharp and therefore, the diamond continues to cut.

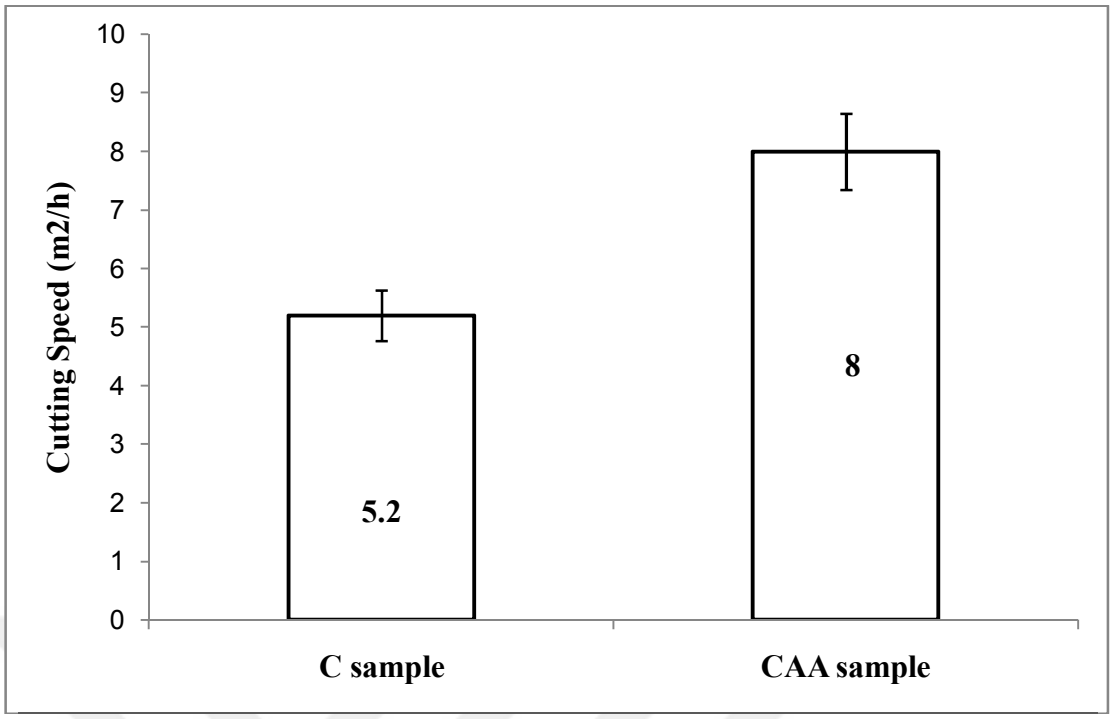

Figure 4.9 : The cutting speed of the samples.

Table 4.5 : The W1 and H1 dimensions of the samples due to the amount of stone

The Amount of Stone Cut (m^2)	The W1 Dimension (mm)		The H1 Dimension (mm)	
	The C Sample	The CAA Samples	The C Sample	The CAA Sample
0	9,60±0,03	9,60±0,02	12,50±0,06	12,50±0,04
70	9,55±0,03	9,60±0,02	12,35±0,26	12,50±0,04
230	9,40±0,05	9,55±0,03	9,70±0,29	12,40±0,06
710	8,50±0,07	9,40±0,07	3,50±0,37	9,70±0,51
820	8,00±0,11	9,25±0,05	2,50±0,55	8,50±0,54
1200	Completed	8,50±0,06	Completed	3,70±0,49
1400	Completed	8,00±0,09	Completed	2,70±0,46

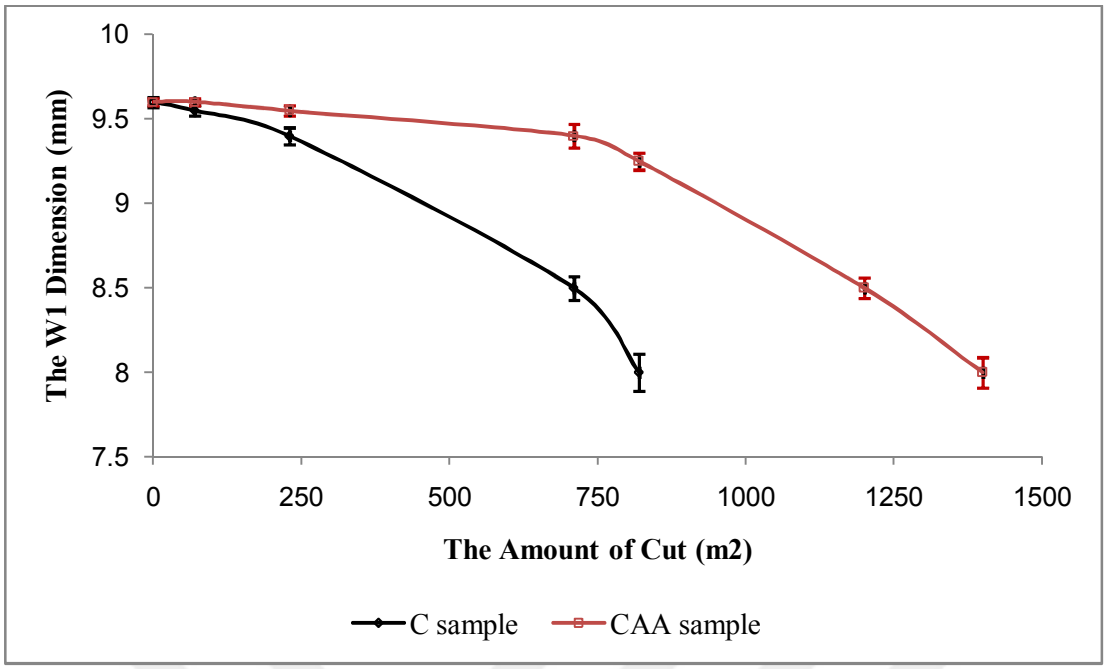

(a)

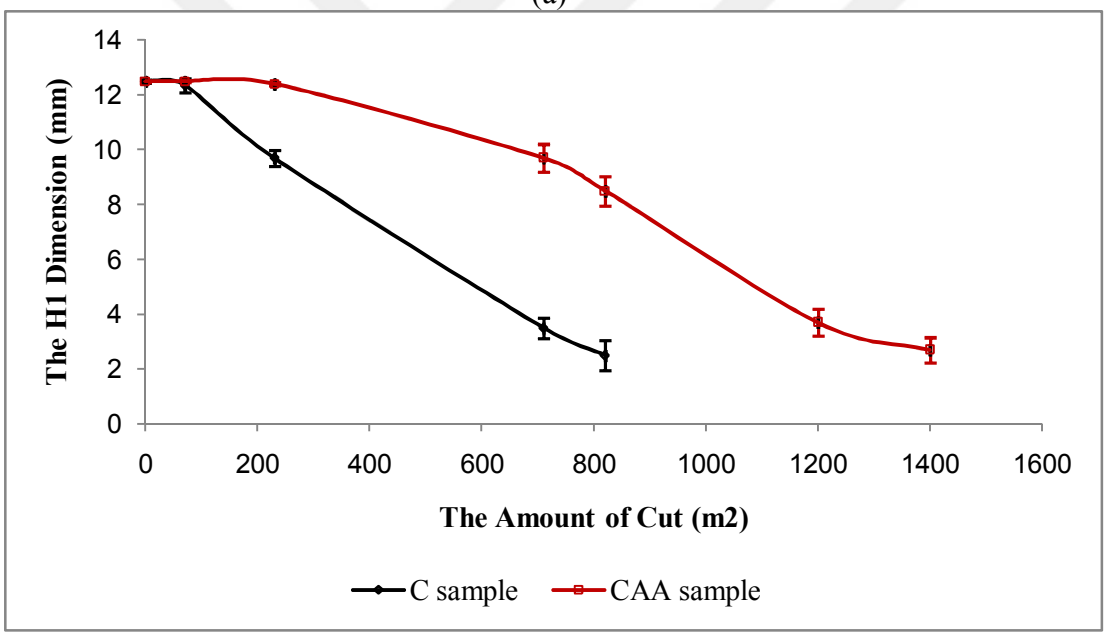

(b)

Figure 4.10 : The dimensions of W1 and H1 of the cutting segments during cutting process.

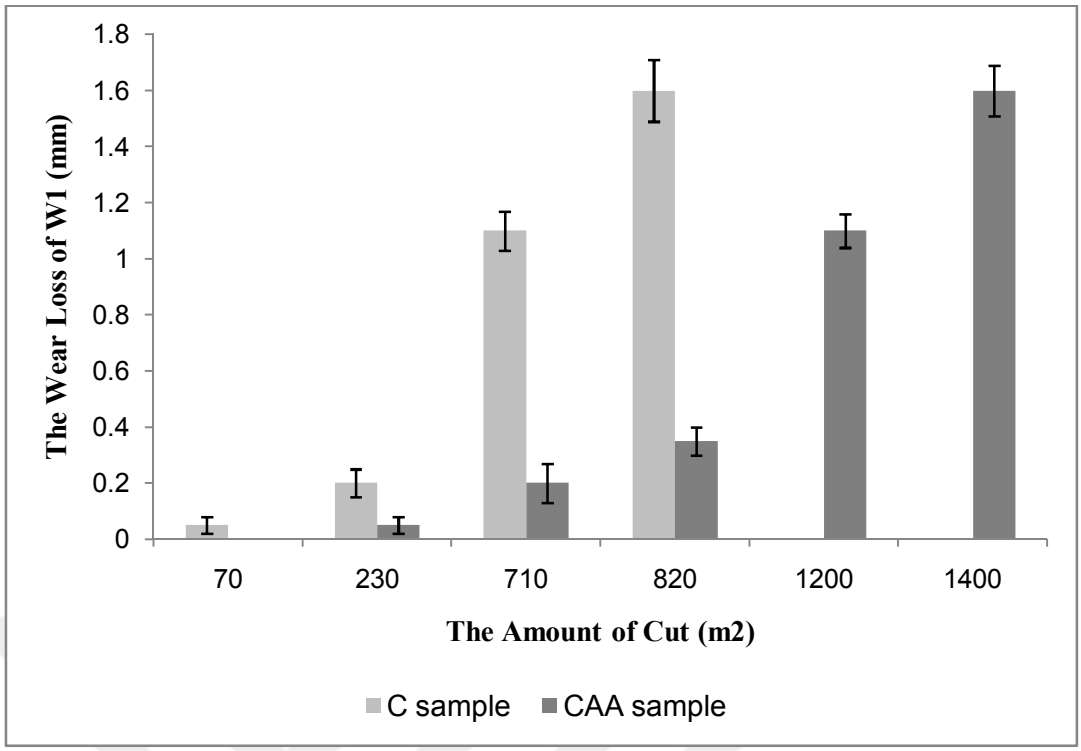

(a)

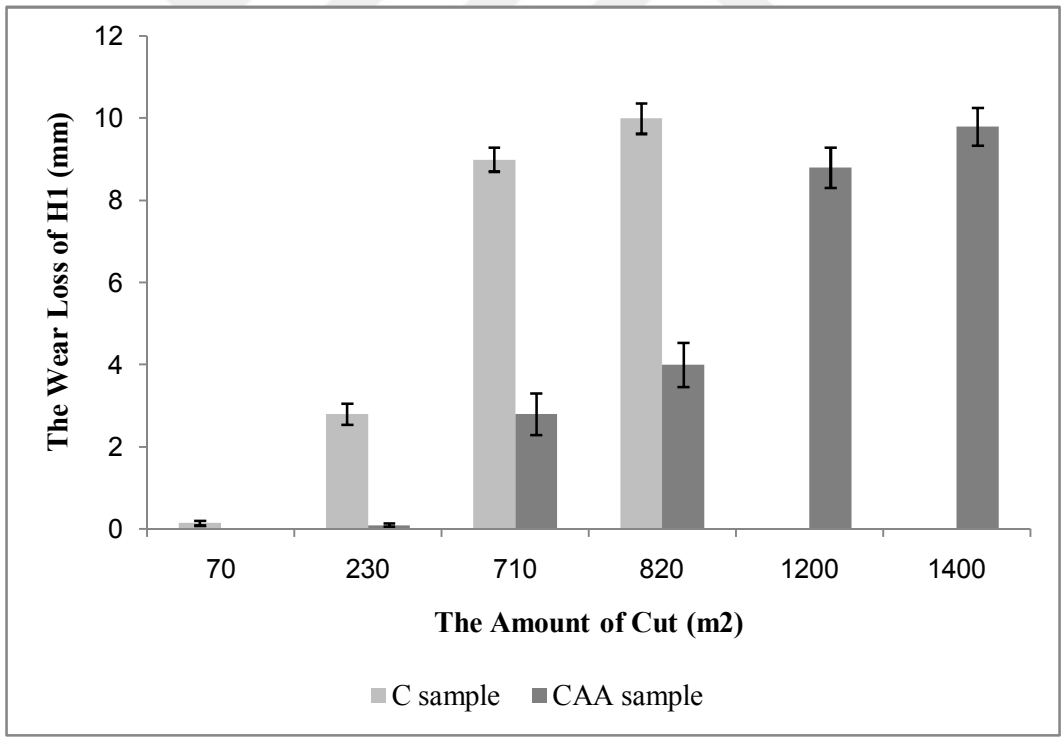

(b)

Figure 4.11 : The wear loss of W1 and H1 of the cutting segments during the cutting process.

Figure 4.12 : The images of segment until cutting process a) C -70 m2 b) CAA -70 m2 c) C-820 m2 d) CAA-820 m2 e) CAA-1400 m2.

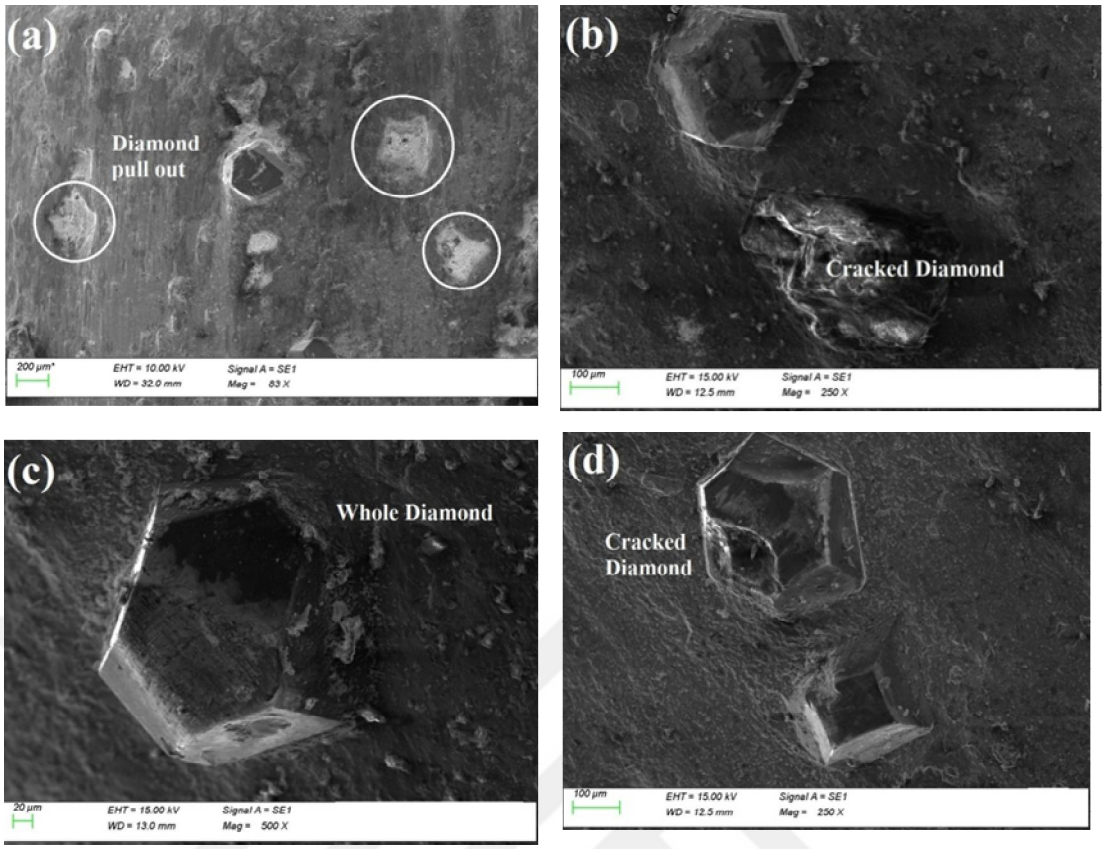

Figure 4.13 : The SEM images of the diamonds after andesite cutting process a) C samples-Diamond pull out, b) C samples- Cracked diamond, c) CAA samples-Whole diamond d) CAA samples-Cracked diamond.

The results of this study showed that optimization of the wear rates of the segments of the diamond saw blades are necessary for better cutting performances. The mechanical properties of the C samples are lower than the mechanical properties of the CAA samples. The C sample that works against an abrasive stone such as andesite has a worn out matrix due to its low wear resistance and intense diamond spillage has occurred due to the worn out matrix. Due to the diamond spillage, it was observed that the cutting speed and the amount of stones cut in the field were low. Diamond spillage was not observed in the CAA sample for which the hardness and wear resistance were increased by the addition of Al and Ag to the matrix when the sample was used for working against the same abrasive rocks. Comparing the field performance of the C and CAA samples, the cutting speed and the amount of cut stone are 35% and 41.4 % greater, respectively, than those of the CAA sample. The CAA samples are determined to be the most suitable matrix mixture for andesite cutting according to the abrasive level of stones. The matrix mixture developed in this study (the CAA sample) has already been applied into industrial products by

using andesitic and basaltic stones in the Ankara and Kayseri, Turkey and mass production is ongoing.

4.4 Conclusion

In the XRD analysis of powders, the acquired peaks for the C sample were Co and NiSn and the acquired peaks for the CAA sample with the addition of Ag and Al were Co, NiSn, Ag, and $Al_{13}Co_4$. For both samples, the highest intensity peaks were obtained for Co as the most significant phase and with the addition of Al and Ag, the Ag phase and the $Al_{13}Co_4$ intermetallic phase were observed in the CAA sample.

Based on the SEM analysis of the sintered samples, it was observed that after the sintering process, the C sample had dense porosity and the CAA sample had low porosity. The Ag phases were accumulated at the grain boundaries of the CAA sample.

The mechanical properties (relative density, compressive strength, hardness and relative wear resistance) of CAA samples are improved relative to those of the C samples due to the addition of Al and Ag and the accompanying decrease in porosity. The $Al_{13}Co_4$ intermetallic phase formed in the structure with the addition of Al and the solid lubricating layer formed with Ag on the surface of the material provided an increase in the mechanical properties. An examination of the worn surfaces occurring after the wear test by SEM analysis supports the results that the wear resistance of the CAA sample is higher than the wear resistance of the C sample.

According to the field tests results, the cutting speed and the amount of stone cut of the CAA samples are higher than those obtained using the C samples for andesite rock production. Based on the hardness and abrasiveness level of rock and wear resistance of the matrices, the CAA matrix is suitable for andesite cutting and has already been developed into industrial products for using andesitic and basaltic stones in the Ankara and Kayseri, Turkey with ongoing mass production.

5. CONCLUSION

In this dissertation, studies were about to increase the field performance of diamond cutting tools used in natural stone production. First of all, Co powders, which are highly used in the metal matrix composition, were examined and the appropriate Co powder, which would positively affect the cutting performance, was determined. By improving the matrix composition in both diamond cutting wires and circular saws, field performances have been increased from soft stones such as marble to hard stones such as granite and andesite.The conclusions of each chapter are given below.

In the first part of the thesis, the Co powders with spherical and rod-like grain shapes were characterized. The conclusions from the this chapter of the thesis are presented as:

- In the particle size distribution analysis, the D95 value for Co-R powder is 5.0 µm, while the same value for Co-S is 3.5 µm. The results showed that the grain size of the Co-S powder was smaller than the grain size of the Co-R powder.
- The behaviours of the powders in cold press process were examined by aeration, permeability, and compressibility tests. According to the FT4 rheometer results, the Co-S powders can easily flow in the gravity of the cold press mould. The high SE value of Co-R powder is proof that it can be difficult in powder flow due to increased mechanical locking and friction effects during cold press mould filling. It has been observed that Co-R powder cannot maintain its stability.
- It has been determined that from the SEM analysis, the Co-R powder had a porous structure. Parallel of this result, it has been seen that the mechanical properties of the Co-S samples were enhanced compared with the Co-R samples.
- All these results supported that the Co-S powder is more convenient for the metal matrices of diamond tools. The Co-S powders and the high fluidity and

compressibility during the cold pressing phase ensured that the structure was void-free during powder filling. High mechanical properties were also detected in the samples with low porosity after sintering. The usage of the Co-S powder will have improved the cutting performance of the diamond tools.

In the second part of the thesis, the matrix composition of diamond cutting wires was determined by considering the hardness and abrasivity properties of granite and marble stones. The conclusions from the this chapter of the thesis are presented as:

- According to the XRD results of the samples, the intensity of the Fe-based and Co-based peaks were increased with increasing Fe and Co contents of the samples.
- The hardness and compression strength values of the both type of the samples, Fe- based and Co-based, were increased with the increasing Fe and Co contents of the samples. The mechanical properties of the Co-based samples are higher than the Fe-based samples.
- The cutting speeds of Fe-30 and Fe-50 samples are high for marble stone production. The diamonds of the Fe-30 and Fe-50 samples were good diamonds. The damaged diamonds removed from the matrix and the new-sharpened diamonds were come to the surface with the abrasion of the metal matrix. However due to the high hardness of the Co-based metal matrix the new diamonds could not come to the cutting surface. Blunted and broken diamonds did not leave the matrix and were not able to continue the cutting process.
- The cutting speed of Co-80 is high for granite stone production. The reasons for obtaining good cutting speed with Co-80 samples in granite cutting are the enhanced mechanical properties of the metal matrix and high thermal resistance of the matrix. The cutting speed of the Fe-80 samples is low for granite stone production. The good diamond were spilled out from the matrix due the low mechanical properties of the metal matrix, so the cutting speed of the Fe-80 samples remained low.
- With the results obtained in this part of the thesis, it has been determined that high cutting speeds can be obtained in marble production with Co- free, Fe-based metal matrices and are more advantageous than Co-based matrices. It

has been observed that studies on Fe-based metal matrices should be continued for hard and abrasive stones such as granite.

In the last part of the thesis, the matrix composition of the circular diamond saw blades was improved by addition on Ag and Al for cutting Ankara andesite stone. The conclusions from the this chapter of the thesis are presented as:

- In SEM examinations, it was observed that silver added to the matrix mixture accumulates in the grain boundaries of the matrix and reduces the porosity between grains.
- It was determined a increase of the mechanical properties of the CAA sample with the addition of Al and Ag. This addition was created a decrease of the porosity of the samples and also the $Al_{13}Co_4$ intermetallic phase formed in the structure.Al and Ag provided an enhancement of the mechanical properties.
- The cutting speed and lifetime of the CAA sample is higher than the cutting speed and lifetime of the C sample.
- The mass production of the matrix composition develop in this thesis is ongoing at industrial products.

The matrix compositions developed in the thesis have been used in different stone types in different countries and mass production continues.

REFERENCES

[1] **Junior, E.P.S., Conceicao, F.T., Fernandes, A.M., Sardinha, D.S., Menegario, A.A.,& Moruzzi, R.B.** (2019). Chemical weathering rates of clastic sedimentary rocks from the Paraná Basin in the Paulista Peripheral Depression, Brazil. *Journal of South American Earth Sciences*, *96*, 102369.

[2] **Irfan, T.Y.** (1999). Characterization of weathered volnanic rocks in Hong Kong. *Quarterly Journal of Engineering Geology and Hydrogeology*, *32*, 317-348.

[3] **Middlemost, E.A.K.** (1972). A simple classification of volcanic rocks. *Bulletin of Volcanology*, *36*, 382–397.

[4] **Duan, K., Li, Y., Wang, L., Zhao, G., &Wu, W.** (2019). Dynamic responses and failure modes of stratified sedimentary rocks. *International Journal of Rock Mechanics and Mining Sciences*, *122*, 104060.

[5] **Brigaud, F., & Vasseur, G.** (1989). Mineralogy, porosity and fluid control on thermal conductivity of sedimentary rocks. *Geophysical Journal International,98*, 525-542.

[6] **Blatt, H., & Jones, R.L.** (1975). Proportions of Exposed Igneous, Metamorphic, and Sedimentary Rocks. *The Geological Society of Amerika Bulletin*, *86*, 1085-1088.

[7] **Vaculikova, L., & Plevova, E.** (2005). Identification of clay minerals and micas in sedimentary rocks. *Acta Geodynamica et Geomaterialia*, *138*, 167-175.

[8] **Sabatakis, N., Koukis, G., Tsiambaos, G., &Papanakli, S.** (2008). Index properties and strength variation controlled by microstructure for sedimentary rocks. *Engineering Geology*, *97*, 80-90.

[9] **Chigira, M., & Oyama, T.** (2000). Mechanism and effect of chemical weathering of sedimentary rocks. *Developments in Geotechnical Engineering*, *84*, 267-278.

[10] **Galimov, E.M.** (1988). Sources and mechanisms of formation of gaseous hydrocarbons in sedimentary rocks. *Chemical Geology*, *71*, 77-95.

[11] **Tsiamboas, G., & Sabatakakis, N.** (2004). Considerations on strength of intact sedimentary rocks. *Engineering Geology*, *72*, 261-273.

[12] **Barker, C.E.** (1983). Influence of time on metamorphism of sedimentary organic matterin liquid-dominated geothermal systems, western North America. *Geology*, *11*, 384–388.

[13] **Chang, C., Zoback, M.D., & Khaksar, A.** (2006). Empirical relations between rock strength and physical properties in sedimentary rocks. *Journal of Petroleum Science and Engineering*, *51*, 223-237.

[14] **Hunt, J.M.** (1961). Distribution of hydrocarbons in sedimentary rocks. *Geochimica et Cosmochimica Acta*, *22*, 37-49.

[15] **Zedef, V., Kocak, K., Doyen, A., Ozsen, H., & Kekec, B.** (2007). Effect of salt crystallization on stones of historical buildings and monuments, Konya, Central Turkey. *Building and Environment*, *42*,1453-1457.

[16] **Picard, M.D.** (1971). Classification of fine-grained sedimentary rocks. *Journal of Sedimentary Research*, *41*, 179-195.

[17] **Middlemost, E.A.K.** (1994). Namingmaterials in the magma/ igneous rock system. *Earth-Science Reviews*, *37*, 215-224.

[18] **Green, T.H., & Ringwood, A.E.** (1968). Genesis of thecalc-alkaline igneous rock suite. *Contributions to Mineralogy and Petrology*, *18*, 105–162.

[19] **Nockolds, S.R., & Allen, R.** (1953). The geochemistry of some igneous rock series. *Geochimica et Cosmochimica Acta*, *4*, 105-142.

[20] **Wang, Q., Xu, J., & Zhao, Z.** (2001). The summary and comment on research on a new kind of igneous rock-Adakite. *Advances in Earth Science*, *16*, 201-208.

[21] **Kansteiner, M., & Biermann, D.** (2019). Influence of the diamond grain shape and orientation on the process forces and the mechanical work in scratchtests on basalt stone. *Diamond and RelatedMaterials*, *94*, 65-72.

[22] **Schaef, H.T., McGrail, B.P., & Owen, A.T.** (2010). Carbonate mineralization of volcanic province basalts. *International Journal of Greenhouse Gas Control*, *4*, 249-261.

[23] **Sari, M., Karpuz, C., & Ayday, C.** (2010). Estimating rock mass properties using Monte Carlo simulation: Ankara andesites. *Computers & Geosciences*, *36*, 959‑969.

[24] **Eyuboglu, A.S., Ozcelik, Y., Kulaksiz, S., & Engin, I.C.** (2003). Statistical and microscopic investigation of disc segment wearrelated to sawing Ankara andesites. *International Journal of Rock Mechanics and Mining Sciences, 40*, 405‑414.

[25] **Chen, L., Zheng, Y.F., Xu, Z., & Zhao, Z.F.** (2021). Generation of andesite through partial melting of basaltic metasomatites in the mantlewedge: Insight from quantitative study of Andean andesites. *Geoscience Frontiers*, *12*, 101124.

[26] **Kang, F., Li, Y., & Tang, C.** (2021). Grain size heterogeneity controls strengthening to weakening of granite overhigh-temperature treatment. *International Journal of Rock Mechanics and Mining Sciences*, *145*, 104848.

[27] **Delgado, N.S., Rey, A.R., Rio, L.M.S., Sarria, I.D., Calleja, L., & Argandona, V.G.R.** (2005). The influence of rock microhardness on the sawability of Pink Porrinogranite (Spain). *International Journal of Rock Mechanics and Mining Sciences*, *42*, 161‑166.

[28] **Buyuksagis, I.S.** (2007). Effect of cutting mode on the sawability of granites using segmented circular diamond sawblade. *Journal of Materials Processing Technology*, *183*, 399–406.

[29] **Luo, S.Y.** (1997). Investigation of the worn surfaces of diamond saw blades in sawing granite. *Journal of Materials Processing Technology,70*, 1-8.

[30] **Chen, X., Liang, H., Richards, J.P., Huang, W., Zhang, J., Wu, J., & Sotiriou, P.** (2018). Age and granite association of skarn W mineralization at Niutangjiedistrict, South China Block. *Ore Geology Reviews*, *102*, 268-283.

[31] **Zhu, Y.F., Zeng, Y., & Gu, L.** (2006). Geochemistry of the rare metal-bearing pegmatite No. 3 vein and related granites in the Keketuohairegion, Altay Mountains, North west China. *Journal of Asian Earth Sciences*, *27*, 61-77.

[32] **Winter, J.D.** (2021). Metamorphism, metamorphic rocks and classification of metamorphic rocks. *Encyclopedia of Geology (Second Edition)*, 345-353.

[33] **Dasgupta, S., & Bhowmik, S.K.** (2021). Types of metamorphism. *Encyclopedia of Geology (Second Edition)*, 354-365.

[34] **Schreyer, W.** (1995). Ultra deep metamorphic rocks: The retrospective view point. *Journal of Geophysical Research*, *100*, 8353-8366.

[35] **Elliott, D.** (1973). Diffusion Flow Laws in Metamorphic Rocks. *Geological Society of America Bulletin*, *84*, 2645-2664.

[36] **Song,S., & Cao, Y.** (2021). Textures and structures of metamorphic rocks. *Encyclopedia of Geology (Second Edition)*, 375-388.

[37] **Wang, X., Zhang, J., Li, X.P., Yin, C., Zhou, H., Liu, J., Liu, X., & Zhao, C.** (2020). Geochronology and geochemistry of low-grade metamorphic rocks from the Erdaowa Group and its significance on the tectonic evolution of the Paleoproterozoic Khondalite Belt, North China Craton. *Precambrian Research*, *350*, 105923.

[38] **Touret, J.L.R.** (2001). Fluids in metamorphicrocks. *Lithos*, *55*, 1-25.

[39] **Han, C., Tian, J., Hu, C., Liu, H., Wang, W., Huan, Z., & Feng, S.** (2020). Lithofacies characteristics and their controlling effects on reservoirs in buried hills of metamorphic rocks: A casestudy of late Paleozoic units in the Aryskumdepression, South Turgay Basin, Kazakhstan. *Journal of Petroleum Science and Engineering*, *191*, 107137.

[40] **Bas, M.J.L., Subbarao, K.V., & Walsh, J.N.** (2002). Metacarbonatiteor marble? –the case of the carbonate, pyroxenite, calcite–apatite rock complex at Borra, Eastern Ghats, India. *Journal of Asian Earth Sciences*, *20*, 127-140.

[41] **Elci, H. & Turk, N.** (2014). Rock mass block quality designation for marble production. *International Journal of Rock Mechanics and Mining Sciences*, *69*, 26-30.

[42] **Brilli, M., Mercadal, M.P.L., Giustini, F., &Plumed, H.R.** (2018). Petrography and mineralogy of the white marble and black stone of Goktepe (Mugla, Turkey) used in antiquity: New data for provenance determination. *Journal of Archaeological Science: Reports*, *19*, 625-642.

[43] **Wang, C.Y., & Clausen, R.** (2002). Marble cutting with single point cutting tool and diamond segments. *International Journal of Machine Tools and Manufacture*, *42*, 1045-1054.

[44] **Soltani, H.M., & Tayebi, M.** (2020). Determination of wear parameters and mechanisms of diamond/copper tools in marble stones cutting. *International Journal of Refractory Metals and Hard Materials*, *87*, 105172.

[45] **Adam, A.A., Fener, M.M., Comakli, R., Ince, I., Balci, M.C., & Kayabali, K.** (2021). Investigation of the relationships between basic physical and mechanical properties and abrasion wearresistance of several natural building stones used in Turkey. *Journal of Building Engineering,*10384.

[46] **Bilgin, N., Yeprem, H.A., Arslan, S., Bilgin, A., Gunay, E., & Marsoglu, M.** (2012). Use of waste marble powder in brick industry. *Construction and Building Materials*, *29*, 449-457.

[47] **Ashmole, I., & Motloung, M.** (2008). Dimensionstone: the late sttrends in exploration and production technology. *The Southern African Institute of Mining and Metallurgy-Surface Mining.*

[48] **Kulaksız, S.** (2007). *Natural stone (marble) mining and processing technologies,* TMMOB Mining Engineers Publications,*126*, 624.

[49] **Gupta, R.K., & Pratap, B.** (2021). Diamond tools processing for marble and granite: Cutting & wear. *Materials Todays Proceedings*, *46*, 2135-2140.

[50] **Zhang, H., Zhang, J., Dong, P., & Sun, Q.** (2018).Investigation of the sawing performance of a new type of diamond frame saw machine. *Diamond and Related Materials*, *84*, 11-19.

[51] **Dong, P., Zhang, J., Ouyang, C., Sun, D., &Wu, J.** (2021). Investigation on sawing performance of diamond frame saw based on reciprocating swing in processing hard stone. *Journal of Materials Processing Technology*, *295*, 117171.

[52] **Dormishi, A., Ataei, M., Mikaeil, R., Khalokakaei, R., & Haghshenas, S.S.** (2019). Evaluation of gang saws' performance in the carbonate rock cutting process using feasibility of intelligent approaches. *Engineering Science and Technology, an International Journal*, *22*, 990-1000.

[53] **Ersoy, A., & Atici, U.** (2004). Performance characteristics of circular diamond saws in cutting different types of rocks. *Diamond and Related Materials,13*, 22‑37.

[54] **Kaplan, M., & Budak, S.** (2011). The effect of Co additives on microstructure and mechanical properties in a marble cutting process, *6th International Advanced Technologies Symposium (IATS'11)*, Elazig, Turkey.

[55] **Rosa, L.G.,Fernandes, J.C., Anjinho, C.A., Coelho, A., & Amaral,P.M.** (2015). Long-term performance of stone-cutting tools. *Journal of Refractory Metals and Hard Materials*, *49*, 276-282.

[56] **Yu, J., Huang, L., Luo, H.,& Hai, Y.** (2019). Study effects on diamond concentration of CuSnFeNi/diamond composite on grinding WC. *The International Journalof Advanced Manufacturing Technology*, *104*, 2863–2873.

[57] **Das, M.K., Li, R., Qin, J., Zhang, X., Das, K., Thueploy, A., Limpanart, S., Boonyongmaneerat, Y., Ma, M., & Liuc, R.** (2017). Effect of electro deposition conditions on structure and mechanical properties of Ni-W/diamond composite coatings. *Surface & Coatings Technology*, *309*, 337-343.

[58] **Che, Z., Wang, Q., Wang, L., Li, J., Zhang, H., Zhang, Y., Wang, X., Wang, J., & Kim, M.J.** (2017). Interfacial structure evolution of Ti-coated diamond particle reinforced Al matrix composite produced by gas pressure infiltration. *Composites Part B, 113*, 285-290.

[59] **Aslantas, K., Ozbek, O., Ucun, I., & Buyuksagıs, S.** (2009). Investigation of the effect of axial cutting force on circular diamond saw blade used in marble cutting process. *Materials and Manufacturing Processes,24*, 1423–1430.

[60] **Bayram, F., & Kulaksiz, S.** (2021). Evaluation of rock cutting performance of diamond segmented frame saw in terms of diamond segment wear. *International Journal of Rock Mechanics and Mining Sciences*, *139*, 104657.

[61] **Sun, Q., Zhang, J., Wang, Z., Zhang, H., & Fang, J.** (2016). Segment wear characteristics of diamond frame saw whencuttingdifferent granite types. *Diamond and Related Materials*, *68*, 143-151.

[62] **Ersoy, A., Buyuksagis, S., & Atici, U.** (2005). Wear characteristics of circular diamond saws in the cutting of different hard abrasive rocks. *Wea*r, *258*, 1422-1436.

[63]**Dhokey, N.B., Utpat, K., Gosavi, A., & Dhoka, P.** (2013). Hot-press sintering temperature response of diamond cutting tools and its correlation with wear mechanism. *Journal of Refractory Metals and Hard Materials*, *36*, 289-293.

[64] **Nitkiewicz, Z., & Swierzy, M.** (2006). Tin influence on diamond–metal matrix hot pressed tools for stone cutting. *Journal of Materials Processing Technology*, *175*, 306-315.

[65] **Ganta, A.J., Konyashin, I., Ries, B., McKie, A., Nilen, R.W.N., & Pickles, J.** (2018). Wear mechanisms of diamond-containing hard metals in comparison with diamond-based materials. *International Journal of Refractory Metals and Hard Materials, 71*, 106–114.

[66] **Xi, X., Nie, Z., Xu, K., Ma, L., Chen, G., Zhang, X., & Zuo, T.** (2013). Structure and properties of secondary cobalt powder. *International Journal of Refractory Metals and Hard Materials, 41*, 90–93.

[67] **Liua, K., Wang, Z., Yin, Z., Cao, L., & Yuana, J.** (2018). Effect of Co content on microstructure and mechanical properties of ultrafine grained WC-Co cemented carbide sintered by spark plasma sintering. *Ceramics International, 44*, 18711–18718.

[68]**Molinari, A., Marchetti, F., Gialanella, S., Scardi, P., & Tiziani, A.** (1990). Study of the diamond-matrix interface in hot-pressed cobalt-based tools. *Materials Science and Engineering: A,130*, 257-262.

[69] **Chandrashekar, M., & Prasad, K.V.S.** (2018). The effect of cobalt on wear behavior of cemented carbide cutting tools for machining of titanium alloy. *Materials today: Proceedings, 5*, 7678-7684.

[70]**Xie, Z., Ni, S., & Song, M.** (2018). Effect of Y_2O_3 doping on FCC to HCP phase transformation in cobalt produced by ball milling and spark plasma sintering. *Powder Technology,324*,1-4.

[71] **Wanjun, T.,& Donghua, C.** (2007). Mechanism of thermal decomposition of cobalt acetate tetrahydrate. *Chemical Papers,6*, 329–332.

[72] **Samal, P.K., & Newkirk, J.W.** Powder Metallurgy.*ASM Handbook*, *Vol7*.

[73] **Wu, J., Tang, J., Wei, X., Ye, N.,& Yu, F.** (2017). Preparation process and mechanism of ultra-fine spherical cobalt powders by hydrogen reduction of calcium cobaltite. *Journal of Alloys and Compound*,*726*, 1119-1123.

[74] **Nakayamaa, N., Horitab, M., Sakagamia, S., Mikic, H., Miyazakid, T.,& Takeishie, H.** (2014). Effect of powder shape and size on mechanical properties of Al thin plate formed by compression shearing method at room temperature. *Procedia Engineering,81*,1163– 1168.

[75] **Nouri, A., & Sola, A.** (2018). Metal particle shape: A practical perspective. *Metal Powder Report*, *73*, 276-282.

[76] **Beckers, D., Ellendt, N., Fritsching, U., & Uhlenwinkel, V.** (2020). Impact of process flow conditions on particle morphology in metal powder production via gas atomization. *Advanced Powder Technology, 31*, 300-311.

[77] **Fariñas, J.C., Moreno, R., Pérez, A., Garcíaa, M.A., García-Hernándezc, M., Salvador, M.D., & Borrell, A.** (2018). Microwave-assisted solution synthesis, microwave sintering and magnetic properties of cobalt ferrite. *Journal of the European Ceramic Society, 38*, 2360-2368.

[78] **Bokhonov, B.B., Korchagina, M.A., Ukhinaa, A.V., & Dudina, D.V.** (2018) Structural and morphological transformations in cobalt-carbon mixtures during ball milling, annealing and Spark Plasma Sintering. *Vacuum, 157*, 210-215.

[79] **Sakkaki, M., Moghanlou, F.S., Vajdi, M., Asl, M.S., Mohammadi, M., & Shokouhimehr, M.** (2020). Wear studies of spark plasma sintered ZrO2 reinforced Ti-6Al-4V alloy. *Ceramics International, 46*, 4998-5007.

[80] **Peng, Z., Luo, X., Xie, Z., & Yang, M.** (2020). Sintering behavior and mechanical properties of spark plasma sintering SiO2-MgO ceramics. *Ceramics International, 46*, 2585-2591.

[81] **Shankarab, E., & Prabu, S.B.** (2017). Influence of WC and cobalt additions on the microstructural and mechanical properties of TiCN-Cr3C2-nano-TiB2 cermets fabricated by spark plasma sintering. *International Journal of Refractory Metals and Hard Materials,69*, 110-118.

[82] **Freeman, R.** (2007). Measuring the flow properties of consolidated, conditioned and aerated powders - A comparative study using a powder rheometer and a rotational shear cell. *Powder Technology*,*174*, 25–33.

[83]**Srinivasan, R., Yogamalar, R., & Bose, A.C.** (2010). Structural and optical studies of yttrium oxide nanoparticles synthesized by co-precipitation method. *Materials Research Bulletin*, *45*, 1165–1170.

[84] **Cleary, P. W.** (2008). The effect of particle shape on simple shear flows. *Powder Technology*, *179*, 144–163.

[85] **Nan, W., Wang, Y., & Wang, J.** (2016). Numerical analysis on the fluidization dynamics of rodlike particles. *Advanced Powder Technology*, *27*, 2265–2276.

[86] **Nan, W., Ghadiri, M., & Wang, Y.** (2017). Analysis of powder rheometry of FT4: Effect of particle shape. *Chemical Engineering Science*, *173*, 374-383.

[87] **Bharadwaj, R., Ketterhagen, W.R.,& Hancock, B.C.** (2010). Discrete element simulation study of a Freeman powder rheometer. *Chemical Engineering Science,65*, 5747–5756.

[88] **Jakub, H., David, Z., Lucie, J., Jiří, Z., & Jan, N.** (2016). Effect of particle shape and size on the compressibility and bulk properties of powders in powder metallurgy. *Metal 2016 Conferences Paper*.

[89] **Fu, X., Huck, D., Makein, L., Armstrong, B., Willen, U.,& Freeman, T.** (2012). Effect of particle shape and size on flow properties of lactose powders. *Particuology,10*, 203– 208.

[90] **Danjo, K.** (1989). Effect of particle shape on the compaction and flow properties of powders. *Chemical and Pharmaceutical Bulletin, 37*, 3070-3073.

[91] **Zhou, K., Liu, B., Yao, Y.,& Zhong, K.** (2014). Effects of grain size and shape on mechanical properties of nanocrystalline copper investigated by molecular dynamics. *Materials Science and Engineering: A.,615*, 92-97.

[92] **Uddin, S.M., Mahmud, T., Wolf, C., Glanz, C., Kolaric, I., Volkmer, C., Höller, H., Wienecke, U., Roth, S.,& Fecht, H.** (2010).Effect of size and shape of metal particles to improve hardness and electrical properties of carbon nanotube reinforced copper and copper alloy composites.*Composites Science and Technology, 70*, 2253–2257.

[93] **Wu, J., Ruan, C., Ma, Y., Wang, Y.,& Luo, Y.** (2018). Vital role of hydroxyapatite particle shape in regulating the porosity and mechanical properties of the sintered scaffolds. *Journal of Materials Science & Technology,34*, 503–507.

[94] **Celik, M.Y., & Sabah, E.** (2008). Geological and technical characterisation of Iscehisar (Afyon, Turkey) marble deposits and the impact of marble waste on environmental pollution. *Journal of Environmental Management*, *87*, 106-116.

[95] **Hamza, R.A., El-Haggar, S., & Khedr, S.** (2011). Marble and granite waste: characterization and utilization in concrete bricks. *International Journalof Bioscience, Biochemistry and Bioinformatics*,*4*, 286-291.

[96] **Lopez, A.J., Pozo- Antonio, J.S., Ramil, A.,& Rivas, T.** (2018). Influence of the commercial finishes of ornamental granites on roughness, colour and reflectance, *Construction and Building Materials*, *182*, 530-540.

[97] **Mostofi, M., Richard, T., Franca, L.,& Yalamanchi, S.** (2018). Wear response of impregnated diamond bits. *Wear*, *410-411*, 34-42.

[98] **Yang, N., Huang, W.,& Lei, D.**(2018). The effects of diamond amorphous layer on the diamond lapping surface. *Procedia CIRP*, *71*, 140-143.

[99] **Sung, J.C.,& Sung, M.** (2009).The brazing of diamond. *Journal of Refractory Metals & Hard Materials*, *27*, 382-393.

[100] **Wang, Y.H., Wang, H.X., Wang, M.Z.,& Zheng, Y.Z.** (2001). Brazing of Ti/Ni- coated diamond. *Key Engineering Materials*, *202-203*, 147-150.

[101] **Zhang, S.J., To, S.,& Zhang, G.Q.** (2017). Diamond tool wear in ultra-precision machining. *Journal of Advanced Manufacturing Technology*, *1*, 4.

[102] **Tonshoff, H.K., Denkena, B., & Apmann, H.H.** (2003) .Diamond tools for wire sawing metal components. *Key Engineering Materials*, *250*, 33-40.

[103] **Zeren, M. & Karagoz, S.** (2006). Defect characterization in the diamond cutting tools. *Materials Characterization*, *57*, 111-114.

[104] **Miranzo, P. Osendi, M.I. Garcia, E. Fernandes, A.J.S. Silva, V.A. Costa, F.M. & Silva, R.F.** (2002). Thermal conductivityenhancementincutting toolsbychemical vapour deposition diamond coating. *Diamond and Related Materials*, *11*, 703-707.

[105] **Oliveira, L.J., & Filgueira, M.**(2008). The use of PM ferritic matrix for the processing of diamond cutting tools. *MaterialsScienceForum*.*591-593*,241-246.

[106] **Zeren, M., & Karagoz, S.** (2007). Sintering of polycrystalline diamond cuttingtools. *MaterialsandDesign*, *28*, 1055-1058.

[107] **Beste, U., Jacobson, S., &Hogmark, S.** (2008). Rock penetration into cemented carbide drill buttons during rock drilling. *Wear*, *264*, 1142-1151.

[108] **Meena, K.L.,& Karunakar, D.B.** (2018). Development of alumina toughened zirconia nanocomposites using spark plasma sintering. *Materials Today: Proceedings*, *5-9*, 16928-16935.

[109] **Villar, M., Muro, P., Sa´nchez, J.M., Iturriza, I., & Castro, F.** (2001). Consolidation of diamond tools using Cu–Co–Fe based alloys as metallic binders. *Powder Metallurgy*, *44-1*, 82-90.

[110] **Oliveira, L.J., & Filgueira, M.** (2007). Processing and characterization of impregnated diamond cutting tools using a ferrous metal matrix. *International Journal of Refractory Metals & Hard Materials*,*25*, 328–335.

[111] **Xu, L., Srinivasakannan, C., Zhang, L., Yan, M., Peng, J., Xia, H.,& Guo, S.** (2016). Fabrication of tungsten copper alloys by microwave hot pressing sintering. *Journal of Alloys and Compounds*, *658*, 23-28.

[112] **Bayer, A.M., Becherer, B.A.,& Vasco, T.** (1989). High speed tool steels. *ASM Handbook*, *Vol 16*, Machining 51-59.

[113] **Gulyaev, A.P.,& Kupalova, I.K.** (1970). Effect of cobalt on the structure and properties of high-speed steels. *Metal Science and Heat Treatment*, *12*, 666- 671.

[114] **Karaca, I.,& Buyukakkas, S.** (2019). Microhardness characterization of Fe- and Co-based superalloys. *Iranian Journal of Science and Technology A, 43*, 1311-1319.

[115] **Chandrashekar, M.,& Prasad, K.V.S.** (2018). The effect of cobalt on wear behaviour of cemented carbide cutting tools for machining of titanium alloy. *Materials Today: Proceedings*,*5*, 7678–7684.

[116] **Gant, A. J., Konyashin, I., Ries, B., Mckie, A., Nilen, R.W.N.,& Pickles, J.**(2018). Wear mechanism of diamond-containing hard metals in comparison with diamond-based materials. *International Journal of Refractory Metals and Hard Materials*, *71*, 106-114.

[117] **Yan, J., Zhang, Z., & Kuriyagawa, T.** (2009). Mechanism for material removal in diamond turning of reaction-bonded silicon carbide. *International Journal of Machine Tools and Manufacture*, *49*, 366-374.

[118] **Anikoh, G.A., Adesida, P.A., & Afolabi, O.C.** (2015). Investigation of physical and mechanical properties of selected rock types in Kogi state using hardness tests. *Journal of Mining World Express*, *4*, 37-51.

[119] **Nesbitt, H.W., & Young, G.M.** (1984). Predictionof some weathering trends of plutonic and volcanic rocks based on thermo dynamic and kinetic considerations. *Geochimica et Cosmochimica Acta*, *48*, 1523-1534.

[120] **Brouwer, H.A.** (1928). Production of trachyte and phonolite from pyroxene andesitic magma associated with limestone. *The Journal of Geology*, *36*, 545-548.

[121] **Kaplan, C.D., Murtezaoglu, F., İpekoglu, B., &Boke, H.** (2013). Weathering of andesite monuments in archaeological sites. *Journal of Cultural Heritage,14*, 77-83.

[122] **Doyuran, V., Ayday, C., & Karahanoglu, N.** (1993). Statistical analyses of discontinuity parameters of Golbasi (Ankara) andesites, Supren (Eskisehir) marble, and Porsuk dam (Eskisehir) peridotitein Turkey. *Bulletin of the International Association of Engineering Geology*, *48*, 15‑31.

[123] **Orhan, M., Isık, N.S., Topal, T., & Ozer, M.** (2006). Effect of weathering on the geomechanical properties of andesite, Ankara ‑Turkey. *Environmenta lGeology*,*50*, 85‑100.

[124] **Sohrabian, B., &Ozcelik, Y.** (2012). Determination of exploitable blocks in an andesite quarry using in dependent component kriging. *International Journal of Rock Mechanics and Mining Sciences*, *55*, 71‑79.

[125] **Ozcelik, Y.** (2011). Determination of the regions used as facingand building stone according to the material characteristics in an andesite quarry. *Engineering Geology*, *118*, 104‑109.

[126] **Karpuz, C., & Pasamehmetoglu, A.G.** (1997). Field characterisation of weathered Ankara andesites. *EngineeringGeology*, *46*, 1-17.

[127] **Skury, A.L.D., Bobrovnitchii, G.S., Azevedo, M.G., &Monteiro, S.N.** (2012). Obtention and characaterization of the Sn-Ni-Fe-Cu alloys applied in diamond saw blade production. *Materials Science Forum*, *727-728*, 305- 309.

[128] **Ucun, I., Aslantas, K., Buyuksagis, I.S., &Tasgetiren, S.**(2011). An investigationon the effect of diamond concentration and matrix material composition in the circular sawing process of granites. *Proceedings of the Institution of MechanicalEngineers, Part C: Journal of Mechanical Engineering Science*, *225*, 1-17.

[129] **Oliveira, H.C.P., Coelho, A., Amaral, P.M., Fernandes, J.C., & Rosa, L.G.** (2013). Comparison between cobalt and niobium as a matrix component for diamond impregnated tools used for stone cutting. *Key Engineering Materials*, *548*, 98-105.

[130] **Tönshoff, H.K., &Warnecke, G.** (1982). Research on stone sawing. *Advances in Ultrahard Materials Application Technology*, *1*, 36-49.

[131] **Buttner, A.** (1974). Diamond tools and stone. *Industrial Diamond Review*, *34*, 89-93.

[132] **Atici, U., & Ersoy, A.** (2009). Correlation of specific energy of cutting saws and drilling bits with rock brittleness and destructionenergy. *Journal of MaterialsProcessingTechnology*, *209*,2602–2612.

[133] **Feng, Y., Yuan, H.L., & Zhang, M.** (2005). Fabrication and properties of silver- matrix composites reinforced by carbon nanotubes. *Materials Characterization*,*55*, 211-218.

[134] **Li, J., Xiong, D., Huang, Z., Kong, J., & Dai, J.** (2009). Effect of Agand CeO_2 on friction and wear properties of Ni-base composite at high temperature. *Wear*, *267*, 576-584.

[135] **Chaki, T.K., &Wang, P.E.** (1994). Densification and strengthening of silver-reinforced hydroxyapatite-matrix composite prepared by sintering. *Journal of MaterialsScience: Materials in Medicine*, *5*, 533-542.

[136] **Suresh, K.R., Niranjan, H.B., Jebaraj, P.M., & Chowdiah, M.P.** (2003). Tensile andwearproperties of aluminumcomposites. *Wear*, *255*, 638-642.

[137] **Rock Characterization Testing and Monitoring Suggested Methods**.(1981). *ISRM Oxford*, 16.

[138] **T.S.E. Testing**. (1987). Examination Methods of Natural Building Stones. *T.S. 669, Ankara: T.S.E. Press*, 82 (in Turkish).

[139] **Ruiz, R.H.E., Campos, R.F., Rodrigues, G.A.T., Ramirez, J.M.H., & Sanchez,R.M.** (2016). Wear resistance analysis of the aluminum 7075 alloy and the nanostructured aluminum 7075 ‐silver nanopartıclescomposites. *Journal of MiningandMetallurgy, Section B: Metallurgy*, *52*, 163-170.

[140] **Ruiz, R.H.E., Campos, R.F., Ramirez, J.M.H., &Sanchez, R.M.** (2016). Mechanical properties of aluminum 7075 ‐ Silver nanoparticles powder composite and its relationship with the powder particle size. *Advanced PowderTechnology*, *27*,1694-1699.

[141] **Azar, G.T.P., Rezaie, H.R., &Razavizadeh, H.** (2012). Synthesis and consolidation of W‐Cu composite powders with silver addition. *International Journal of RefractoryMetalsand Hard Materials*, *31*, 157-163.

[142] **Zhang, X., Ba, Z., Wang, Z., He, X., Shen, C., & Wang, Q.** (2013). Influence of silver addition on microstructure and corrosion behavior of Mg‐Nd‐Zn‐Zr alloys for biomedical application. *Materials Letters*, *100*, 188-191.

[143] **Wu, X.Z., Xiao, D.H., Zhu, Z.M., Li, X.X., &Chen, K.H.** (2014). Effect of minor silver addition on microstructure and properties of Al-8Zn-1.Cu-1.3Mg-0.1Zr alloys. *Advanced Materials Research*, *834-836*, 360-363.

[144] **Mandal, P.K., & Robi, P.S.** (2018). Influence of micro-alloying with silver on microstructure and mechanical properties of Al-Cu alloy. *Materials Science and Engineering A*, *722*, 99-111.

[145] **Chou, C.W., Hsu, S., Chang, H., Tseng, S.M., & Lin, H.R.** (2006). Enhanced thermal and mechanical properties and biostability of polyurethane containing silver nanoparticles. *Polymer Degradation and Stability*, *91*, 1017-1024.

CURRICULUM VITAE

Name Surname: Berrak BULUT

Education

Ph.D :2021, Istanbul TechnicalUniversity, Faculty of Chemical and Metallurgy Engineering, Metallurgy and Materials Engineering.

M.Sc. : 2014, Istanbul Technical University, Faculty of Chemical and Metallurgy Engineering, Metallurgy and Materials Engineering.

B.Sc. : 2011,Yildiz Technical University, Faculty of Chemical and Metallurgy Engineering, Metallurgy and Materials Engineering.

B.Sc. : 2013, Anadolu University, Faculty ofManagementDepartment of Business Administration.

PUBLICATIONS AND PRESENTATIONS ON THE THESIS:

PUBLICATIONS

- **Bulut B.**, Gunduz O., Baydogan M., Kayali E.S., "Determination of matrix composition for diamond cutting tools according to the hardness and abrasivity properties of rocks to be cut", International Journal of Refractory Metals and Hard Materials, 2020.

- **Bulut B.**, Baydogan M., Kayali E.S., "Effect of aluminium and silver addition on the wear characteristics of circular diamond saw blades for cutting Ankara andesite rocks", Wear, 2021.

- **Bulut B.**, Unal F., Baydogan M., Kayali E.S., "Effect of particle morphology on physical, mechanical and wear properties of cobalt metal powders", Transactions of the Indian Institute of Metals, 2021.

- **Bulut B.**, Tazegul O., Baydogan M., Kayalı E.S., "Characterization of Diamond Tools for Cutting Natural Stones Using Fe-Co-Cu Base Alloy as a

Metal Matrix", 18. Uluslararası Metalurji ve Malzeme Kongresi Bildiriler Kitabı, 489-492,2016.

- **Bulut B.**, Tazegul O., Baydogan M., Kayalı E.S.," The Comparison of the Sintering Methods for Producing Diamond Tools Which are Used in Natural Stone Cutting",16.Uluslararası Malzeme Sempozyumu Bildiriler Kitabı,1582-1589,2016.

- **Bulut B.**, Tazegul O., Baydogan M., Kayalı E.S.," The Comparison of the Sintering Methods for Producing Diamond Tools",Journal of Achievements of Materials and Manufacturing Engineering, 76 (1), 30-34,2016.

- **Bulut B.**, Tazegul O., Baydogan M., Kayalı E.S., "Investigation and Application of Fe-Co-Cu Based Diamond Cutting Tools with Different Bronze Content Used in Marble Production", Advanced Structured Materials, 65, 307-314,2017.

PRESENTATIONS

- MDA 2016, International Conference on Materials Design and Application,30 June-1 July 2016, Porto,Portugal.
- IMMC 2016, 18. International Congress of Metallurgy and Materials, 29 September-1 October 2016, Istanbul,Turkey.
- IMSP2016,16.International SymposiumofMaterials,12-14October2016, Denizli,Turkey.
- PPM, Porous and Powders Materials, 12-15 October 2017, Kusadasi,Aydin, Turkey.
- UDCS2019, 4. International Symposium of Iron and Steel, 4-6 April2019, Karabuk,Turkey.
- IMSMATEC2019, 21-23 June 2019, Kapadokya,Turkey.